

BRINK, S

TITANIUM(IV) COMPLEXES OF THIANTHRENE AND DIBENZODIOXIN
AS POSSIBLE ANTITUMOUR AGENTS

MSc (Chemistry)

UP

1998

Titanium(IV) complexes of thianthrene and dibenzodioxin as possible antitumour agents

by

Susanna Brink

Submitted in partial fulfilment of the degree

MAGISTER SCIENTIAE

in

CHEMISTRY

in the Faculty of Natural Sciences of the

UNIVERSITY OF PRETORIA

PRETORIA

September 1998

Acknowledgements

I would like to thank the following people who made the completion of this work possible:

My Creator

My supervisor, Prof Simon Lotz

The Foundation for Research and Development

All my friends and fellow students

My parents and grandmother

Brief Contents

Summary

Samevatting

Abbreviations

List of Compounds

Part I Review and Aim

1. A Review of the Antitumour Properties of Titanocene Dichloride
2. Aim of Study

Part II Synthesis, Characterization and Discussion of New Titanium Complexes

3. Titanocene Complexes with Dibenzodioxinyl as Ligand
4. Titanocene Complexes with Thianthrenyl as Ligand
5. Titanocene Complexes with Dibenzodioxin-1-thiolate as Ligand
6. Titanocene Complexes with Thianthrene-1-thiolate as Ligand
7. Titanocene Complexes with a Ring-Opened Thianthrene Ligand

Part III Comparison of Structural Features and Antitumour Properties

8. Comparison of Geometries
9. Possible Mechanisms for Antitumour Activity

Part IV Experimental

10. Experimental

Appendix

Contents

Summary	vi
Samevatting	vii
Abbreviations	viii
List of Compounds	x
<u>Part I</u>	1
<u>Review and Aim</u>	1
1. A Review of the Antitumour Properties of Titanocene Dichloride	2
1.1 Background	2
1.2 Antitumour Properties of Bis(cyclopentadienyl) Metal Complexes	4
1.3 Metallocene Diacido Complexes	6
1.4 Carcinostatic Activity of Titanocene Dichloride	11
1.5 Proposed Mechanism of Action for Titanocene Dichloride	12
1.6 Intercalation	17
2. Aim of Study	20
2.1 Aim and Motivation of Study	20
2.2 The Ligands	22
2.3 Construction of Thesis	24
<u>Part II</u>	25
<u>Synthesis, Characterization and Discussion of New Titanium Complexes</u>	25
Information Concerning all Complexes	26
3. Titanocene Complexes with Dibenzodioxinyl as Ligand	27
3.1 Synthesis	27
3.2 Characterization	29
• <i>Mass Spectrometry</i>	29
• <i>¹H NMR Spectroscopy</i>	31
• <i>COSY</i>	34
• <i>¹³C NMR Spectroscopy</i>	36
• <i>HETCOR</i>	38
• <i>X-ray Crystallography</i>	39

3.3 Conclusion	43
4. Titanocene Complexes with Thianthrenyl as Ligand	45
4.1 Synthesis	45
4.2 Characterization	47
• <i>Mass Spectrometry</i>	47
• <i>¹H NMR Spectroscopy</i>	48
• <i>¹³C NMR Spectroscopy</i>	52
4.3 Conclusion	53
5. Titanocene Complexes with Dibenzodioxin-1-thiolate as Ligand	54
5.1 Synthesis	54
5.2 Characterization	56
• <i>Mass Spectrometry</i>	56
• <i>¹H NMR Spectroscopy</i>	57
• <i>COSY</i>	62
• <i>¹³C NMR Spectroscopy</i>	63
• <i>HETCOR</i>	65
5.3 Conclusion	66
6. Titanocene Complexes with Thianthrene-1-thiolate as Ligand	67
6.1 Synthesis	67
6.2 Characterization	68
• <i>Mass Spectrometry</i>	68
• <i>¹H NMR Spectroscopy</i>	69
• <i>COSY</i>	73
• <i>¹³C NMR Spectroscopy</i>	74
6.3 Conclusion	75
7. Titanocene Complexes with a Ring-Opened Thianthrene Ligand	76
7.1 Introduction	76
7.2 Synthesis	77
7.3 Characterization	78
• <i>Mass Spectrometry</i>	78
• <i>¹H NMR Spectroscopy</i>	79
• <i>¹³C NMR Spectroscopy</i>	82
7.4 Conclusion	84

<u>Part III</u>	<u>Comparison of Structural Features and Antitumour Properties</u>	85
8.	Comparison of Geometries	86
8.1	Chalcanthrenes	86
8.2	Chalcanthrenethiolates	88
8.3	Conclusion	91
9.	Possible Mechanisms for Antitumour Activity	92
9.1	Geometry and Intercalation	92
9.2	Geometry and Covalent Bonding	93
9.3	Conclusion	93
9.4	Future	94
<u>Part IV</u>	<u>Experimental</u>	95
	Information Concerning all Reactions	96
10.	Experimental	97
10.1	Experimental Procedures	97
•	<i>Lithiation of Dibenzo[1,4]dioxin</i>	97
•	<i>Lithiation of Thianthrene</i>	97
•	<i>Preparation of</i>	
-	<i>Chlorobis(cyclopentadienyl)(dibenzodioxinyl)titanium(IV) 1</i>	97
-	<i>μ-oxobis{bis(cyclopentadienyl)(dibenzodioxinyl)titanium(IV)} 2</i>	97
•	<i>Preparation of</i>	
-	<i>Chlorobis(cyclopentadienyl)(thianthrenyl)titanium(IV) 3</i>	98
-	<i>μ-oxobis{bis(cyclopentadienyl)(thianthrenyl)titanium(IV)} 4</i>	98
•	<i>Preparation of</i>	
-	<i>Lithiated Dibenzodioxin-1-thiolate 5a</i>	98
-	<i>Dibenzodioxin-1-thiol 5</i>	98
-	<i>Dibenzodioxin-1-butylthioether 5b</i>	98
•	<i>Preparation of</i>	
-	<i>Lithiated Thianthrene-1-thiolate 8a</i>	99
-	<i>Thianthrene-1-thiol 8</i>	99
•	<i>Preparation of</i>	
-	<i>Chlorobis(cyclopentadienyl)(dibenzodioxinylthiolato)titanium(IV) 6</i>	99

Contents	v
<i>-Bis(cyclopentadienyl)bis(dibenzodioxinylthiolato)titanium(IV) 7</i>	99
• <i>Preparation of</i>	
<i>-Chlorobis(cyclopentadienyl)(thianthrenylthiolato)titanium(IV) 9</i>	99
<i>-Bis(cyclopentadienyl)bis(thianthrenethiolato)titanium(IV) 10</i>	99
• <i>Preparation of the Titanium(IV) complex with Thianthrene as Ring-Opened Ligand 11</i>	99
10.2 Crystal Structure Determination of [TiCp ₂ (Db)Cl]	100
Appendix	103

Titanium(IV) complexes of thianthrene and dibenzodioxin as possible antitumour agents

Candidate: Susanna Brink

Promotor: Prof Simon Lotz

Department: Chemistry

Degree: Magister Scientiae

Summary

This study involves the synthesis and characterization of new organometallic complexes of Ti(IV). Such complexes are designed to act as possible antitumour agents and thus include ligands with specific functions. As target for biological activity, the DNA double helix was identified. These complexes include (i) a labile halogen ligand which is capable of forming a covalent bond with DNA, (ii) a planar condensed 3-membered ring system which may act as intercalator in the major groove of DNA and (iii) two bulky, non-labile stopper ligands which will control the degree of intercalation. The complexes represent two groups, namely those where the transition metal is bonded directly to the planar ring system and those where a sulphur atom is located between the metal and the ring system. The sulphur acts as a spacer and causes the ring system to be out of the plane of the metal fragment.

New complexes $[\text{TiCp}_2(\text{R})\text{Cl}]$, $[\text{TiCp}_2(\text{R})_2]$, $[\text{TiCp}_2(\text{SR})\text{Cl}]$ and $[\text{TiCp}_2(\text{SR})_2]$ ($\text{R} = \text{thianthrene, dibenzodioxin}$) were prepared by adding the lithiated rings or the metallated thiolates to titanocene dichloride. Also studied was the insertion of titanocene dichloride into ring-opened, dilithiated thianthrene. The composition of the new complexes were determined by using NMR studies, mass spectrometry and micro analysis. The structure of $[\text{TiCp}_2(\text{Db})\text{Cl}]$ was confirmed by a single crystal X-ray diffraction study. Since the molecular geometries of the complexes are of utmost importance for their interaction with DNA, their three-dimensional structures were also studied using computer generated spacefill models. From these results, the structures of the complexes were obtained and together with their physical features, the complexes $[\text{TiCp}_2(\text{Db})\text{Cl}]$ and $[\text{TiCp}_2(\text{DbS})\text{Cl}]$ were selected as the best candidates for *in vivo* and *in vitro* tests. The latter did not form part of this study.

Samevatting

Hierdie studie behels die sintese en karakterisering van nuwe organometaalkomplekse van Ti(IV). Sulke komplekse is ontwerp om te dien as moontlike antikankermiddels en sluit dus ligande met spesifieke antitumor funksies in. As teiken vir die biologiese aktiwiteit is die DNA dubbel heliks geïdentifiseer. Hierdie komplekse bevat (i) 'n labiele halogeen ligand wat na verplasing 'n direkte kovalente binding met DNA moontlik maak, (ii) 'n planêre gekondenseerde 3-lid ringsisteem wat as interkaleerder kan optree en (iii) twee groot, nie-labiele stopperligande wat die mate van interkalering sal beheer. Die komplekse verteenwoordig twee groepe naamlik die waar die oorgangsmetaal direk aan die planêre ringsisteem gekoppel is en in die vlak van die ringsisteem voorkom en die waar 'n swaelatoom tussen die metaal en die ringsisteem voorkom. Die swael dien in die tweede geval as 'n spasiëerder en veroorsaak dat die ringsisteem uit die vlak van die metaalfragment lê.

Nuwe komplekse $[\text{TiCp}_2(\text{R})\text{Cl}]$, $[\text{TiCp}_2(\text{R})_2]$, $[\text{TiCp}_2(\text{SR})\text{Cl}]$ en $[\text{TiCp}_2(\text{SR})_2]$ ($\text{R} =$ tiantreen, dibensodioksien) is berei deur die gelitiseerde ringe of die gemetalleerde tiolate by titanoseendichloried te voeg. Daar is ook gekyk na die invoeging van titanoseendichloried in 'n ring-geopende, digelitiseerde tiantreen. Die nuwe komplekse is gekarakteriseer deur gebruik te maak van KMR-studies, massaspektrometrie en mikro-analises. Die struktuur van $[\text{TiCp}_2(\text{Db})\text{Cl}]$ is bevestig met 'n enkel kristal X-straal diffraksie studie. Omdat die molekulêre geometrieë van die komplekse van die uiterste belang vir hul interaksie met DNA is, is hulle drie-dimensionele stukture ook gesimuleer deur middel van ruimtevullende rekenaar modelle. Uit hierdie resultate, die samestelling van die komplekse en die fisiese hanteerbaarheid (stabiliteit) daarvan, blyk dit dat $[\text{TiCp}_2(\text{Db})\text{Cl}]$ en $[\text{TiCp}_2(\text{DbS})\text{Cl}]$ die geskikste kandidate is vir *in vivo* en *in vitro* studies. Laasgenoemde het nie deel gevorm van hierdie studie nie.

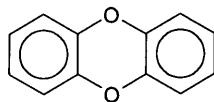
Abbreviations

A	Adenine
<i>Anal. Calc.</i>	Micro analysis calculated values
Bu	Butyl
BT	Benzothiophene
C	Cytosine
COSY	Correlation spectroscopy
Cp	Cyclopentadienyl
d	Doublet
d ⁿ	Superscript indicates the number of valence electrons in the d-orbital
DbT	Dibenzothieryl
dd	Doublet of doublets
dt	Doublet of triplets
Db	Deprotonated dibenzodioxin
DbH	Dibenzo[1,4]dioxin
DbSBu	Dibenzodioxinbutylthioether
DbS	Dibenzodioxinthiolate
DbSH	Dibenzodioxin-1-thiol
DNA	Deoxyribonucleic acid
ED ₉₀	Effective dose (dose at which 90% of the mice used are cured)
EELS	Electron energy loss spectroscopy
EhAT	Ehrlich ascites tumour
G	Guanine
ICP	Inductive coupled plasma
J	Coupling constant
HeLa	Human cervix epitherioid carcinoma
HETCOR	Heteronuclear correlation spectroscopy
L	Ligand
LD ₅₀	Lethal dose (dose at which 50% of the mice used are killed)

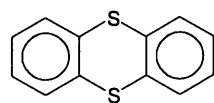
M	Transition metal
[M ⁺]	Molecular ion
Mp	Melting point
NMR	Nuclear magnetic resonance
ppm	Parts per million
R	Heteroaromatic ligand
RNA	Ribonucleic acid
s	Singlet
HSDbT	Dibenzothienylthiol
HSBT	Benzothienylthiol
t	Triplet
T	Thymine
THF	Tetrahydrofuran
Th	Deprotonated thianthrene
ThH	Thianthrene
ThS	Thianthrenethiolate
ThSH	Thianthrenethiol
TMEDA	Tetramethylethylenediamine
U	Uracil
UV	Ultraviolet
X	Labile ligand
Å	Angstrom (10 ⁻⁸ m)
δ	Chemical shift
Δ	Difference between two values
μ	Indicates a bridged ligand
η ⁿ	Superscript indicates the number of coordinated carbons

List of Compounds

Organic Starting Compounds

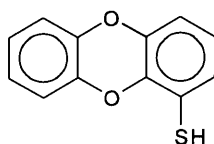


Dibenzo[1,4]dioxin

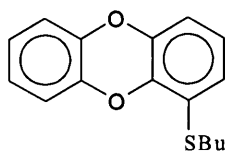


Thianthrene

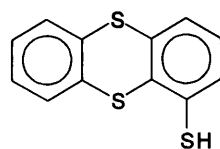
Organic Synthesized Compounds



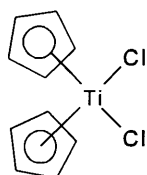
Dibenzodioxin-5-thiol **5** [DbSH]

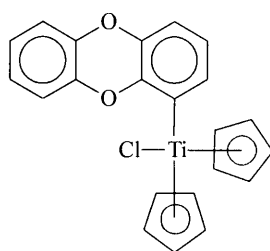
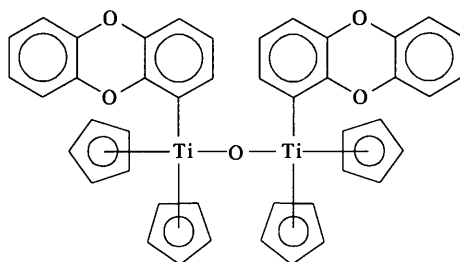
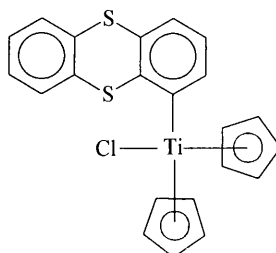


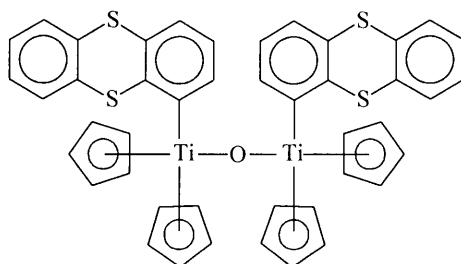
Dibenzodioxinbutylthioether **5b** [DbSBu]



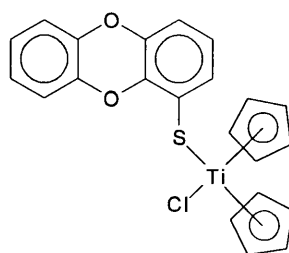
Thianthrene-5-thiol **8** [ThSH]

Organometallic Starting Complex

 Titanocene dichloride [TiCp₂Cl₂]

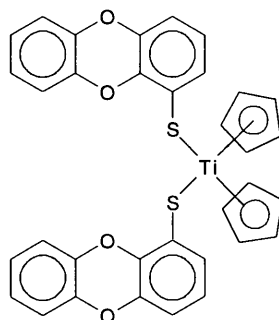
Organometallic Synthesized Complexes

 Chlorobis(cyclopentadienyl)(dibenzodioxinyl)titanium(IV) **1** [TiCp₂(Db)Cl]

 μ -oxobis{bis(cyclopentadienyl)(dibenzodioxinyl)titanium(IV)} **2** [{TiCp₂(Db)}₂O]

 Chlorobis(cyclopentadienyl)(thianthrenyl)titanium(IV) **3** [TiCp₂(Th)Cl]



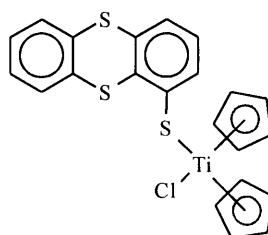
μ -oxobis(bis(cyclopentadienyl)(thianthrenyl)titanium(IV)) **4** [$\{\text{TiCp}_2(\text{Th})\}_2\text{O}$]



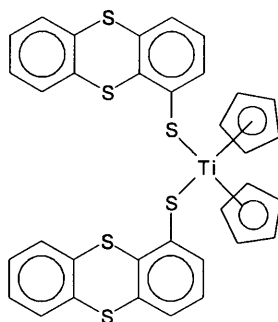
Chlorobis(cyclopentadienyl)(dibenzodioxinethiolato)titanium(IV) **6** [$\text{TiCp}_2(\text{DbS})\text{Cl}$]



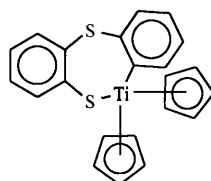
Bis(cyclopentadienyl)bis(dibenzodioxinethiolato)titanium(IV) **7** [$\text{TiCp}_2(\text{DbS})_2$]



Chlorobis(cyclopentadienyl)(thianthrenethiolato)titanium(IV) **9** [$\text{TiCp}_2(\text{ThS})\text{Cl}$]



Bis(cyclopentadienyl)bis(dibenzodioxinyl)titanium(IV) **10** [TiCp₂(Db)₂]



Titanocene with ring-opened thianthrene as ligand **11** [TiCp₂(SC₆H₄SC₆H₄)]

Part I

Review and Aim

- 1. A Review of the Antitumour Properties of Titanocene Dichloride 2**
- 2. Aim of Study 20**

1. A Review of the Antitumour Properties of Titanocene Dichloride

1.1 Background

Organometallic compounds were synthesized since 1760¹. For a long time little research was done to investigate the possible biological activities of organometallic complexes. This was mainly due to various cases of metal poisoning and it was just assumed that such compounds would not be effective as therapeutic agents. In the 19th century, a suspension of lead acetate in benzene, better known as Fowlers² solution, was one of the first examples of a metal compound being used to treat cancer. Many compounds based on Fowlers solution, were used until recent times³. Today cisplatin (**Fig. 1.1**) is one of the most widely used compounds to treat certain malignant tumours. It was first synthesized in 1844 by Michele Peyrone⁴, but it was only in 1969 that Barnett Rosenberg discovered the tumour-inhibiting properties of cisplatin⁵.

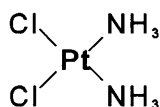


Fig. 1.1. *cis*-Diamminedichloroplatinum(II).

Soon after this discovery research was based on producing cisplatin analogues and all new tumour-inhibiting compounds were compared to and modelled on cisplatin. Scientists did not take into account that they could also have studied other compounds, which might have a

1. L. D. Cadet de Gassicourt, *Memoires de Mathématique et de Physique*, 1760, 3, 623.

2. Lissauer, *Berliner Klin. Wochenschrift*, 1865, 2, 403.

3. G. Tarchiani, S. Vitale, *Clin. Ther.*, 1964, 31, 101.

4. M. Peyrone, *Annalen der Chemie und Pharmazie*, 1844, Band LI, 1ff.

5. B. Rosenberg, L. Van Camp, *Nature*, 1969, 222, 385.

different mode of biological activity. The range of tumours inhibited by cisplatin is very narrow and the aim must be to find other compounds that will inhibit cisplatin-resistant tumours. Carboplatin and other second generation platinum complexes are presently used to minimize some of the undesirable side effects associated with cisplatin treatments⁶. Certain tumours also build up a resistance against cisplatin during treatment. Today there are only a few non-platinum complexes in clinical trials, including germanium compounds, gallium salts and budotitane, while others, such as ruthenium and metallocene complexes, are undergoing preclinical tests⁷.

The first transition metal complex after cisplatin to enter clinical studies was budotitane (**Fig. 1.2**), which belongs to the class of bis(β -diketonato) metal complexes. The antitumour activities of some of these compounds were reported as early as 1982⁸. About 200 compounds from this group were studied as possible antitumour agents and ultimately budotitane was selected for further testing⁹. The antitumour effects of this complex have been discussed in a recent review¹⁰. The structure-activity relation of budotitane is believed to be completely different from that of cisplatin. This was concluded from the fact that its activity is dependent on the planar aromatic group of the β -diketonato ligand. Therefore, it is anticipated that they act through an intercalating mechanism. As a result, this lead to further investigations in the intercalation properties of complexes with DNA. It was shown that metallaintercalators could act in the same way as planar organic systems which are capable of intercalation into the grooves of double stranded DNA helixes (see Section 1.6).

The first metallocene, ferrocene, was discovered independently by Pauson¹¹ and Miller¹² in 1951. Its then, unusual structure and new type of bond, the π -sandwich type of bond, attracted a lot of

6. A. J. Wagstaff, A. Ward, P. Benfield, R. C. Heel, *Drugs*, **1989**, *37*, 162.

7. B. K. Keppler, M. R. Berger, T. Klenner, M. E. Heim, *Adv. Drug Res.*, **1990**, *19*, 243.

8. H. J. Keller, B. K. Keppler, D. Schmähel, *Arzneim. Forsch.*, **1982**, *32*, 806.

9. M. E. Heim, H. Flechtner, B. K. Keppler, *Prog. Clin. Biochem. Med.*, **1989**, *10*, 217.

10. B. K. Keppler, C. Friesen, H. Vongerichten, E. Vogel in *Metal Complexes in Cancer Chemotherapy*, B. K. Keppler (ed.), VCH, Weinheim, **1993**, 299.

11. T. J. Kealy, P. L. Pauson, *Nature (London)*, **1951**, *168*, 1039.

12. S. A. Miller, J. A. Tebboth, J. F. Tremaine, *J. Chem. Soc.*, **1952**, 632.

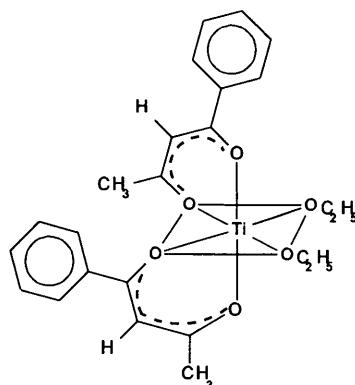


Fig. 1.2. Budotitane.

interest to such compounds. Since then, numerous other metallocenes of groups 3-11 were synthesized and over the last few years, it has become apparent that some of these metallocenes display biological activities. We will now focus specifically on bis(cyclopentadienyl) metal complexes, as they represent the basis of this study.

1.2 Antitumour Properties of Bis(cyclopentadienyl) Metal Complexes

Bis(cyclopentadienyl) metal complexes can be neutral or ionic and the cyclopentadienyl rings are arranged in a sandwich or an open clam shell structure, depending on the type and number of other ligands around the metal centre (**Fig. 1.3**)¹³.

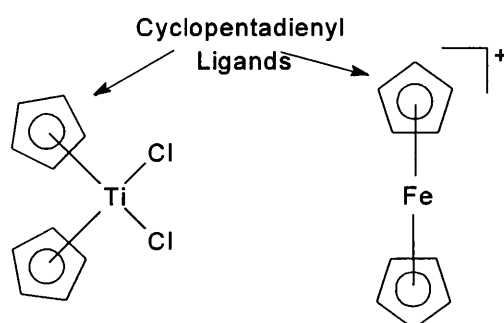


Fig. 1.3. Neutral and ionic bis(cyclopentadienyl) metal complexes with an open clam shell and a sandwich structure, respectively.

13. P. Köpf-Maier in *Metal Complexes in Cancer Chemotherapy*, B.K. Keppler (ed.), VCH, Weinheim, 1993, 262.

The complexes classified as neutral compounds include metallocene complexes with diacido ligands and those with substituted cyclopentadienyl rings. The diacido complexes (**Fig. 1.4 A**) contain early transition metals Ti, V, Nb and Mo in oxidation state +4 and the Cp rings are tilted. The acido ligands can be varied and are represented by halides, carboxylates, phenolates or thiophenolates. The molecular geometry is in the form of a distorted tetrahedron. Decasubstituted metallocenes (**Fig. 1.4 B and C**) contain main group metals Sn and Ge in oxidation state +2. The Cp rings are pentasubstituted by phenyl or benzyl and are arranged in a sandwich or, due to steric reasons, in a distorted sandwich structure, respectively^{14,15}. These compounds contain no covalently bound acido ligands.

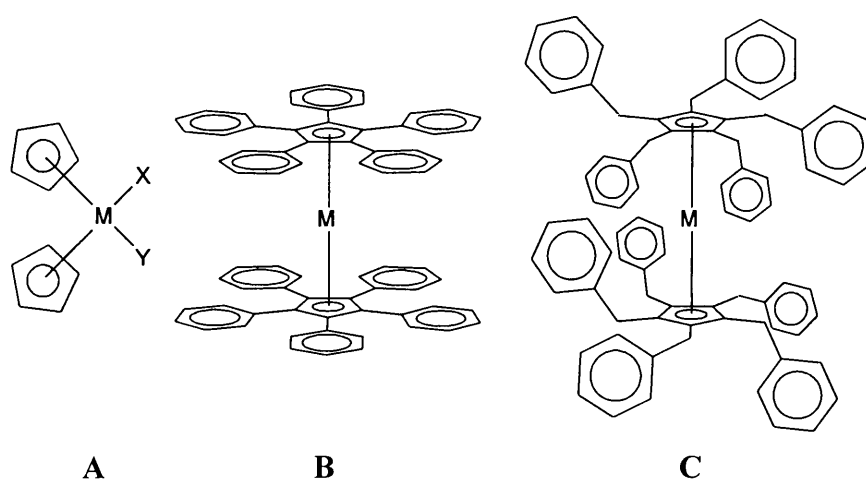


Fig. 1.4. Neutral bis(cyclopentadienyl) metal complexes: (A) diacido complexes, (B) phenyl decasubstituted metallocenes and (C) benzyl decasubstituted metallocenes.

The ionic compounds are better soluble in water and include titanocenium, ferricenium, rhenocenium and highly oxidized niobocenium and molybdenocenium complexes. The titanocenium complexes contain Ti in oxidation state +4 and can have two neutral donor ligands or one anionic and one neutral ligand. The ferricenium complex has Fe in oxidation state +3 and because there are no other acido or neutral ligands, it has a sandwich structure. The rhenocenium dichloride complex (**Fig. 1.5**) contains the middle transition heavy metal, Re in oxidation state

14. M. J. Heeg, C. Janiak, J. J. Zuckerman, *J. Am. Chem. Soc.*, **1984**, *106*, 4259.

15. H. Schumann, C. Janiak, E. Hahn, C. Kolax, J. Loebel, M. D. Rausch, J. J. Zuckerman, M. J. Heeg, *Chem. Ber.*, **1986**, *119*, 2656.

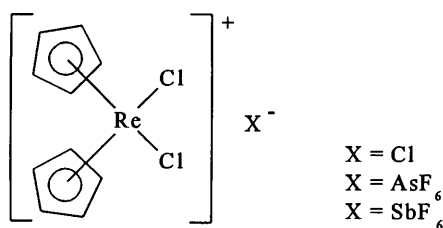


Fig. 1.5. Bis(cyclopentadienyl)dichlororhenium(V) salt

+5 and has two chloro ligands. The niobocenium complex has Nb in oxidation state +5 and two chloro ligands. The molybdenocenium complex has Mo in oxidation state +6, with two chloro ligands. The last two complexes have the same molecular structure as titanocene dichloride and also similar antitumour activity. Of these, the neutral metallocene diacido complexes will be discussed further, as they represent the structural entity chosen for this study.

1.3 Metallocene Diacido Complexes

Metallocene dihalides represent the first organometallic antitumour agents. The structure-activity relation was studied by chemical variation. The molecules can be modified at three different positions, (a) the central metal atom, (b) the acido ligands and (c) the protons on the cyclopentadienyl rings (**Fig. 1.6**)^{16,17}.

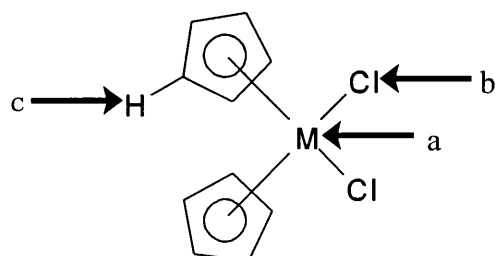


Fig. 1.6. Positions where metallocene dichloride can be modified.

16. H. Köpf, P. Köpf-Maier in *Platinum, Gold and Other Metal Chemotherapeutic Agents*, S. J. Lippard (ed.), ACS Symposium Series, **1983**, 315.

17. I. Haiduc, C. Silvestru, *Organometallics in Cancer Chemotherapy*, Vol II, CRC Press, **1990**, 36.

(a) Variation of the central metal atom was done using eight different early transition metals of groups 4-6 (Ti, V, Nb, Mo, Ta, W, Zr and Hf). There was a strong dependence of the antitumour action against Ehrlich ascites tumour (EhAT) upon the metal atom used. The metals in the first two rows, Ti, V, Nb and Mo, showed high cure rates at optimum doses, while the higher homologues, Ta and W, showed very low cure rates and for Zr and Hf, no cures were observed. If we look at their positions on the Periodic Table, we notice a diagonal relation between Ti - Nb and V-Mo (**Fig. 1.7**). The atomic radii of these diagonal pairs are very similar and we can see that the size of the metal determines the Cl-M-Cl bonding angle, the M-Cl bonding distance and therefore the intramolecular non-bonding Cl...Cl distance (bite distance) (**Fig. 1.8**). This bite distance of about 3.2Å corresponds to the bite distance of cisplatin and to the distance between two DNA-base donor atoms. After dissociation of the Cl ligands, cross-links can be build up by forming covalent bonds between the metal and DNA heteroatoms (**Fig. 1.9**)¹⁸. Zirconium and hafnium, with their bigger radii, are believed to be inactive because of their larger bite distances. These distances exceed the critical value believed to be between 3.50Å and 3.60Å and this probably makes it difficult for them to form DNA-metal cross-links. The fact that the bite distance of cisplatin and antitumour active metallocene dichlorides are of similar size, does not necessarily mean that the modes of interaction with DNA are the same.

H																	He
Li	Be											B	C	N	O	F	Ne
Na	Mg											Al	Si	P	S	Cl	Ar
K	Ca	Sc	Ti	V	Cr	Mn	Fe	Co	Ni	Cu	Zn	Ga	Ge	As	Se	Br	Kr
Rb	Sr	Y	Zr	Nb	Mo	Tc	Ru	Rh	Pd	Ag	Cd	In	Sn	Sb	Te	I	Xe
Cs	Ba	La	Hf	Ta	W	Re	Os	Ir	Pt	Au	Hg	Tl	Pb	Bi	Po	At	Rn
Fr	Ra	Ac	Db	Jl	Rf	Bh	Hn	Mt									

Fig. 1.7. The diagonal relation of transition metals on the Periodic Table.

18. I. A. G. Roos, *Chem. Biol. Interact.*, 1977, 10, 39.

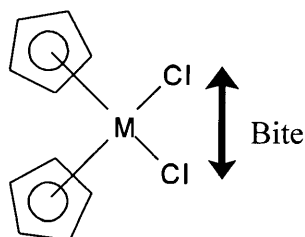


Fig. 1.8. The intramolecular non-bonding Cl...Cl bite distance.



Fig. 1.9. Possible binding modes of cisplatin with DNA.

(b) Variation of the acido ligands in titanocene dichloride with other halides or pseudohalides like F, Br, I, NCS and N₃ had no effect on the level of antitumour activity¹⁹. All these ligands are labile and dissociate in a similar way in aqueous solutions, meaning that the coordination sites of the metal, for interaction with the DNA, are released in the same way. However, some of these ligands can be used to increase the therapeutic range and index. The therapeutic range is defined as the difference between the lethal dose (LD₅₀) and the effective dose (ED₉₀), while the therapeutic index is defined as the ratio of LD₅₀ to ED₉₀²⁰. Titanocene dihalides in acidic medium, buffered to pH 5.1-5.7, increased the therapeutic index and reduced the side-effects. This is explained by the tendency of titanocene dihalides to partially cleave off their acido ligands in a hydrolysis equilibrium²¹. In neutral or basic solutions the drugs have acidic properties which lead to side-effects. In cisplatin the kinetics of Cl-substitution is also very important²².

19. P. Köpf-Maier, B. Hesse, R. Voightländer, H. Köpf, *J. Cancer Res. Clin. Oncol.*, **1980**, *97*, 31.

20. I. Haiduc, C. Silvestru, *Organometallics in Cancer Chemotherapy*, Vol II, CRC Press, **1990**, 44.

21. E. Samuel, *Bull. Soc. Chim. France*, **1966**, 3548.

22. M. J. Cleare, *Coord. Chem. Rev.*, **1974**, *12*, 349.

Titanocene derivatives with thiolate ligands, such as $\text{Cp}_2\text{Ti}(\text{SR})_2$ ²³ and Cp_2TiS_5 ²⁴ (**Fig. 1.10**), have low activity against EhAT, which is ascribed to their hydrophobic character and the strength of the Ti-S bonds. This probably inhibits dissociation of the thiolate ligand and cause interference prohibiting the coordination of the titanium metal to the DNA bases. It is interesting to note that compounds with thiolato and alkoxo ligands, with fluoro substituted aromatic rings (**Fig. 1.11**) had a 100% cure rate against EhAT, at optimal doses²⁵.

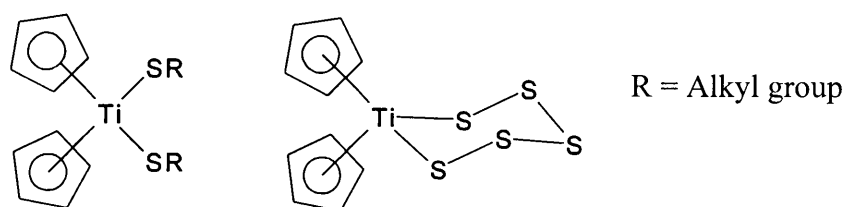


Fig. 1.10. Tumour inactive titanocene derivatives with anionic thiolate ligands.

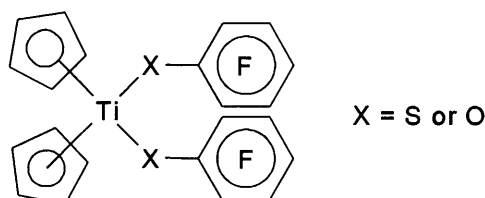


Fig. 1.11. Tumour active titanocene derivatives with aromatic thiolate ligands.

Complexes where only one chloro ligand is replaced by an aromatic thiolato ligand displayed much weaker antitumour properties than the parent compound, titanocene dichloride²⁶. Note that the ligands in (**Fig. 1.12**) consist only of one benzene ring. It was anticipated in this study that replacing a chloro ligand with a heteroaromatic system containing three to four coplanar rings, might increase the antitumour activity, because of a different mechanism than covalent bond formation with DNA bases.

23. H. Köpf, M. Schmidt, *Z. Anorg. Allg. Chem.*, **1965**, *340*, 139.

24. H. Köpf, B. Block, M. Schmidt, *Chem. Ber.*, **1968**, *101*, 272.

25. P. Köpf-Maier, H. Köpf, *J. Organomet. Chem.*, **1988**, *342*, 167.

26. P. Köpf-Maier, S. Grabowski, H. Köpf, *Eur. J. Med. Chem. Chim. Ther.*, **1984**, *19*, 347.

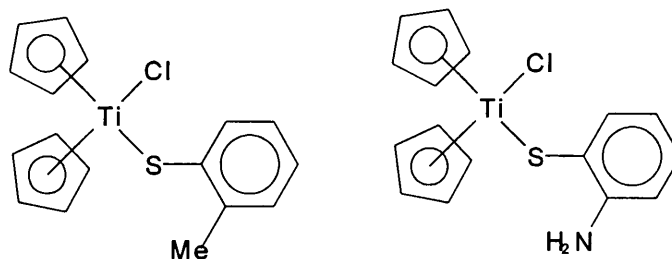


Fig. 1.12. Titanocene derivatives with one anionic thioligand.

(c) The modification of the cyclopentadienyl ligands showed that the activity on tumours is strongly influenced by one substitution on one of the rings. The activity was even more reduced when a second substituent was introduced and full substitution lead to complete inactivity against tumours²⁷. The same result was obtained when one of the rings was replaced by an acido ligand. The replacement of Cp rings by the bulkier η^5 -systems, indenyl or tetrahydroindenyl (**Fig. 1.13**) showed that replacement of one of the rings had little effect on the antitumour activity, but when both were replaced there was a decrease in the cure rate^{27,28}. It is clear that the Cp-rings are necessary because they act as carrier ligands to enable the transport of the active metal centre to intracellular target sites. Reasons for this can be steric effects, changes in solubility properties and altered ring ligand-metal bond stability.

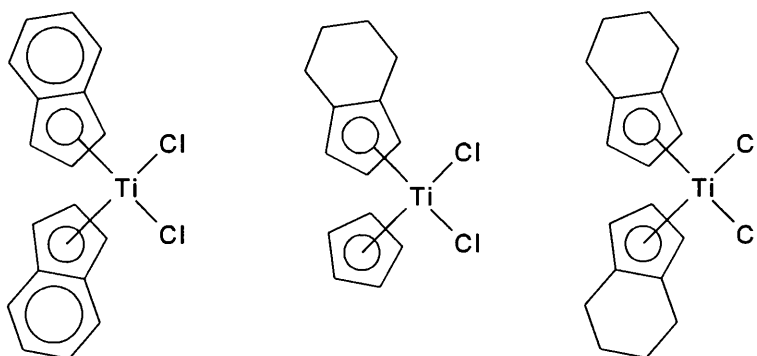


Fig. 1.13. Titanocene derivatives where cyclopentadienyl is replaced by other η^5 -systems.

27. P. Köpf-Maier, W. Kahl, N. Klouras, G. Hermann, H. Köpf, *Eur. J. Med. Chem.*, **1981**, *16*, 275.

28. E. Samuel, R. Setton, *J. Organomet. Chem.*, **1965**, *4*, 156.

Of the metallocene dichlorides, titanocene dichloride is the best investigated because of the low toxicity and high antitumour activity it displayed. In group 3, no metallocenes were screened as antitumour agents. In group 4 only titanocene dichloride was effective²⁹. In group 5 the vanadium analogue was less effective than titanocene³⁰, while the niobium analogue was more effective but had a narrower range for optimal doses³¹. Tantalocene dichloride is much less effective than the other metallocenes³². In group 6, no organometallic compounds of chromium have been screened. Molybdenocene dichloride is less toxic than titanocene but also less effective, though it is more effective than vanadocene³³. Tungstenocene dichloride is of low toxicity but the antitumour effects are limited³¹.

We will now concentrate on titanocene dichloride, since it is the most studied metallocene dihalide complex and displays promising antitumour properties. It is presently in phase II of clinical trials as a drug for colon cancer.

1.4 Carsinostatic Activity of Titanocene Dichloride

There are many simple and complex titanium compounds that display antitumour properties. As early as 1928 an aqueous lipase solution was treated with titanium tetrachloride and used in the treatment of cancer³⁴.

In 1979, Köpf and Köpf-Maier discovered the cytostatic properties of titanocene dichloride after it was tested *in vivo* and *in vitro*²⁹. At optimal doses it was effective against EhAT³⁵, sarcoma

29. H. Köpf, P. Köpf-Maier, *Angew. Chem.*, **1979**, *91*, 509; *Angew. Chem. Int. Ed. Engl.*, **1979**, *18*, 477.

30. P. Köpf-Maier, H. Köpf, *Z. Naturforsch.*, **1979**, *34b*, 805.

31. P. Köpf-Maier, M. Leitner, H. Köpf, *J. Inorg. Nucl. Chem.*, **1980**, *42*, 1789.

32. P. Köpf-Maier, H. Köpf, *Drugs of the Future*, **1986**, *11*, 297.

33. P. Köpf-Maier, M. Leitner, R. Voigtlander, H. Köpf, *Z. Naturforsch.*, **1979**, *34c*, 1174.

34. D. Gardener, *J. Trop. Med.*, **1928**, *31*, 194; *Chem. Abstr.*, **1928**, *22*, 4648.

35. P. Köpf-Maier, W. Wagner, B. Hesse, H. Köpf, *Eur. J. Cancer*, **1981**, *17*, 665.

180³⁶, B16 melanoma and colon 38 adenocarcinoma³⁷, human epidermoid (HEp-2) tumour cells³⁸ and Lewis lung carcinoma³⁹. The drug also showed antitumour activity against human colon, gastro-intestinal carcinomas and lung malignancies, which were xenografted into athymic mice⁴⁰. The activity was dose dependant, but the toxic effects were much lower than that of cisplatin and the metal was concentrated in the liver.

In vivo studies showed that titanocene dichloride is not selective and all treated cells were destroyed⁴¹. The number of dead cells also increased with an increased concentration of the drug. It was also observed that titanocene dichloride damaged the EhAT cells in such a way that they continued to die days after the drug was removed.

1.5 Proposed Mechanism of Action for Titanocene Dichloride

To investigate the mode of action of titanocene dichloride in biological systems, four experiments were used⁴². Firstly, ³H-labelled precursors of DNA, RNA and protein synthesis were incorporated into the acid insoluble fraction of EhAT cells, after *in vivo* and *in vitro* treatment with titanocene dichloride, to reveal the different influences of the precursors on these synthesis pathways. The results showed that the nucleic acid metabolism is much more sensitive to titanocene dichloride than the protein metabolism. DNA synthesis was suppressed significantly while RNA and protein synthesis were slightly and irreversibly inhibited. The *in vitro* interaction of nucleic acids (calf thymus DNA and calf liver RNA) with titanocene dichloride can be demonstrated by monitoring the UV absorptions. The maximum, at 258nm, is

36. P. Köpf-Maier, F. Preiß, T. Marx, T. Klapötke, H. Köpf, *Anticancer Res.*, **1986**, *6*, 33.

37. P. Köpf-Maier, H. Köpf, *Arzneim. Forsch. Drug Res.*, **1987**, *37*, 532.

38. M. S. Murthy, L. N. Rao, L. Y. Kuo, J. H. Toney, T. J. Marks, *Inorg. Chim. Acta*, **1988**, *152*, 117.

39. S. I. Chang, *Yao Hsueh T'ung Pao*, **1981**, *16*, 57.

40. P. Köpf-Maier, *J. Struct. Biol.*, **1990**, *105*, 35.

41. P. Köpf-Maier, W. Wagner, H. Köpf, *Cancer Chemother. Pharmacol.*, **1981**, *5*, 237.

42. H. Köpf, P. Köpf-Maier in *Platinum, Gold and Other Metal Chemotherapeutic Agents*, S. J. Lippard (ed.), ACS Symposium Series, **1983**, 325 and the references therein.

shifted to a lower wavelength and the absorbance of the band increases, which indicates an alteration of the secondary structure of the nucleic acids.

Secondly, the cytokinetic behaviour of EhAT cells, after *in vivo* treatment with optimum doses of titanocene dichloride, was pursued to recognize alterations in the cell transit through the cell cycle. It was noted that there were marked mitotic depressions and cell accumulations in the late S and G₂ phases. Several days after application, the treated cell populations were removed by cells from the defensive system of the host. This *in vitro* treatment caused cell arrests in the G₂ phase after the treatment was stopped and this G₂ block was reversible when low concentrations of the drug were used. This cytokinetic behaviour is similar to that of other cytostatic drugs which are believed to attack DNA, for example, cyclophosphamide, anthracyclines and cisplatin.

Thirdly, cellular events during the inhibition of proliferation were studied by observing light-microscopic and ultrastructural alteration patterns. These morphological studies showed that the treatment of titanocene dichloride induces the formation of giant cells and also the appearance of abnormal mitotic figures. This is also analogous to the cytostatic drugs mentioned in the previous paragraph. The observable alterations after *in vivo* and *in vitro* treatment are the following: chromatin condensation and nuclear segmentation, the development of the morphological signs of an unbalanced cellular growth and later the formation of necroses of the tumour cells. A surprising event is the appearance of complete type-A virus particles few days after treatment. This leads to a massive immigration of cells from the defence system of the host and the final event is the destruction of the tumour cells.

Fourthly, electron energy loss spectroscopy (EELS) studies after *in vivo* and *in vitro* treatment was used to reveal that titanium is mainly enriched in the nuclear heterochromatin. It was also detected in minor concentrations in the euchromatin, the nucleolus and the cytoplasmic ribosomes. No metal atoms were detected in other regions of the cell.

From the above it is clear that the metal complexes attack the nucleic acids. The interactions of

metallocenes with DNA have recently been reviewed⁴³. Further studies included investigations of the binding of metallocenes to the potential donor sites of 2'-deoxynucleoside 5'-monophosphates (**Fig. 1.14**), such as the nitrogen atoms of the nucleobases and the oxygen atoms of the phosphate groups, as seen in the molybdenocene complexes in **Fig. 1.15**⁴⁴. Also studied was the direct interaction of titanocene dichloride with bases of nucleic acids by formation of covalent bonds. In literature there are a few examples of purine and uracil complexes which show that the titanocene moiety can be attached to purine and pyrimidine bases^{45,46,47,48}. For titanocene dichloride, complexation to nucleobases in water is weak and interactions to nucleobases at pH 2-4 happen with simultaneous binding to the base and the oxygen of the phosphate⁴⁹. These complexes cannot be characterized due to the lability of the Cp-Ti bond. At pH > 6, almost no

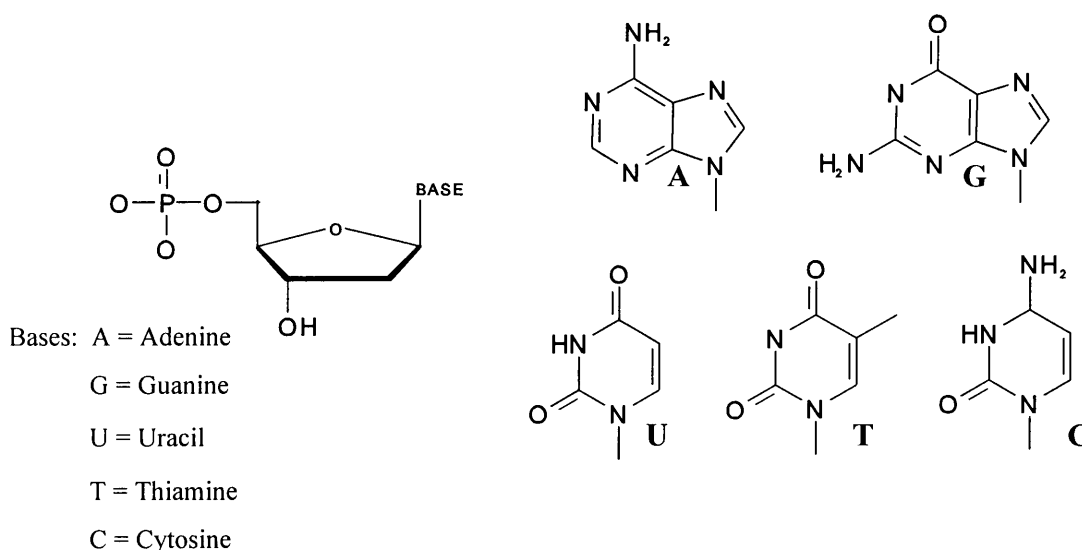


Fig. 1.14. Structures of the 2'-deoxynucleoside 5'-monophosphates.

43. L. Y. Kuo, H. Andrew, T. J. Marks in *Metal Ions in Biological Systems*, A. Sigel, H. Sigel (eds.), Marcel Dekker, Inc., New York, 1996, 33, 53.

44. B. Lippert in *Progress in Inorganic Chemistry*, S. J. Lippard (ed.), John Wiley and Sons, New York, 1989, p 1.

45. D. Cozac, A. Mardhy, A. Morneau, *Can. J. Chem.*, 1986, 64, 751.

46. A. L. Beauchamp, F. Bélanger-Garlépy, A. Mardhy, D. Cozac, *Inorg. Chim. Acta*, 1986, 124, 23.

47. A.L Beauchamp, D. Cozac, A. Mardhy, *Inor. Chim. Acta*, 1984, 92, 191.

48. D. Cozac, A. Mardhy, M. J. Olievier, A. L. Beauchamp, *Inorg. Chem.*, 1986, 25, 2600.

49. J. H. Murray, M. M. Harding, *J. Med. Chem.*, 1994, 37, 1936.

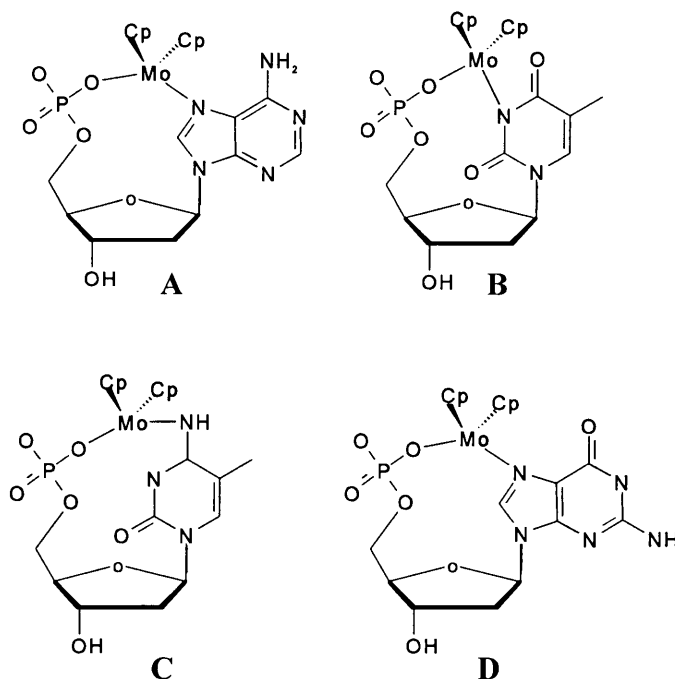


Fig. 1.15. Structures of Cp_2M^{2+} binding modes to (A) 5'-dMAP, (B) 5'-dTTP, (C) 5'-dCMP and (D) Me(5'-dGMP) as observed for the $\text{Cp}_2\text{Mo}^{2+}$ fragment.

complexation of aqueous titanocene dichloride to nucleotides or nucleobases was observed. Two of these complexes were synthesized and characterized in nonaqueous media. In the $\text{Cp}_2\text{Ti(IV)Cl(purinato)}$ complex⁴⁷ (**Fig. 1.16**), the Cp_2TiCl^+ moiety binds to the N9 position and in the $\text{Cp}_2\text{Ti(III)-(theophyllinato)}$ complex⁴⁸ (**Fig. 1.16**), the Cp_2Ti^+ moiety simultaneously binds to the O6 and the N7 sites. In both complexes the nucleobase ligand planes are situated in the equatorial plane of the $\text{Cp}_2\text{Ti}^{2+}$ wedge.

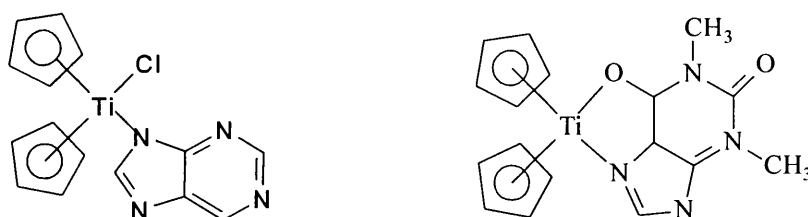


Fig. 1.16. Chlorobis(η^5 -cyclopentadienyl)purinatotitanium(IV) and Chlorobis(η^5 -cyclopentadienyl)theophyllinatotitanium(III).

In aqueous medium titanocene dichloride is undergoing Cp protonolysis with a half-life of about 57h⁵⁰ (Fig. 1.17). In unbuffered solution, to be a good antitumour agent, compounds are expected to have stable M-Cp bonds over a period of days. The ring loss for titanocene dichloride is also extensive at near physiological pH values and the compound precipitates as “Ti(η⁵-C₆H₅)_{0.31}O_{0.30}(OH)”, with the loss of 1.69 equivalents of CpH per titanium. For chloride hydrolysis (Scheme 1.1) the rate of the first chloride released is too fast to be measured and when the dissolution of metallocene dichloride is complete, [Cl⁻]/[M] > 10, suggesting that chloride aquation is closely connected with the dissociation process⁵¹. The aquated species of Cp₂M(H₂O)₂²⁺ were investigated further and the pK_a values show that its acidity declines as M becomes more electron rich.

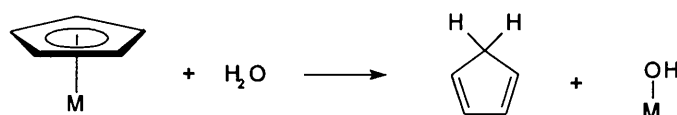
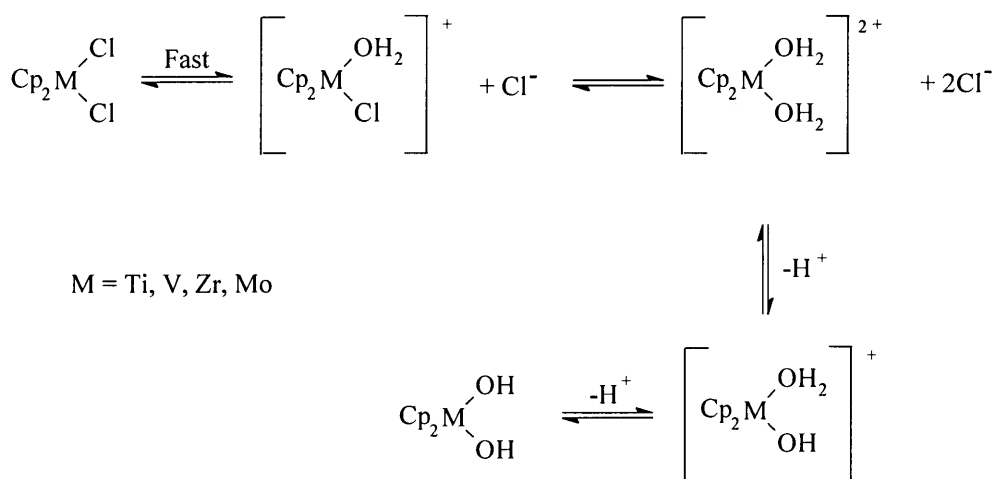


Fig. 1.17. Protonolysis of cyclopentadienyl.



Scheme 1.1.

50. J. H. Toney, T. J. Marks, *J. Am. Chem. Soc.*, 1985, 107, 947.

51. L. Y. Kuo, M. G. Kanatzidis, M. Sabat, A. L. Tipton, T. J. Marks, *J. Am. Chem. Soc.*, 1991, 113, 9027.

Inductive coupled plasma (ICP) spectroscopy was used to examine $\text{Cp}_2\text{Ti}(\text{H}_2\text{O})_2^{2+}$ with salmon testis DNA. At pH 5.3 and 7.0, DNA-bis(cyclopentadienyl)titanium(IV) and DNA-mono(cyclopentadienyl)titanium(IV) adducts, with unknown binding modes were formed, respectively⁵². These adducts were stable at neutral pH for up to 48h.

The Cp ligands of metallocenes make them too large to fit into the major groove, and as a result, no binding in the major groove of DNA is expected^{52,53}. When the metallocene is located at the 5' terminus of the DNA helix, minimum nonbounded contacts are encountered because of the binding through the terminal phosphate and a nucleobase.

1.6 Intercalation

Several modes of interaction of transition metal complexes with DNA have been recognized⁵⁴. From the above we saw that one of the important binding modes of transition metal complexes to DNA is covalent bond formation with base, sugar and phosphate heteroatoms. A second type does not form covalent bonds with the metal, but rely on intermolecular interactions such as hydrogen bonding and π -stacking as found in intercalation. **Fig. 1.18** shows structures which display covalent bonds of *cis*-diammineplatinum(II)²⁺ to the N7 of neighbouring guanine, the formation of an osmate ester with ribose hydroxyl groups, and electrostatic interaction between $[\text{Mg}(\text{H}_2\text{O})_6]$ and guanosine phosphate. Also illustrated is the $[\text{Co}(\text{NH}_3)_6]^{3+}$ complex, hydrogen bonded simultaneously to the guanine base (G10) and phosphate backbone (P9)⁵⁵ and an example of a metal complex, (terpyridyl)(2-hydroxyethanethiolate)platinum(II), which intercalates into the grooves between the base pairs⁵⁶. In this section we will discuss factors facilitating intercalation, which has two possible modes for transition metals. Intercalation can be affected by ligands and may include the transition metal or not. The term metallointercalation is used to describe intercalation which includes the metal.

52. M. L. McLaughlin, J. M. Cronan, Jr., T. R. Schaller, R. D. Snelling, *J. Am. Chem. Soc.*, **1990**, *112*, 8949.

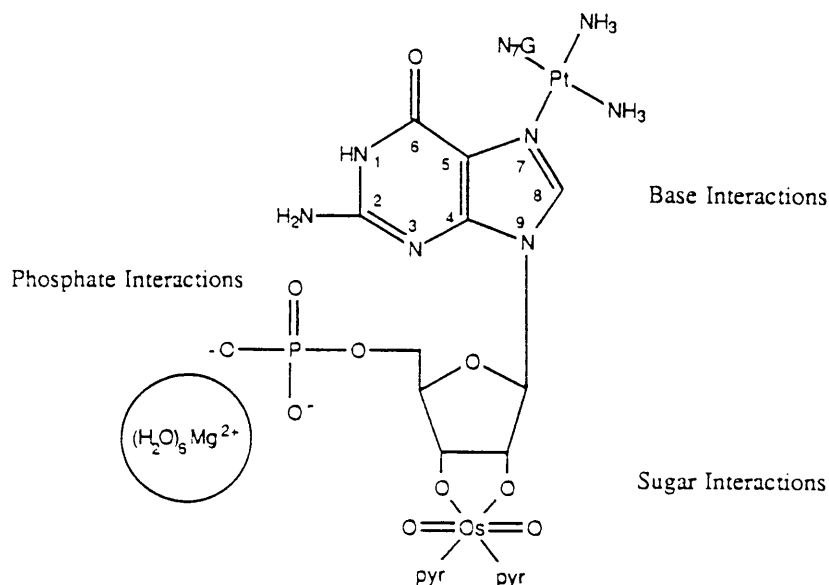
53. M. M. Harding, G. J. Harden, L. D. Field, *FEBS Lett.*, **1993**, *322*, 291.

54. J. K. Barton, *Progress in Inorg. Chem.: Bioinorg. Chem.*, **1990**, *38*, 413.

55. R. V. Gessner, G. J. Quigley, A. H. -J. Whang, G. A. Van der Marel, J. H. Van Boom, A. Rich, *Biochemistry*, **1985**, *24*, 237.

56. A. H. -J. Whang, J. Nathans, G. A. Van der Marel, J. H. Van Boom, A. Rich, *Nature (London)*, **1978**, *276*, 471.

COVALENT



NON-COVALENT

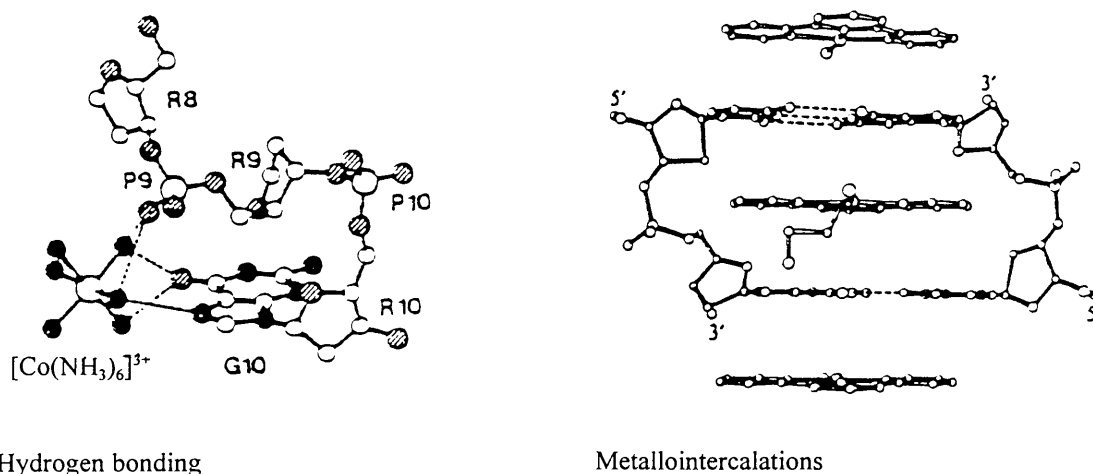


Fig. 1.18. Binding modes of transition metal complexes to DNA. (Reproduced from Ref. 54)

One of the most important cytostatic mechanisms of coplanar polycyclic compounds is their intercalation with DNA⁵⁷. Intercalation is understood as the insertion of a chromophoric (planar) part of a molecule between two stacked base pairs (Fig. 1.19). This causes basically two changes

57. U. Pindur, M. Haber, K. Sattler, *J. Chem. Ed.*, 1993, 70, 263.

in DNA. Firstly, the DNA tertiary structure (helix) is lengthened and somewhat unwound, while the primary and secondary structures remain intact. With intercalation, the average separation between two stacked base pairs increases from 3.4\AA to $7\text{-}8\text{\AA}$. At biochemical level a blockage of the matrix functions occurs. Secondly, there is a significant change in the torsional angles of the sugar phosphate skeleton. This causes reading errors in the replication process and cell proliferation comes to a standstill. Intercalative binding in DNA is believed to arise from electrostatic, van der Waals and hydrophobic forces. For an optimal intercalation, the planar part of the molecule (the chromophore) must have a minimum surface of 28\AA^2 (optimum at three to four condensed five or six membered rings).

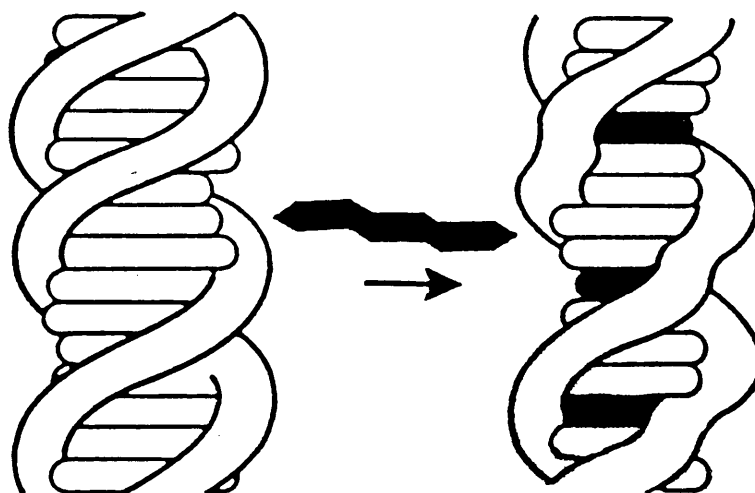


Fig. 1.19. Schematic representation of intercalation between stacked base pairs of DNA. (Reproduced from Ref. 57)

For carefully designed transition metal complexes, intercalation is also possible. They are usually small molecules containing flat heterocycles as ligands, which can be stacked between the base pairs. For metallointercalation it is important that the metal must be in the same plane as the planar ligand. It is important to note that intercalation is not restricted only to flat compounds. Partial intercalation is possible through two modes of intercalation. Firstly, surface or groove bound interaction in the minor groove and secondly, insertion into the major groove of DNA.

2. Aim of Study

2.1 Aim and Motivation of Study

In this study, new transition metal complexes, which could potentially display antitumour properties, were designed, synthesized and characterized. In the design of the complexes, the aim was to try and incorporate ligands, which could be easily substituted to form covalent bond sites, as well as contain a planar polycyclic ring system for intercalation. To achieve this goal the complexes will have to meet certain requirements which are: (**Fig. 2.1**)

1. The metal centre (**M**) must be in a high oxidation state to prevent oxidation in the body.
2. A labile ligand (**X**), which will dissociate readily to leave a free coordination site on the metal to allow for covalent bonding to DNA.
3. A planar heteroaromatic ligand (**R**) with three to four rings to intercalate between base pairs.
4. Some stable stopper ligands to direct the intercalation and covalent bonding.
5. The orientation of the ring plane with respect to the other ligands is important and special attention should be paid to get the correct structural features, to achieve the above goals.

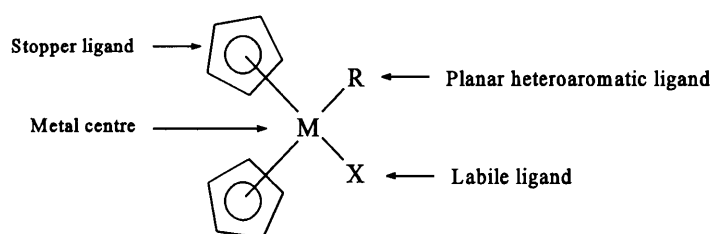


Fig. 2.1. A designer model of the features of a new series of antitumour complexes.

As titanocene dichloride is a very versatile precursor, which can be used to synthesize a great spectrum of new complexes, it was clear that it would be possible to combine labile ligands with polycyclic condensed heteroaromatic rings. Also, titanium being a “body friendly” metal, made it an attractive metal to utilize. Alternatively, CpTiCl_3 could have been used, but for this study Cp_2TiCl_2 was selected because of its stability and proven success in the field of drug design.

Therefore, the covalent binding properties of titanocene dichloride are to be combined with the intercalation features of new aromatic ring ligands, to synthesize a series of compounds, which could potentially display antitumour properties. The mechanism of these complexes with DNA is expected to be different from that of titanocene dichloride, because only one labile ligand will be available for dissociation to allow for covalent bond formation between the metal and DNA. By contrast, no cross-links are expected as is the case for titanocene dichloride, where two chloro ligands dissociate to give vacant sites for covalent bonding.

Titanocene chloride will end up as a σ -substituent after replacing one or both chloro ligands (**X**), with monolithiated ring or monolithiated thiolate ligands from the chalcathrene family of heteroaromatic substrates (**R**) (**Fig. 2.2**). This will result in two classes of complexes (**Fig.2.3**). The first type has direct metal-carbon bond to the heteroaromatic ligand and second a sulfur atom as spacer between the metal and the carbon of the heteroaromatic ligand. The latter will be more flexible than the first, because of rotation of the ring around the sulfur bonds of the spacer unit. Thus, it is expected that these may intercalate more effectively with DNA.

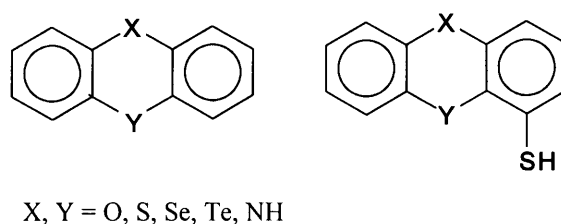


Fig. 2.2. Chalcathrenes and chalcathrenethiols.

The site and effectiveness of lithiation of these ligands, as well as their subsequent reactivity with titanocene dichloride, will be studied. The resulting complexes will be compared with each other in terms of their geometries, and possible interactions with DNA will be proposed and discussed. The degree by which the aromatic character of the rings in the new complexes will be affected, due to the metal-carbon bond in the first class, will also be studied with different methods of spectroscopy. Structurally, features and properties will be discussed, using NMR spectroscopy, mass spectrometry and as far as possible, X-ray crystallography.

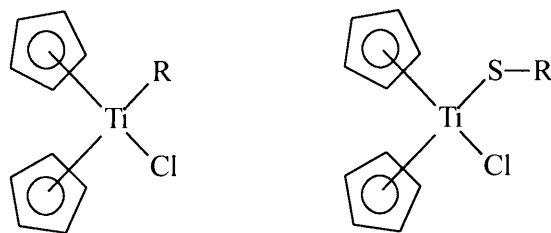


Fig. 2.3. The two types of complexes: One with a direct metal-carbon bond and the other with a sulfur atom as spacer. (R=Heteroaromatic ligand)

2.2 The Ligands

In our laboratories, we found that $[\text{TiCp}_2(\text{SDbT})\text{Cl}]$ displayed enhanced antitumour properties *in vivo* towards B16 sarcoma tumours, compared to that of $[\text{TiCp}_2(\text{SBT})\text{Cl}]$ (SDbT = dibenzothiénylthiolate, SBT = benzothiénylthiolate), while $[\text{TiCp}_2(\text{DbT})\text{Cl}]$ compared to $[\text{TiCp}_2(\text{BT})\text{Cl}]$ (DbT = dibenzothiényl, BT = benzothiényl), showed greater inhibition *in vitro* of Hela cell growth (**Fig. 2.4**). Therefore, it was decided to use thianthrene as a possible intercalator, as it represents a substrate with three condensed rings. Dibenzodioxin was also used to make a comparative study between the two types of heteroatoms in the rings, as they display very different structural features with regard to the planarity of the rings. It was also decided to use the thiolate derivatives of these two compounds, as similar compounds showed more

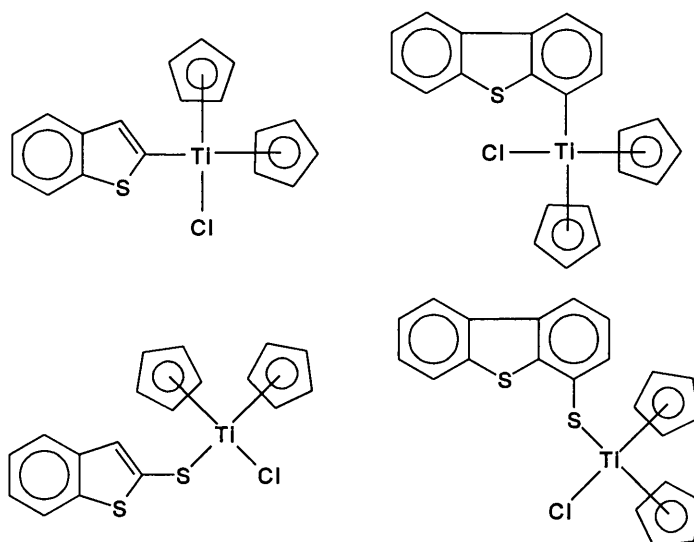


Fig. 2.4. Titanocene derivatives synthesized as possible antitumour agents in our laboratories.

promising antitumour properties *in vivo* than the derivatives without the sulfur atom¹.

Dibenzo[1,4]dioxin (**Fig. 2.5**) was first mentioned in the literature by Cullinane in 1936². Since then, dibenzodioxin and its derivatives were studied frequently, but not much is known about its biological activities. It is known to be poisonous with a LD₅₀ value of 1120mg/kg. Under standard conditions, dibenzodioxin is very stable and is easily lithiated at the 1-position by *n*-BuLi and can also be double lithiated³. It has been characterized by various methods, which include ¹H and ¹³C NMR spectroscopy⁴, mass spectrometry⁵ and X-ray crystallography⁶.

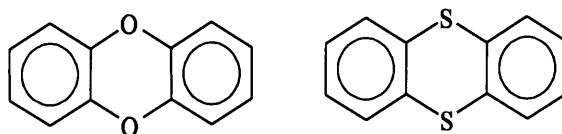


Fig. 2.5 Dibenzo[1,4]dioxin and thianthrene.

Thianthrene (**Fig. 2.5**) was first synthesized in 1948 by Macallum and its chemistry is well documented in literature⁷. In 1990 an excellent review on thianthrenes was published by Joule⁸. Like dibenzodioxin, it is stable at normal room conditions and is also deprotonated at the 1-position, applying the lithiation conditions used for dibenzodioxin. However, it is less reactive than dioxin and cannot be double lithiated easily⁹. Very little is known about its possible applications in the pharmaceutical industry. It has also been characterized by various methods,

-
1. R. Meyer, *Titanium, Molybdenum and Platinum Complexes with Potential Antitumour Properties*, Ph. D. (Chemistry) Thesis, University of Pretoria, 1998.
 2. N. M. Cullinane, *Rec. Trav. Chim. (J. R. Neth. Chem. Soc.)*, **1936**, 55, 881.
 3. B. D. Palmer, M. Boyd, W. A. Denny, *J. Org. Chem.*, **1990**, 55, 438-441.
 4. M. E. Amato, A. Grassi, K.J. Irolic, G.C. Pappalardo, L. Radics, *Organometallics*, **1993**, 12, 775.
 5. N. P. Buu-Hoi, G. Saint-Ruf, M. Mangane, *J. Heterocycl. Chem.*, **1972**, 9, 691.
 6. P. Singh, J. D. McKinney, *Acta Cryst.*, **1978**, B34, 2956.
 7. A. D. Macallum, *J. Org. Chem.*, **1948**, 13, 154.
 8. J. A. Joule, *Adv. Heterocycl. Chem.*, **1990**, 48, 301-393.
 9. H. Gilman, C. G. Stuckwisch, *J. Am. Chem. Soc.*, **1943**, 65, 1461-1464.

which include ^1H and ^{13}C NMR spectroscopy¹⁰, mass spectrometry¹¹ and X-ray crystallography¹².

No information could be found on dibenzo[1,4]dioxinethiol and thianthrenethiol (**Fig. 2.6**) and their synthesis and characterization will be discussed in Chapters 5 and 6, respectively.

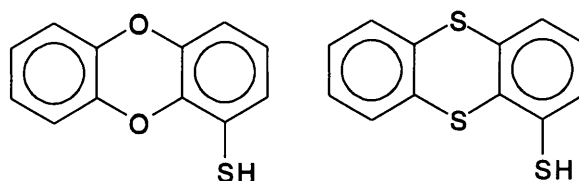


Fig. 2.6. Dibenzo[1,4]dioxinethiol and thianthrenethiol.

2.3 Construction of Thesis

In Part II the chemistry of the new complexes will be discussed. Each reaction will be treated in a separate chapter, which will make it easier to distinguish between the results and also to compare them at a later stage. A scheme of the planned route for the synthesis of each compound will be given and the results discussed. The purity of the compounds will be tested by chemical analysis and the structures and features of the products will be obtained by using mass spectrometry and techniques of NMR spectroscopy.

In Part III the complexes will be compared with each other in terms of geometry and these similarities and differences will be used to postulate and discuss their possible antitumour properties. Some suggestions will be made for future extension of this work.

In Part IV the experimental procedures for the compounds are given.

10. M. E. Amato, A. Grassi, K.J. Irolic, G.C. Pappalardo, L. Radics, *Organometallics*, **1993**, *12*, 775.

11. G. Saint-Ruf, J. Servion-Sidoine, J. P. Cioc, *J. Heterocycl. Chem.*, **1974**, *11*, 287.

12. K. L. Gallaher, S. H. Bauer, *J. Chem. Soc. Faraday Trans. 2*, **1975**, *71*, 1173.

Part II

Synthesis, Characterization and Discussion

Information Concerning all Complexes	26
3. Titanocene Complexes with Dibenzodioxinyl as Ligand	27
4. Titanocene Complexes with Thianthrenyl as Ligand	45
5. Titanocene Complexes with Dibenzodioxin-1-thiolate as Ligand	54
6. Titanocene Complexes with Thianthrene-1-thiolate as Ligand	67
7. Titanocene Complexes with Thianthrene as Ring-Opened Ligand	76

Information Concerning all Complexes

The lithiation of the heteroaromatic rings was done by making a TMEDA-LiBu(THF) complex¹. This method produces better yields than without TMEDA. It is important to note that dibenzodioxin and dibenzodioxinthiol are much more reactive than thianthrene and thianthrenethiol and therefore the reaction times for the first mentioned are half of that needed for the last mentioned.

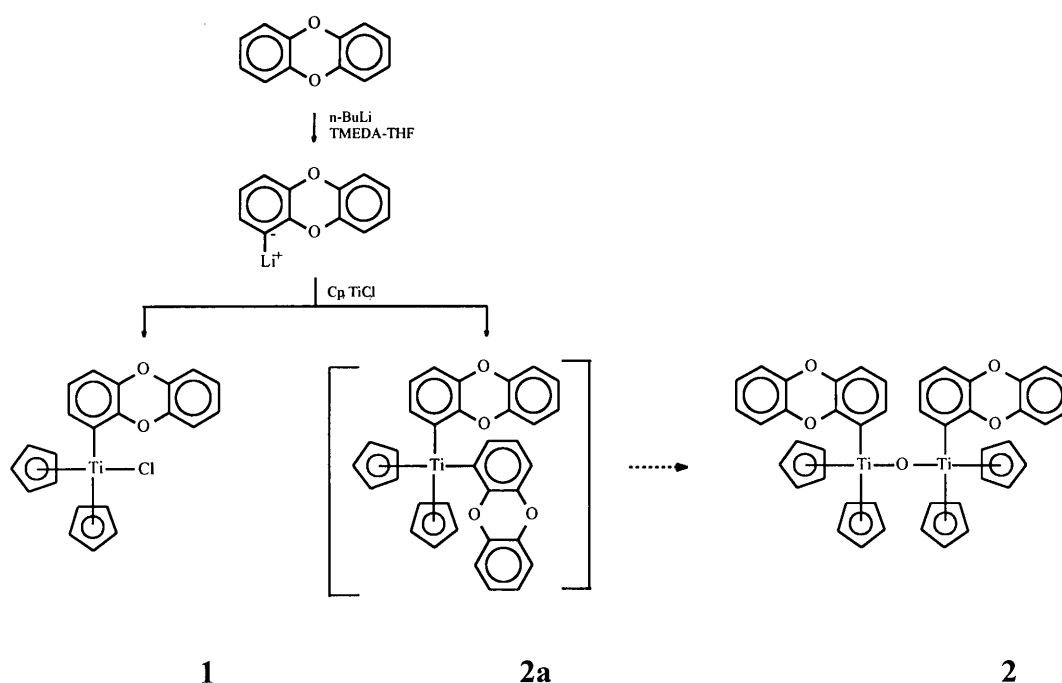
The products in this chapter were characterized as far as possible by mass spectrometry, ¹H and ¹³C NMR spectroscopy, 2D-experiments in NMR spectroscopy and the molecular structure of [TiCp₂(Db)Cl] **1** was determined by X-ray crystallography. The ¹H NMR spectra for all the new compounds were included, because of the overlapping of the aromatic protons. Although the chemical shift ranges of most of these complexes are very similar, the spectra have different characteristic patterns.

1. L. Brandsma, H. Verkuijsse, *Preparative Polar Organometallic Chemistry 1*, Springer-Verlag, Berlin, Heidelberg, 1987, 18.

3. Titanocene Complexes with Dibenzodioxinyl as Ligand

3.1 Synthesis

Dibenzo[1,4]dioxin [DbH] was readily deprotonated by BuLi and a high yield of the metallated product was obtained when the BuLi-TMEDA complex was used². On addition of titanocene dichloride to the lithiated agent, the reaction immediately changed colour from bright red to orange-brown. The solvent was removed and column chromatography gave a yellow fraction before the major fraction, which was orange (**Scheme 3.1**).

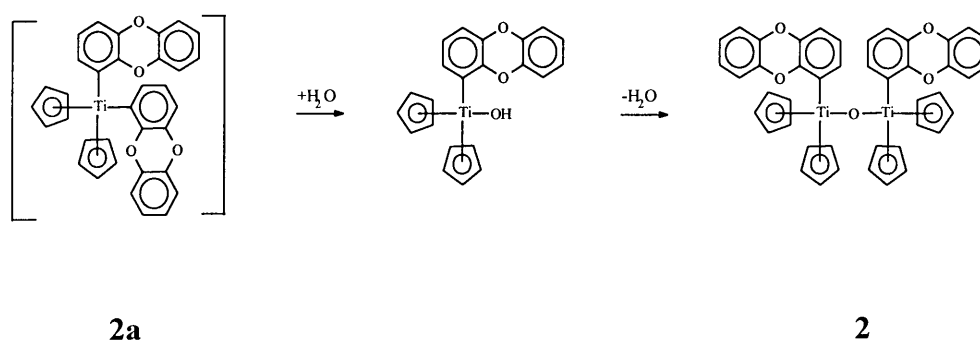


Scheme 3.1

2. B. D. Palmer, M. Boyd, W. A. Denny, *J. Org. Chem.*, 1990, 55, 438.

The expected product, the orange fraction, was characterized as chlorobis(cyclopentadienyl) (dibenzodioxinyl)titanium(IV) **1** [TiCp₂(Db)Cl]. Solvent mixtures such as dichloromethane-hexane or toluene-hexane did not produce crystals of a good enough quality for X-ray structural studies. After many attempts, the slow crystallisation from a THF-hexane mixture, afforded crystals suitable for a single crystal X-ray determination.

The yellow product, bis(cyclopentadienyl)bis(dibenzodioxinyl)titanium(IV) **2a** [TiCp₂(Db)₂] was very unstable and NMR studies showed decomposition with regeneration of the free ligand. The solution slowly turned black every time the compound was dissolved in a chlorinated solvent. In the end **2a** was filtered successfully with benzene. The yellow product **2a** converted to a second yellow product, of which the composition was verified by mass and NMR spectra. The oxygen bridged dinuclear complex, (μ-oxo)bis{bis(cyclopentadienyl)(dibenzodioxinyl) titanium(IV)} **2** [{TiCp₂(Db)}₂O], fitted the data. The bis(dibenzodioxinyl) complex **2a** is very unstable and slowly reacts with water from the column material. As a result, the water protonates one of the Db ligands, leading to the release of DbH and the formation of a hydroxo complex (**Scheme 3.2**). Two hydroxo complexes combined by water elimination to give the oxobridged dinuclear complex **2**. During the conversion water acts as catalyst.



Scheme 3.2

A possible reason why **2a** could not be isolated, is the steric hindrance. A space filling model revealed that there is not enough space for both ligands to co-exist in addition to the two Cp rings around one titanium atom (**Fig. 3.1**). Furthermore, the formation of **2** is proof of the fact that in the reaction mixture, **1** has a highly activated chloro ligand, which in the presence of Li[Db] will lead to the displacement of the second chloro ligand.

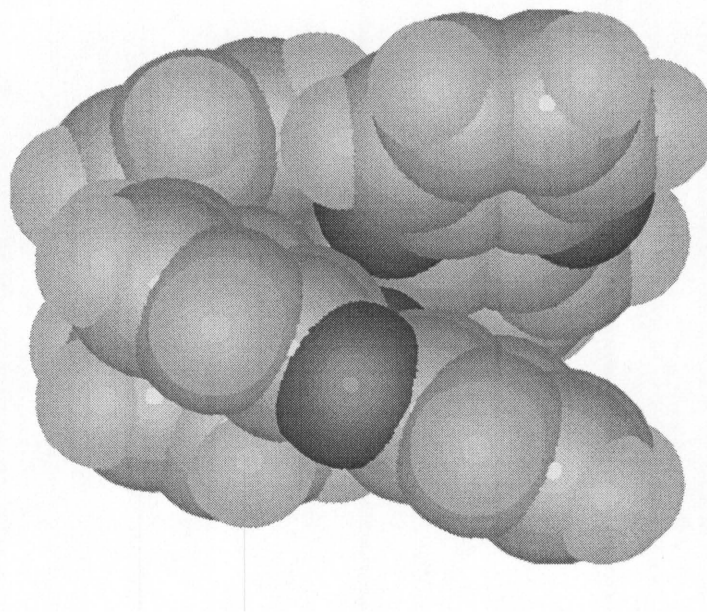


Fig. 3.1. A computer generated model of $[\text{TiCp}_2(\text{Db})_2]$.

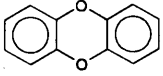
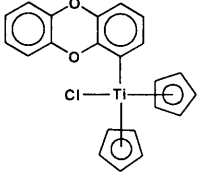
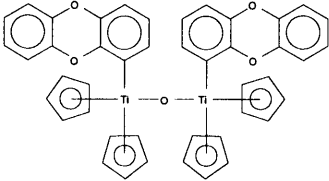
3.2 Characterization

Mass spectrometry

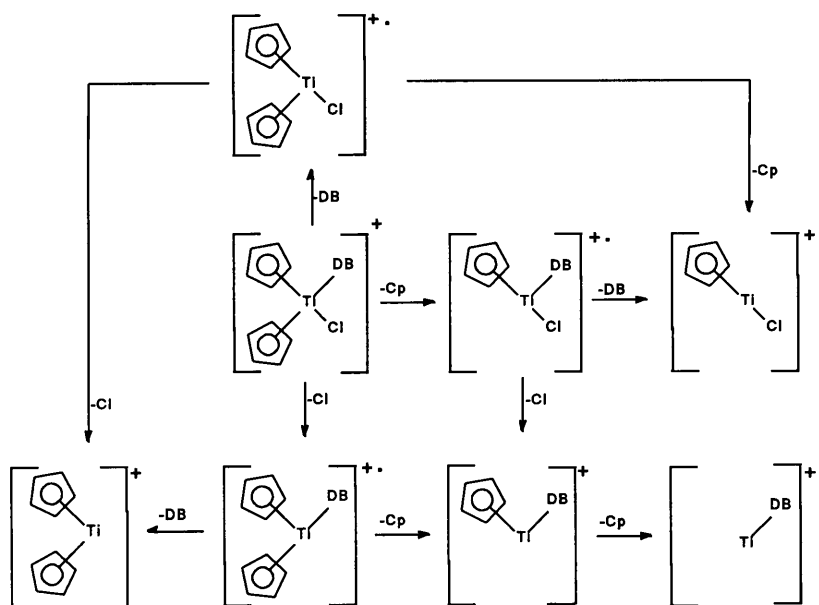
The mass spectra for dibenzodioxin³, **1** and **2** are summarized in **Table 3.1**. The intensity of the molecular ion peak for **1** is low (3%), which means that the compound is relatively unstable under the experimental conditions during the measurement. The dominant pathway (96%), corresponds to the initial fragmentation of a chloro ligand from the molecular ion. According to other fragment ions, several possible pathways exist, as shown in **Scheme 3.3**. One pathway shows the initial loss of a chloro ligand, followed by the loss of the Db ligand or one or both Cp ligands. In the second, the Cp is lost first, followed by the Db ligand or the chloro ligand and then a Cp ligand. In another pathway the loss of the Db ligand is followed by that of a chloro ligand or a Cp ligand. The fragmentation pattern for dibenzodioxin is also observed in the lower part of the spectrum for **1**.

3. N. P. Buu-Hoï, G. Saint-Ruf, M. Mangane, *J. Heterocycl. Chem.*, 1972, 9, 691.

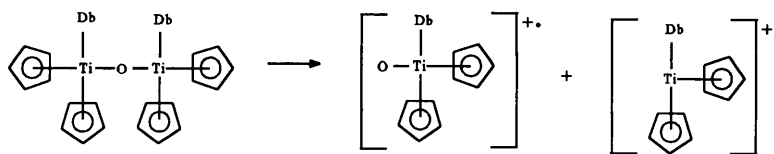
Table 3.1. Mass spectral data for dibenzodioxin³, [TiCp₂(Db)Cl] and [{TiCp₂(Db)}₂O].

	 1	 2
Mass peaks, m/z (I%)	Mass peaks, m/z (I%)	Mass peaks, m/z (I%)
184 (100) [M] ⁺ 156 (4) [M-CO] ⁺ 155 (6) [M-CHO] ⁺ 128 (24) [M-2CO] ⁺ 92 (10) [M/2] ⁺	396 (3) [M] ⁺ 361 (96) [TiCp ₂ (Db)] ⁺⁺ 366 (13) [Db-Db] ⁺ 331 (10) [TiCp(Db)Cl] ⁺⁺ 295 (29) [TiCp(Db)] ⁺ 248 (23) [TiCp ₂ Cl ₂] ⁺ 230 (22) [Ti(Db)] ⁺⁺ 213 (12) [TiCp ₂ Cl] ⁺⁺ 184 (100) [DbH] ⁺ 178 (7) [TiCp ₂] ⁺ 148 (32) [TiCpCl] ⁺	738 * [M] ⁺ 430 (53) [Ti(Db) ₂ O] ⁺ 378 (1) [TiCp ₂ (Db)O] ⁺⁺ 366 (3) [Db-Db] ⁺ 361 (3) [TiCp ₂ (Db)] ⁺⁺ 312 (3) [TiCp(Db)O] ⁺⁺ 247 (6) [Ti(Db)O] ⁺ 184 (13) [DbH] ⁺

* Not observed


Scheme 3.3.

Cleavage of **2** into two fragments can be seen in **Scheme 3.4**. The molecular ion peak was not observed.



Scheme 3.4.

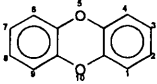
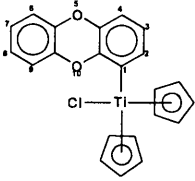
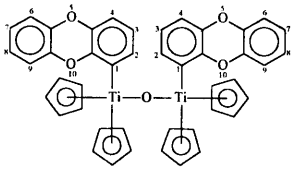
¹H NMR Spectroscopy

The data of the ¹H NMR spectra for dibenzodioxin⁴, **1** and **2** is summarized in **Table 3.2**. According to Amato, *et al*⁴ there are upfield shifts for the H1, H4, H6 and H9 in DbH, when compared with the other chalcantrenes, due to the modification of the paramagnetic term by oxygen. In the heteroaromatic ligand of **1**, the protons were shifted upfield, with the greatest shifts recorded for the ring coordinated to titanium. Lithiation of the ligand caused an increase of electrondensity on the ligand, while addition of the titanium fragment decreased the electrondensity. Thus the titanium removed less electrondensity than was obtained through lithiation. Hence an initial upfield shift of the protons (Li) and then a downfield shift (Ti) was observed, with the protons closest to the metal fragment being influenced most.

The mechanism for this shift of electrondensity can be explained in two possible ways. The first by a σ -inductive effect where Ti is the more electropositive element in the bond with a carbon. This results in a polarized σ -bond between the metal and carbon, C1, with the electrondensity shifted more towards the side of the carbon, leaving the metal partially electropositive and the carbon partially electronegative. The second mechanism involves a π -resonance effect whereby the empty d-orbitals of titanium act as π -acceptors. This causes electrondensity to shift to the metal, leaving the carbon atom with a positive charge. This positive charge is spread over the rest of the molecule as can be seen in **Fig. 3.2**.

4. M. E. Amato, A. Grassi, K.J. Irolic, G.C. Pappalardo, L. Radics, *Organometallics*, 1993, 12, 775.

Table 3.2. ¹H NMR spectroscopic data for dibenzodioxin⁴, [TiCp₂(Db)Cl] and [{TiCp₂(Db)}₂O].

			
		1	2
Chemical Shift, δ (ppm) [†]			
H1	6.81	---	---
H2	6.85	6.74 (dd)	6.34 and *7.05 (dd)
H3	6.85	6.55 (dd)	6.72 and *6.69 (t)
H4	6.81	6.48 (dd)	6.29 and *6.62 (dd)
H6	6.81	6.67-6.70 (multiplet)	6.80-6.95 (multiplet)
H7	6.85		
H8	6.85		
H9	6.81		
Cp	---	6.43 (s)	6.05, *6.08 and 6.27 (s)
Coupling Constant, ⁿ J _{H-H} (Hz)			
J ₁₂	8.0	---	---
J ₁₃	1.5	---	---
J ₁₄	0.4	---	---
J ₂₃	7.5	7.4	8.2 and *7.5
J ₂₄	1.5	1.6	1.5 and *1.6
J ₃₄	8.0	7.7	8.2 and *7.5
J ₆₇	8.0	□	□
J ₆₈	1.5	□	□
J ₆₉	0.4	□	□
J ₇₈	7.5	□	□
J ₇₉	1.5	□	□
J ₈₉	8.0	□	□

[†] d¹-CDCl₃ used as solvent.

□ Difficult to calculate, due to multiplet.

* Two sets of values due to two heteroaromatic ring systems.

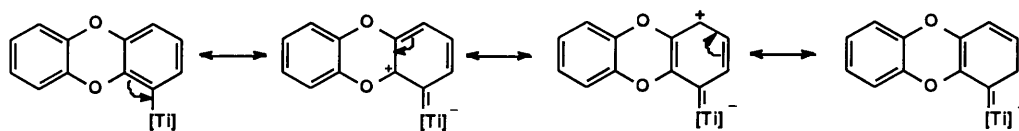


Fig. 3.2. The π -inductive effect in $[\text{TiCp}_2(\text{Db})\text{Cl}]$.

The other ring was less influenced, except for H9 which has a $\Delta\delta \pm 0.25$ ppm downfield from its expected value. A possible explanation is an interaction between one of the oxygen atoms of Db and titanium. Titanium is a d^0 species and has 16 valence electrons in its coordination sphere in **1**, which leaves one available coordination site on the metal. This site can be occupied by an interaction between the lone pair of an oxygen and the metal centre (**Fig. 3.3**). Examples of this effect are known in literature and was shown by a crystal structure of $[\text{TiCp}_2(\text{CH}_2\text{OCH}_3)\text{Cl}]^5$.

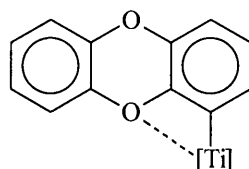


Fig. 3.3. The interaction between an oxygen atom of Db and titanium.

The chemical shifts for H6-H9 were difficult to assign due to their overlapping signals (**Fig. 3.4**), but were not strongly affected. From the values of the free ligand, it can only be said that H6 should be more upfield than H7 and H8. The two Cp rings resonate as a singlet due to the similar chemical environments. In **1** there is more electrondensity on the metal fragment, compared to titanocene dichloride, which causes a downfield chemical shift of the Cp rings.

The spectrum for **2** is much more complex (**Fig. 3.5**). There are two different signals for the four Cp rings. One shows a strong singlet which indicates that the two Cp rings are free to rotate and the second is split into two singlets with a ratio of 4:1, about 0.2ppm upfield from the first signal. This means that on these Cp rings one proton is influenced in each instance. The most

5. G. Erker, R. Schlund, C. J. Krüger, *J. Organomet. Chem.*, 1988, 338, C4.

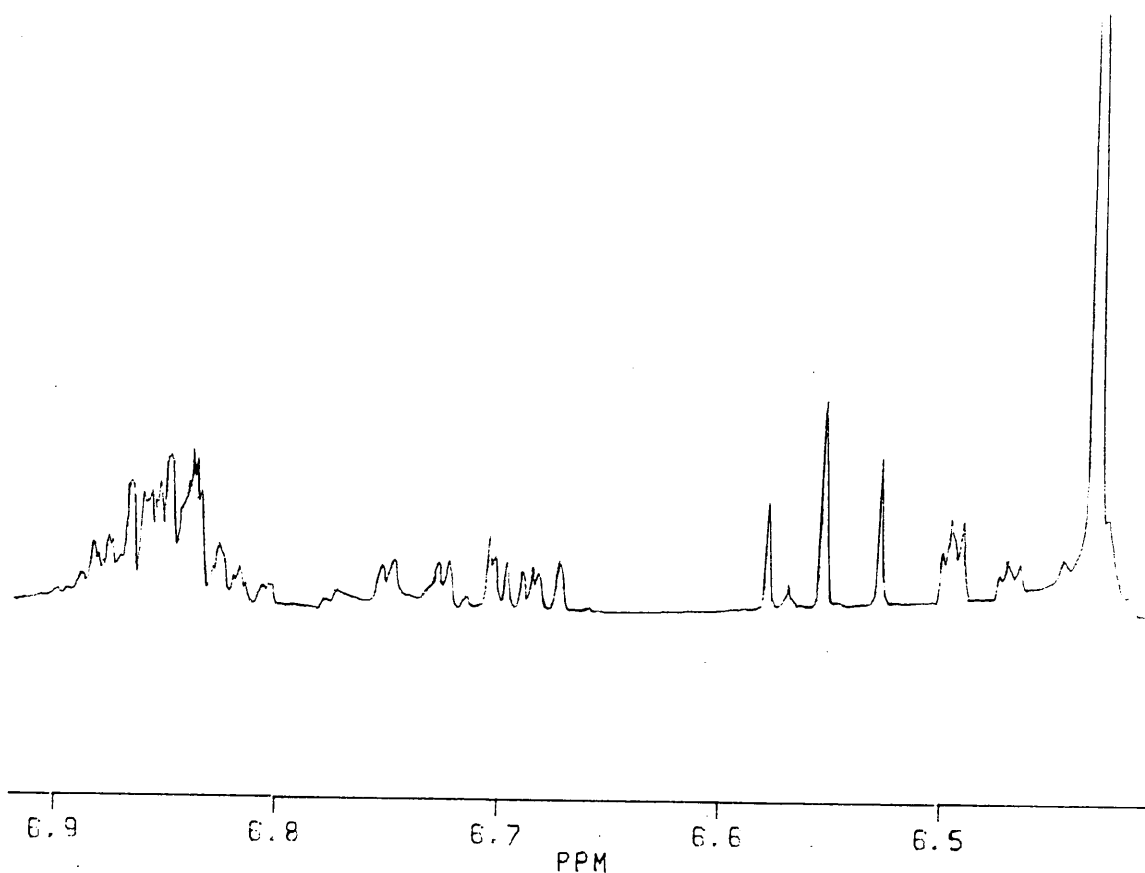


Fig. 3.4. The ^1H NMR spectrum of $[\text{TiCp}_2(\text{Db})\text{Cl}]$ showing the multiplet.

probable atoms to influence these are the oxygens in the heteroaromatic systems, or the ring currents of the rings, because two of the Cp ligands will be very close to the aromatic rings. For the rest of the spectrum there are also two sets of signals for the heteroaromatic rings. A further possible explanation is that the two heteroaromatic rings are caught in two different chemical environments, because of the bulkiness of the Db ligands. Therefore the molecule may have two isomers, with Db rings in different conformations. One H2 displays a significant downfield shift, while the other is very upfield, which can only be due to ring current effects.

COSY

Two-dimensional homonuclear shift correlation spectroscopy (COSY) was used to aid in the unambiguous assignment of the different protons in **1**. Although helpful for most protons, this remained difficult for the protons in the multiplet (**Fig. 3.6**).

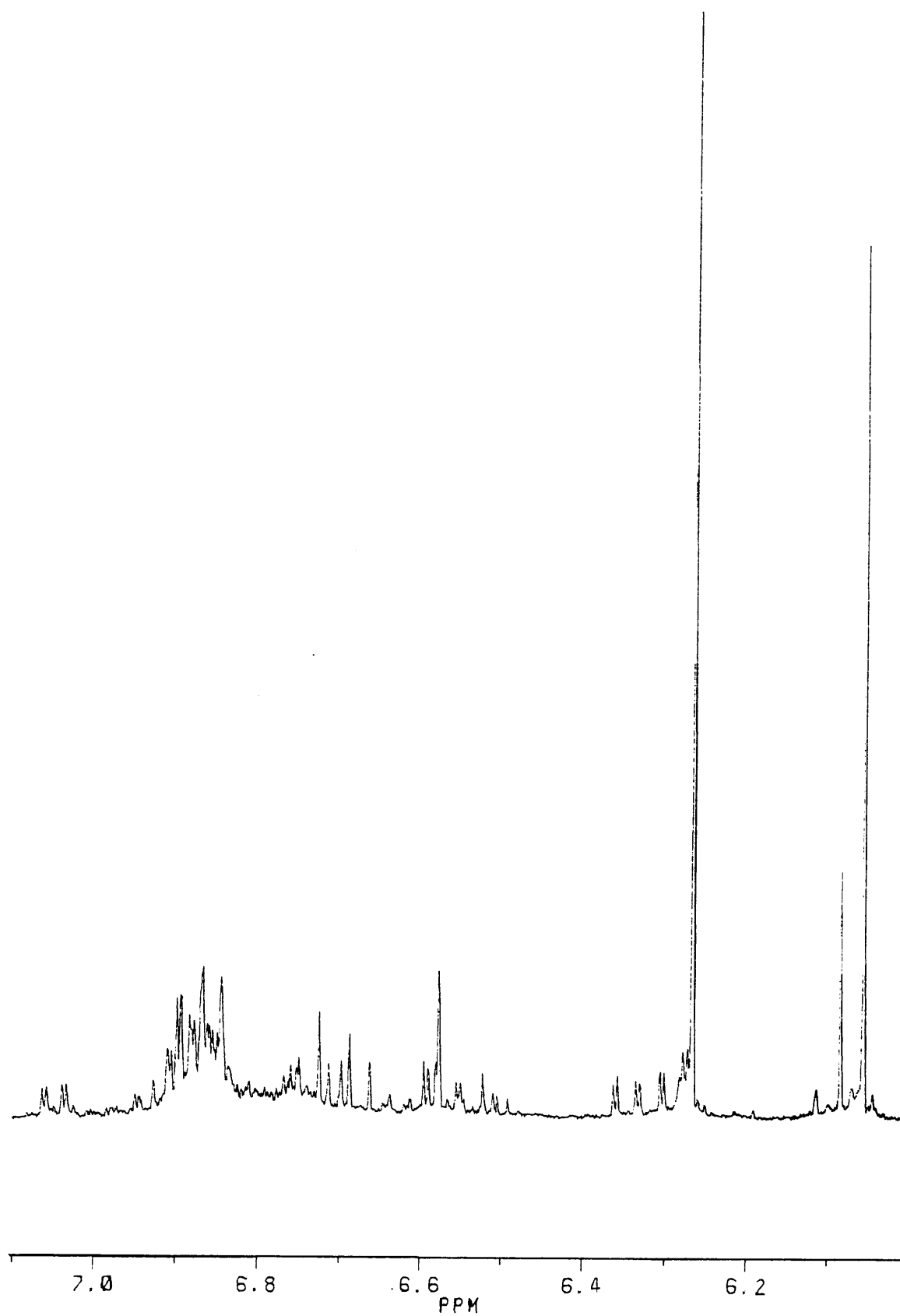


Fig. 3.5. The ¹H NMR spectrum of [$\{\text{TiCp}_2(\text{Db})\}_2\text{O}$] showing the multiplet.

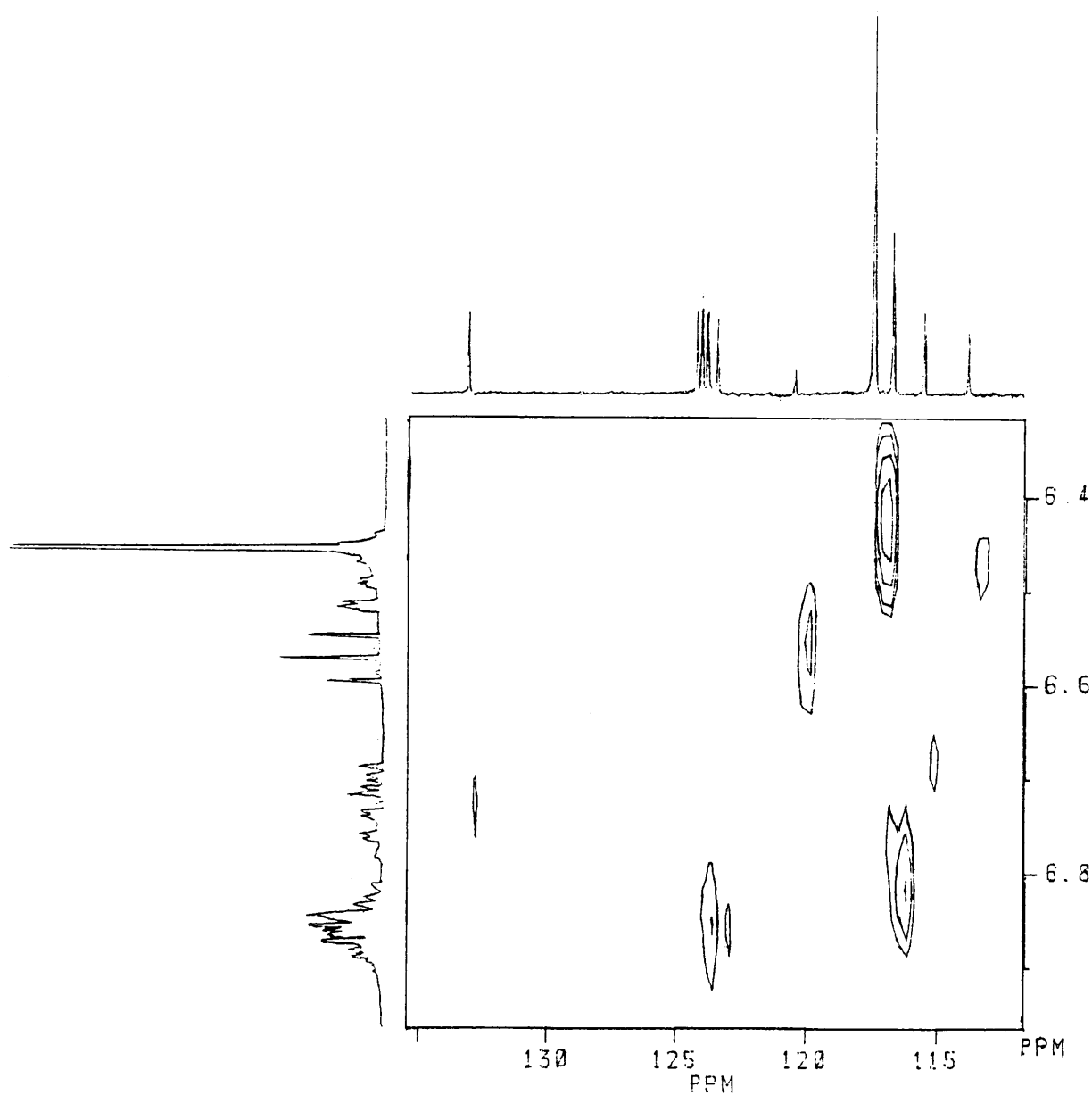


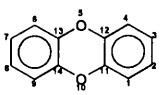
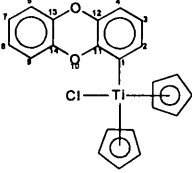
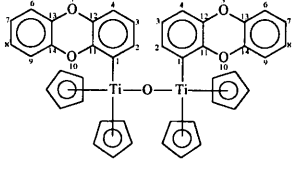
Fig. 3.6. The 2-D spectrum (COSY) for $[\text{TiCp}_2(\text{Db})\text{Cl}]$.

¹³C NMR Spectroscopy

The ¹³C NMR spectral data for dibenzodioxin⁶, **1** and **2** is given in **Table 3.3**. The carbon-metal bond causes C1 to be shifted downfield dramatically. This is due to electron density being

6. M. E. Amato, A. Grassi, K.J. Irolic, G.C. Pappalardo, L. Radics, *Organometallics*, 1993, 12, 775.

Table 3.3. ^{13}C NMR data for dibenzodioxin⁶, $[\text{TiCp}_2(\text{Db})\text{Cl}]$ and $[\{\text{TiCp}_2(\text{Db})\}_2\text{O}]$.

			
		1	2
Chemical Shift, δ (ppm) [†]			
C1	116.2	175.1	176.0 and *178.7
C2	123.6	133.0	132.2 and *132.4
C3	123.6	120.1	120.8 and *122.7
C4	116.2	113.4	113.1 and *113.5
C6	116.2	116.3	116.3 and *116.5
C7	123.6	‡124.0 or	‡123.1, 123.5, 123.6
C8	123.6	123.2	or 123.8
C9	116.2	115.1	115.4 and *116.1
C11	142.1	150.2	°150.1
C12	142.1	‡143.1, 143.0 or 142.6	°142-145
C13	142.1		
C14	142.1		
Cp	---	117.1	114.6, *112.6 and 114.4

[†] $\text{d}^1\text{-CDCl}_3$ used as solvent.

[‡] Difficult to assign to specific carbons.

^{*} Two sets of values due to two heteroaromatic ring systems.

[°] Carbons not clear on spectrum.

transferred to the metal centre from Db. The neighbouring carbons, C2 and C11, also have downfield shifts, but much less than that of C1. The rest of the chemical shifts are quite similar to those of the free ligand, while the Cp signal is upfield due to increased electron density on the metal fragment, when compared to titanocene dichloride.

The ^{13}C NMR for **2** has similar chemical shifts as for **1**. Again there is a 4:1 ratio of Cp rings and for the heteroaromatic ligands there are also two sets of signals as in H NMR spectrum. The signals for C11-C14 were difficult to assign on the spectrum.

HETCOR

The HETCOR spectrum of **1** is shown in Fig. 3.7. This was used to assign and correlate the specific proton resonances to their corresponding carbons. H2-H4 were assigned without problems, but H6-H9 were impossible to assign.

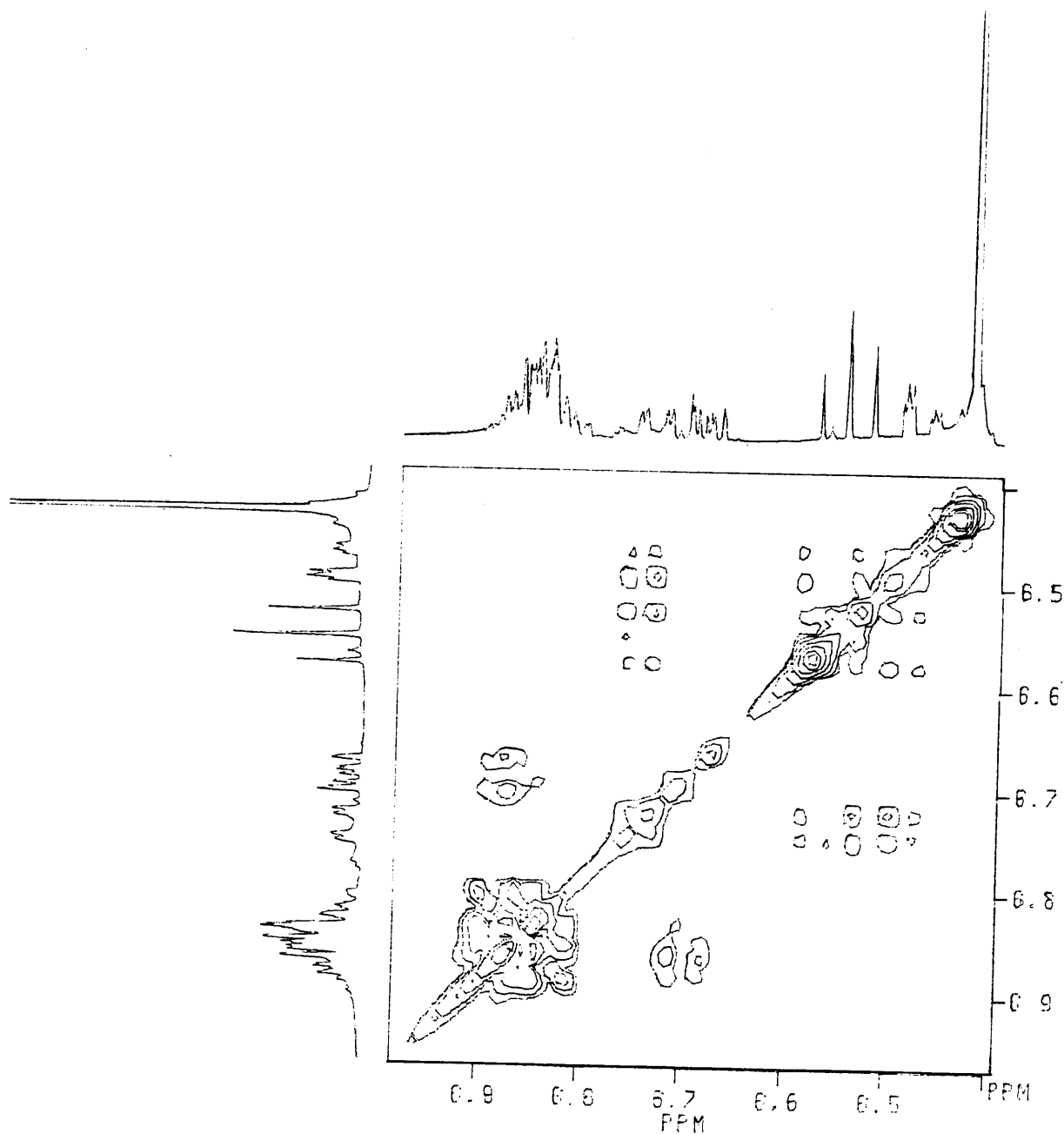


Fig. 3.7. The 2-D spectrum (HETCOR) for $[TiCp_2(Db)Cl]$.

X-ray Crystallography

The final confirmation of the structure of **1** was obtained from a single crystal X-ray diffraction study. The complex was recrystallized from a 1:1 THF:hexane solution by using the layering technique. It gave bright orange crystals with a diamond shape. In **Fig. 3.8** the structure of the molecule is given in an ORTEP diagram, which also indicates the labelling scheme that was used. Solvent molecules, one THF and one hexane, crystallize with every molecule of **1** and because of their thermal motions, low temperature data collection was essential. **Fig. 3.9** shows a ball-and-stick model of the same structure and the solvent molecules. The most important bond lengths and angles are listed in **Table 3.4**. Other structural information is given in Chapter 10 (Experimental section) and as an **Appendix**.

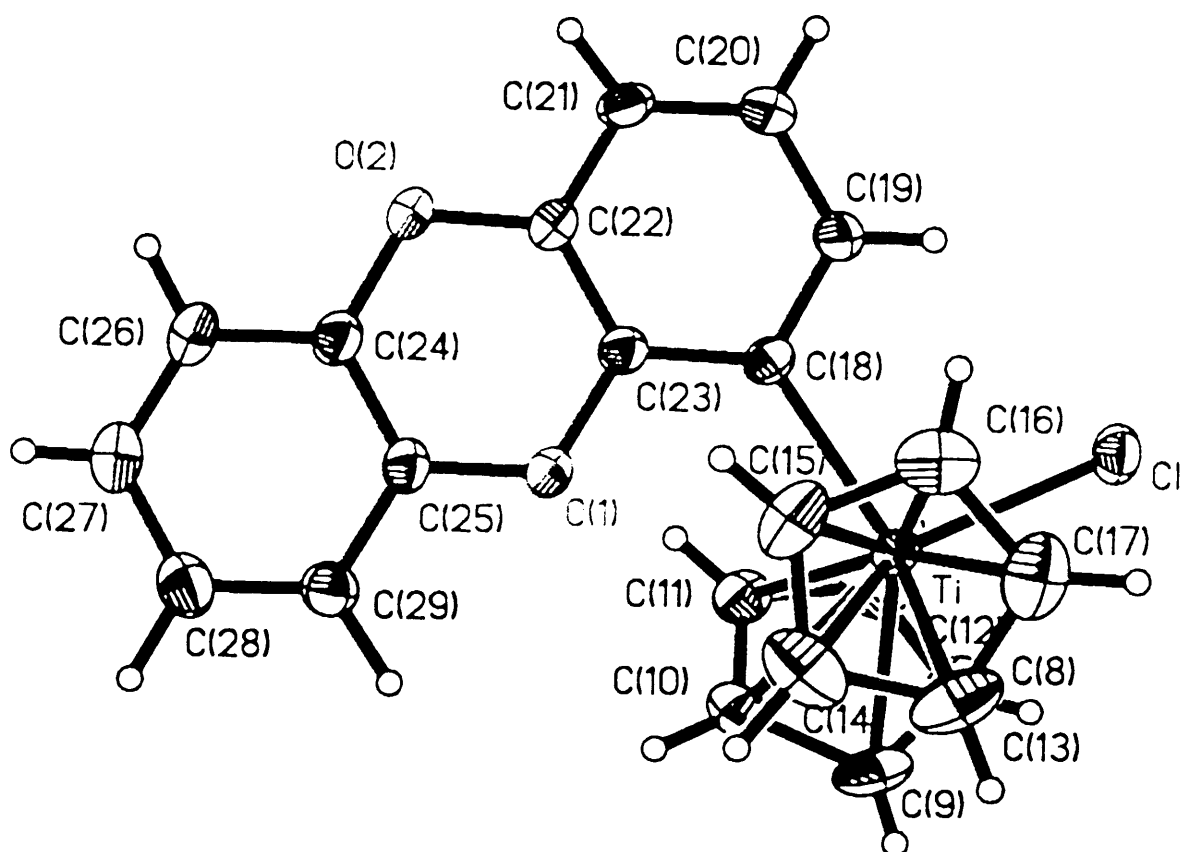


Fig. 3.8. An ORTEP diagram for [TiCp₂(Db)Cl].

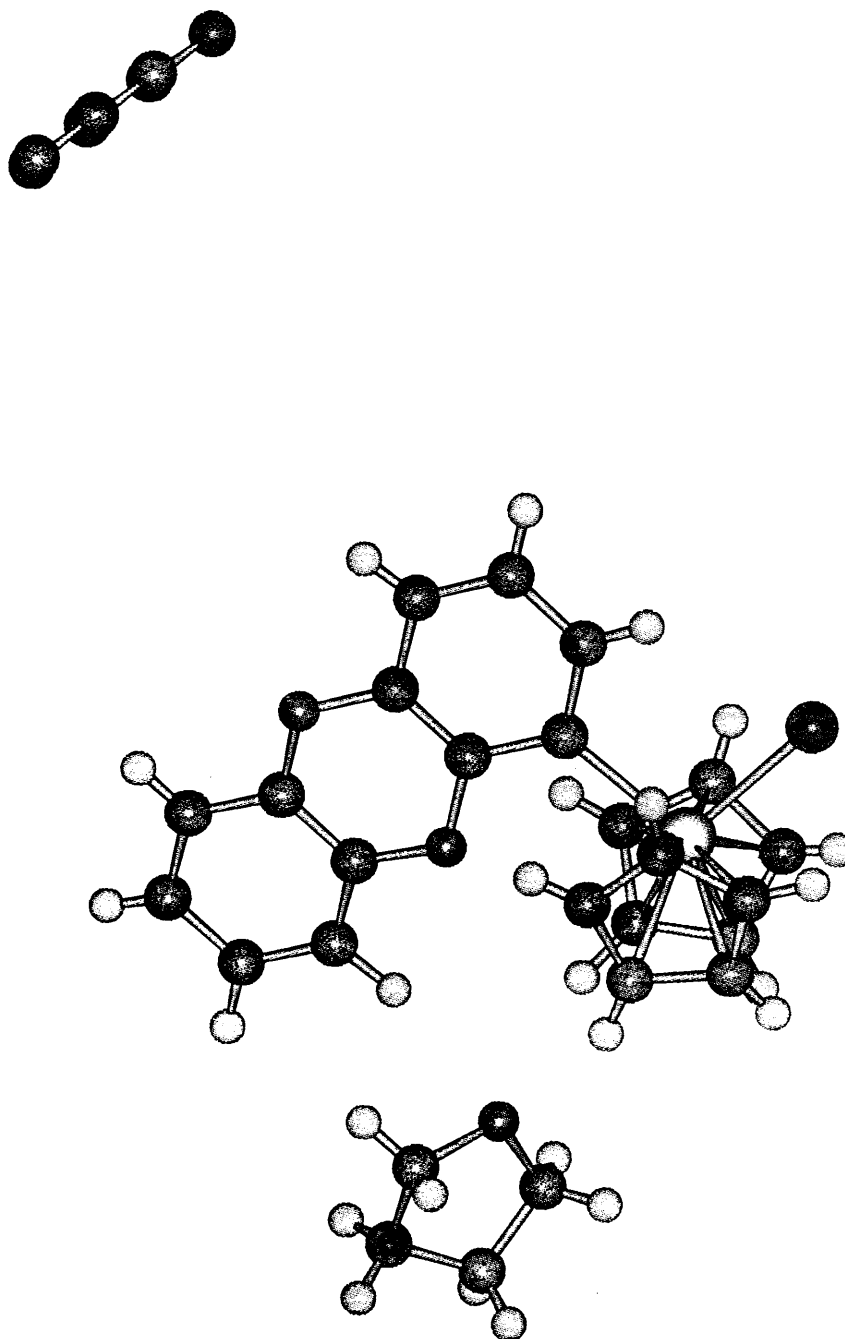
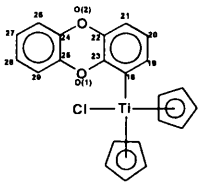
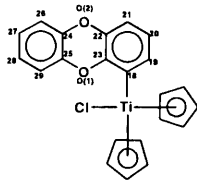


Fig. 3.9. Ball and stick model for $[\text{TiCp}_2(\text{Db})\text{Cl}]$.

Table 3.4. Selected bond lengths and bond angles and [TiCp₂(Db)Cl].

	Bond Length (Å)		Bond Angle (Deg)
Ti-Cl	2.3684(7)	Cl-Ti-C(18)	97.42(7)
Ti-C(18)	2.208(2)	Ti-C(18)-C(19)	118.5(2)
C(18)-C(19)	1.397(4)	Ti-C(18)-C(23)	126.2(2)
C(19)-C(20)	1.403(4)	C(18)-C(19)-C(20)	122.4(2)
C(20)-C(21)	1.376(4)	C(19)-C(20)-C(21)	120.7(2)
C(21)-C(22)	1.383(4)	C(20)-C(21)-C(22)	118.4(2)
C(22)-C(23)	1.392(3)	C(21)-C(22)-C(23)	120.7(2)
C(18)-C(23)	1.404(3)	C(22)-C(23)-C(18)	122.6(2)
O(1)-C(23)	1.389(3)	C(23)-C(18)-C(19)	115.2(2)
O(1)-C(25)	1.379(3)	C(18)-C(23)-O(1)	117.1(2)
O(2)-C(22)	1.389(3)	C(22)-C(23)-O(1)	120.4(2)
O(2)-C(24)	1.378(3)	C(23)-O(1)-C(25)	116.3(2)
C(24)-C(25)	1.397(4)	O(1)-C(25)-C(24)	121.5(2)
C(24)-C(26)	1.387(4)	O(1)-C(25)-C(29)	118.7(2)
C(26)-C(27)	1.388(4)	C(21)-C(22)-O(2)	117.1(2)
C(27)-C(28)	1.398(4)	C(23)-C(22)-O(2)	122.2(2)
C(28)-C(29)	1.383(4)	C(22)-O(2)-C(24)	115.7(2)
C(29)-C(25)	1.387(4)	O(2)-C(24)-C(25)	121.3(2)
H(19)-Cl	2.699	O(2)-C(24)-C(26)	118.3(2)
H(27)-Cl	2.885	C(24)-C(26)-C(27)	119.6(3)
		C(26)-C(27)-C(28)	119.6(3)

Four ligands surround the titanium centre in a distorted tetrahedral arrangement, with positions defined by the centra of the Cp rings and the chloro and Db ligands. The Cp rings and titanium belong to the open clam shell class of compounds and the rotational relationship between the two

Cp rings is close to that of an eclipsed configuration. The bulky Db ligand causes an enlargement of the angle between the two non Cp ligands. In titanocene dichloride this Cl-Ti-Cl angle⁷ is 94.6°, which is smaller than the 97.4° of Cl-Ti-C(18) of **1**. This angle in **1** is very similar to the values of 96.7 and 98.4° recorded for the two molecules in the unit cell of [TiCp₂(DbT)Cl]⁸ (DbT = Dibenzothienyl). The dihedral angle, Cl-Ti-C(18)-C(19) of -6.6(2)° reveals that the chloro ligand is approximately in the plane of the Db rings and in an *anti* conformation with respect to the nearest oxygen atom.

The dihedral angle of C(5)-O(1)-C(25)-C(22) is 12.2(4)°, which shows that the dibenzodioxin ring is almost planar. The titanium atom is also in the plane of the dioxin ligand. In the structure there is also a highly distorted THF molecule and a hexane that appears to have seven carbons, but this is due to positional disorders. Bearing in mind the numerous unsuccessful attempts to obtain crystals of **1**, it is believed that the solvent molecules were involved in the packing process of the crystal.

As a result of the orientation of the Db ring, the hydrogen on C(19) is forced close to the chloro ligand. In fact, the H(19)...Cl non bonding distance of only 2.699Å is very short and typical of hydrogen bonding, as illustrated with the literature value of 2.92-3.18Å for OH...Cl⁹. The effect of hydrogen bonding would be to reduce the Ti-C(18)-C(19) angle, whereas interaction of Ti with the O(1) oxygen of the dibenzodioxinyl ligand will reduce the Cl-Ti-C(18) angle.

If we compare the bond lengths of the free ligand¹⁰ to those of **1**, we can see that they differ very little and that coordination to titanium has very little effect on the bond lengths. The intra-atomic non-bonding distance between H(19) and Cl is 2.699Å. We ascribe the big chemical shift of H2 observed in the NMR spectra, to this hydrogen bonding. There is also an interatomic hydrogen bond interaction between the Cl of one molecule and the H(27) of the other, which is measured at 2.885Å.

7. A. Clearfield, D. K. Warner, C. H. Salderiaga-Molina, R. Ropal, J. Bernal, *Can. J. Chem.*, **1975**, *53*, 1622.

8. S. Lotz, P. H. Van Rooyen, R. Meyer, unpublished results.

9. N. N. Greenwood, A. Earnshaw in *Chemistry of the Elements*, Pergamon Press, Oxford, **1984**, 65.

10. P. Singh, J. D. McKinney, *Acta Cryst.*, **1978**, *B34*, 2956.

The Ti-C(18) (Db) bond distance of 2.208 Å is significantly shorter than the observed Ti-C (sp³, phenyl) bond distance of 2.27(1) Å for TiCp₂Ph₂¹¹ and is comparable with the Ti-C(Ph) distance of 2.193(3) Å recorded for the titanacycle [TiCp₂(C₆H₄-C₆H₄S)]¹² and the average value of 2.188(5) Å for [TiCp₂(C₆H₄-C₆H₄)]¹³. Complexes displaying significant π-interaction between titanium and a sp²-bonded carbon atom, should have Ti-C bond distances of about 2.00-2.10 Å^{14,15,16,17}, which is a little shorter than the corresponding distance in **1**.

The short Ti-C distance in **1** suggests that some multiple bonding interaction exists between the titanium and the Db carbon atom. Titanium(IV) has no electrons in the d-orbitals and will therefore, only be capable of accepting electron density from the π-cloud of the Db ligand. The σ-bonded Db ligand exhibits some carbene character, which supports observations of the ¹³C NMR data that the relevant carbon resonances are shifted downfield into the carbene region (**Fig. 3.2**).

If important, one would expect that the adjacent bonds of the phenyl bonded to the titanium should be lengthened. Although not significant, these are the longest C-C distances in the ring.

3.3 Conclusion

The aim was to synthesize [TiCp₂(Db)Cl] **1** and it was done successfully by the method described. The product, an orange complex, was fully characterized by mass spectrometry, NMR spectroscopy and finally confirmed by X-ray crystallography. The potential antitumour properties

11. V. Kocman, J. C. Rucklidge, R. J. O'Brien, W. Santo, *J. Chem. Soc., Chem. Commun.*, **1976**, 1340.

12. P. R. Stafford, T. B. Rauchfuss, A. K. Verma, S. R. Wilson, *J. Organomet. Chem.*, **1996**, 526, 203.

13. C. A. Mike, T. Nelson, J. Graham, A. W. Cordes, N. T. Allison, *Organometallics*, **1988**, 7, 2573.

14. P. Binger, P. Müller, P. Phillips, P. Gabor, R. Mynott, A. T. Herrmann, F. Langhauser, C. Krüger, *Chem. Ber.*, **1992**, 125, 2209.

15. M. M. Francl, W. J. Hehre, *Organometallics*, **1983**, 2, 457.

16. R. Beckhaus, S. Flatiu, S. Trojanov, P. Hofmann, *Chem. Ber.*, **1992**, 125, 291.

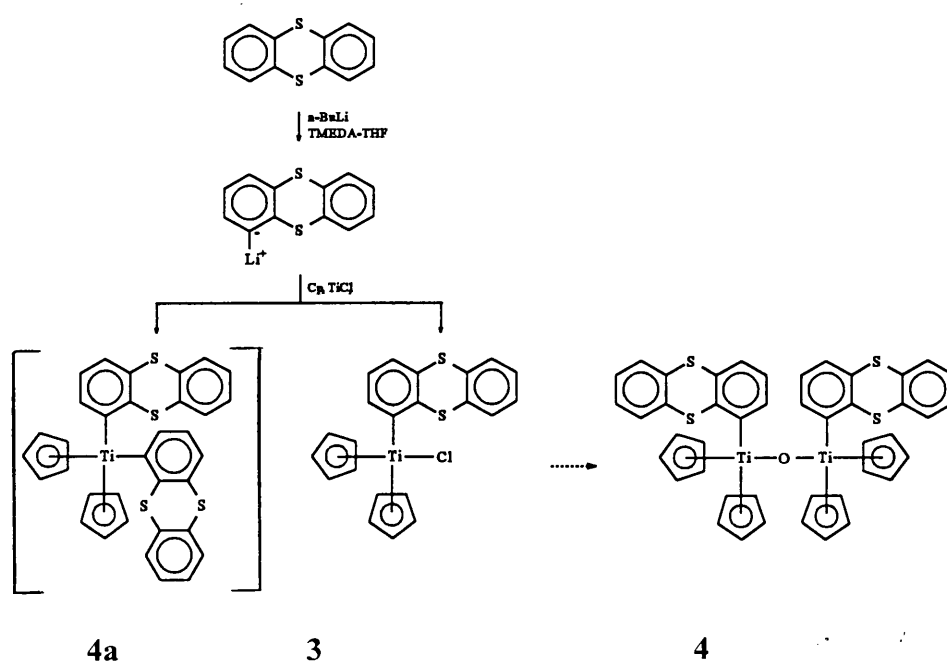
17. A. K. Rappe, *Organometallics*, **1987**, 6, 354.

of **1** will be discussed in Part III. This reaction also gave a second yellow product which was characterized by NMR spectroscopy and mass spectrometry as $[\{\text{TiCp}_2(\text{Db})\} \text{O}]$ **2**. The spectroscopic data also revealed that the chloro ligand is the most labile ligand in **1** and from the structural data it was clear that the Db ring was favourably orientated for intercalation. Both features are essential for the objectives of this study.

4. Titanocene Complexes with Thianthrenyl as Ligand

4.1 Synthesis

Lithiation of thianthrene [ThH] proceeded in a high yield and on addition of titanocene dichloride, the colour changed from red to orange-brown. On the silica column, with 6:4 hexane:dichloromethane as eluent, an orange product was collected first, characterized as chlorobis(cyclopentadienyl)(thianthrenyl)titanium(IV) **3** [$\text{TiCp}_2(\text{Th})\text{Cl}$]. A yellow fraction, bis(cyclopentadienyl)bis(thianthrenyl)titanium(IV) **4a** [$\text{TiCp}_2(\text{Th})_2$], followed on the column, but was too unstable to purify. Complex **3**, after purification and column chromatography was found to be unstable and converted into a second yellow product, μ -oxobis{bis(cyclopentadienyl)(thianthrenyl)titanium(IV)} **4** [$\{\text{TiCp}_2(\text{Th})\}_2\text{O}$] (**Scheme 4.1**). Due to the instability of **3**, the only



Scheme 4.1.

way to characterize it was through measuring a ^1H NMR spectrum as soon as possible. Attempts to obtain ^{13}C NMR and mass spectra failed, as the complex already started to decompose to **4** during measurement. In comparison with **1**, complex **3** is far less stable, indicating that the Th ligand has a stronger activation effect on the remaining chloro ligand, than was the case with the Db ligand. The yellow fraction in this case clearly originated from **3**. We ascribe the fact that **4a** was too unstable to isolate, to steric hindrance, as is shown in a computer generated model (**Fig 4.1**). Comparing stabilities one could conclude that $\mathbf{1} > \mathbf{3}$ and $\mathbf{2a} > \mathbf{4a}$. The mechanism for the formation of **4** differs from that which was discussed in Chapter 3. The desired complex **3** has a highly activated chloro ligand, which in the presence of traces of water converts into the corresponding hydroxo complex **3a**. In a subsequent reaction, **3a** forms the dinuclear complex **4**, by the elimination of water between two of molecules of **3a** or the elimination of hydrochloric acid between molecule **3** and **3a** (**Scheme 4.2**).

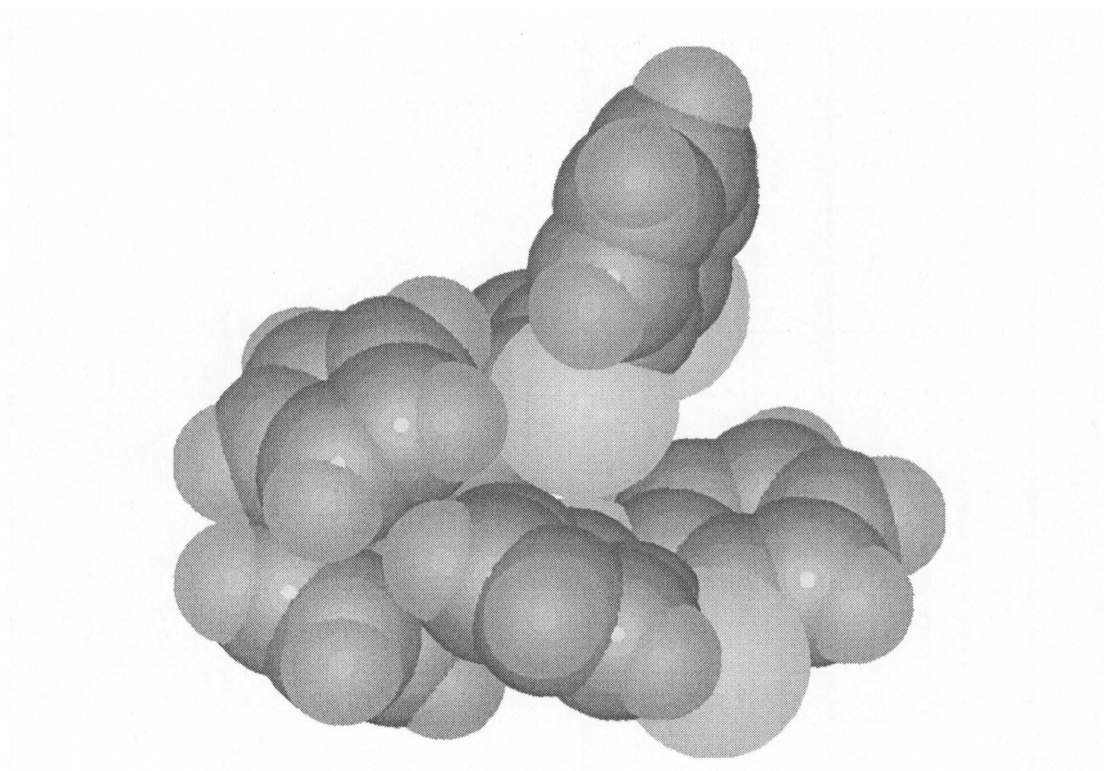
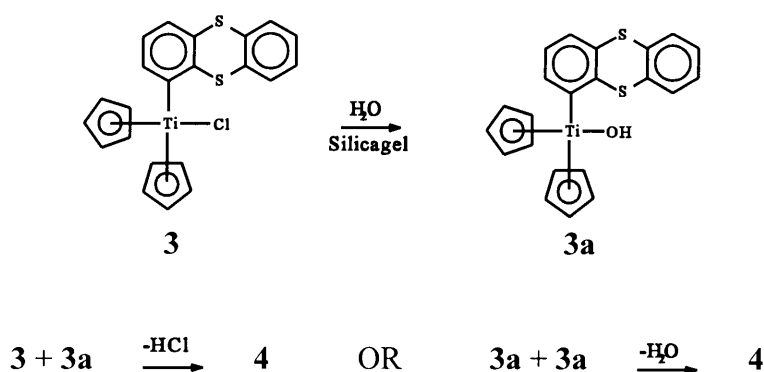


Fig. 4.1. A computer generated model of $[\text{TiCp}_2(\text{Th})_2]$.

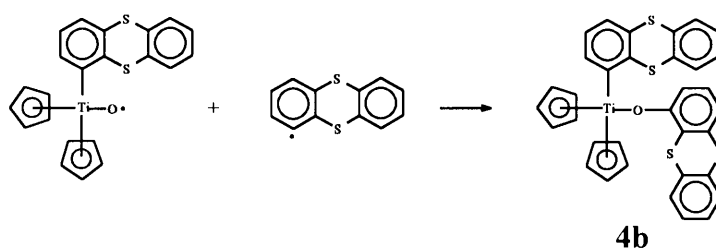


Scheme 4.2.

4.2 Characterization

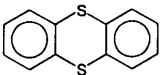
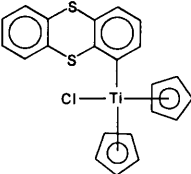
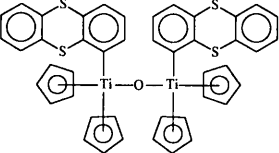
Mass spectrometry

Data for the mass spectra of thianthrene, **3** and **4** is shown in **Table 4.1**. The spectra for **3** and **4** are almost identical, because **3** already converted to **4**. There is a weak signal for the $[M^+]$ in the spectrum of **3**, which indicates the instability of this complex. A fragment indicating thianthrene with an oxygen atom bound to it, is detected on many fragments in both spectra. The fragmentation pattern of **4** is similar to that of **2**, which was discussed in Chapter 3. Again the molecule splits into two parts and the fragments $[\text{TiCp}_2(\text{Th})\text{O}]^+$ and $[\text{TiCp}_2(\text{Th})]^+$ are of highest intensity in the spectrum of **4**. Very important in this case, is that the fragment with the oxygen atom combines with a thianthrene unit which was lost by other metal centres to form complex **4b** (Scheme 4.3). In Scheme 4.4 the fragmentation pattern of complex **4b**, as constructed from fragment ions observed, is shown.



Scheme 4.3.

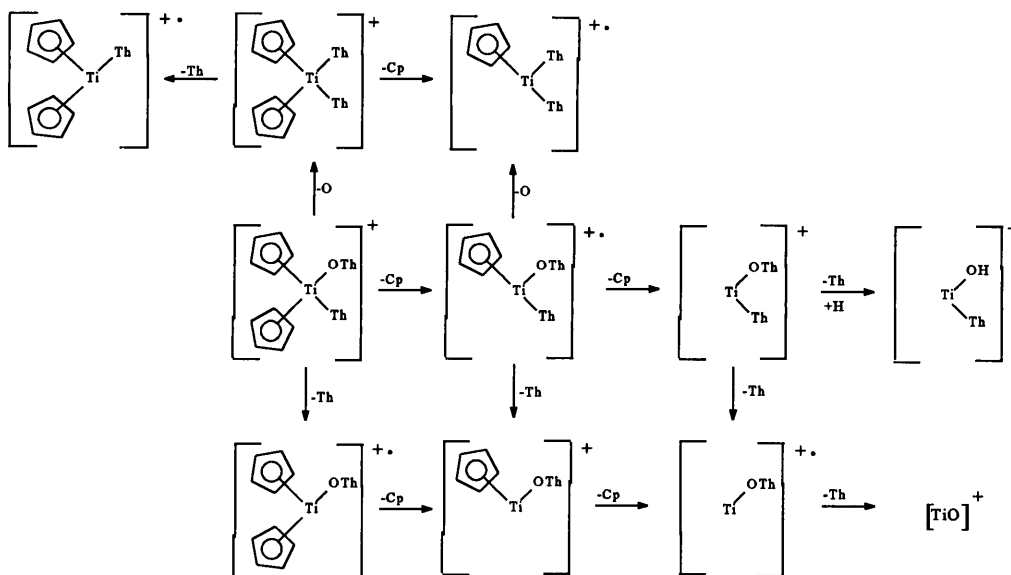
Table 4.1. Mass spectral data for thianthrene, [TiCp₂(Th)Cl] and [{TiCp₂(Th)}₂O].

	 3	 4
Mass peaks ¹ , m/z (I%)	Mass peaks, m/z (I%)	Mass peaks, m/z (I%)
216 (100) [M] ⁺	624 (11) [TiCp ₂ (OTh)(Th)] ⁺⁺	624 (2) [TiCp ₂ (OTh)(Th)] ⁺
184 (70) [M-S] ⁺	608 (1) [TiCp ₂ (Th) ₂] ⁺	608 (1) [TiCp ₂ (Th) ₂] ⁺
171 (22) [M-CSH] ⁺	559 (10) [TiCp(OTh)(Th)] ⁺⁺	559 (1) [TiCp(OTh)(Th)] ⁺⁺
152 (5) [M-2S] ⁺	494 (18) [Ti(OTh)(Th)] ⁺	543 (1) [TiCp(Th) ₂] ⁺⁺
139 (22) [M-(CS ₂ H)] ⁺	430 (2) [Th-Th] ⁺	494 (7) [Ti(OTh)(Th)] ⁺⁺
	428 (3) [TiCp ₂ (Th)Cl]	430 (5) [Th-Th] ⁺
	409 (28) [TiCp ₂ (OTh)] ⁺⁺	409 (77) [TiCp ₂ (OTh)] ⁺⁺
	393 (11) [TiCp ₂ (Th)] ⁺⁺	393 (42) [TiCp ₂ (Th)] ⁺⁺
	344 (31) [TiCp(OTh)] ⁺	344 (60) [TiCp(OTh)] ⁺
	280 (59) [Ti(Th)OH] ⁺⁺	280 (100)[Ti(Th)OH] ⁺⁺
	247 (27) [TiCp ₂ Cl ₂]	232 (72) [Th-OH] ⁺
	216 (21) [Th-H] ⁺	216 (66) [Th-H] ⁺
	178 (15) [TiCp ₂] ⁺	178 (51) [TiCp ₂] ⁺
	113 (6) [TiCp] ⁺⁺	113 (13) [TiCp] ⁺⁺
	64 (9) [TiO] ⁺	64 (11) [TiO] ⁺

¹H NMR Spectroscopy

The ¹H NMR data of thianthrene, **3** and **4** is tabulated in **Table 4.2**. The spectrum for **3** was solved by comparing resonances of the spectrum to those in Chapter 3. Again the three protons of the ring where the metal was bound displayed upfield shifts, caused by the residual electron density after attaching a more electropositive substituent. The proton, H₂, which is closest to the

1. N. P. Buu-Hoi, G. Saint-Ruf, M. Mangane, *J. Heterocycl. Chem.*, 1972, 9, 691.

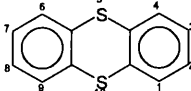
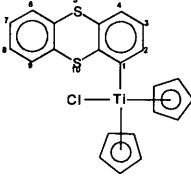
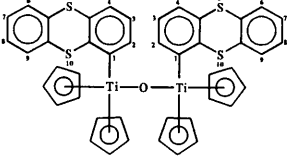


Scheme 4.4.

site of coordination is affected most. Charge distribution, explaining this occurrence was given in Chapter 3 (**Scheme 3.2**). The protons on the other ring were very little affected and because of overlapping, they could only be identified as multiplets (**Fig. 4.2**). The Cp signal is upfield from that of titanocene dichloride, because the replacement of a chloro ligand causes the electron density on the Cp rings to be higher for **3**.

The peaks in the ^1H NMR spectrum of the yellow product **4** (**Fig. 4.3**) were also solved by comparing the chemical shifts with those of **2**. The resonances of the ring protons containing the metal substituent were upfield and the protons closest to the metal were affected most. As in **2** there were two sets of signals for the heteroaromatic ligand, but the chemical shifts of some protons are not clear due to overlapping. One of the H4 signals overlaps with the Cp signal. The protons of the uncoordinated ring had about the same chemical shifts than **3**. The Cp signal for **4** is upfield from the Cp signal for **3**, which means that the electron density on the metal fragment is higher in **4**. Whereas **2** displayed two Cp signals of which one was split in a 4:1 ratio in the

Table 4.2. ¹H NMR spectroscopic data for thianthrene, [TiCp₂(Th)Cl] and [{TiCp₂(Th)}₂O].

			
Chemical Shift, δ (ppm) [†]			
H1	7.48	---	---
H2	7.24	7.14 (dd)	6.98 and *7.68 (dd)
H3	7.23	6.86 (t)	6.93 and *7.06 (t)
H4	7.48	6.77 (dd)	6.38 and *6.59 (dd)
H6	7.48	7.45-7.57 (multiplet)	7.46-7.55 (multiplet)
H9	7.48		
H7	7.23	7.20-7.27 (multiplet)	7.22-7.27 (multiplet)
H8	7.24		
Cp	---	6.41 (s)	6.38 (s)
Coupling Constant, ⁿ J _{H,H} (Hz)			
J ₁₂	7.7	---	---
J ₁₃	1.5	---	---
J ₁₄	0.4	---	---
J ₂₃	7.5	7.4	7.5 and *7.5
J ₂₄	1.5	1.1	1.3 and *1.3
J ₃₄	7.7	7.5	#7.6
J ₆₇	7.7	□	□
J ₆₈	1.5	□	□
J ₆₉	0.4	□	□
J ₇₈	7.5	□	□
J ₇₉	1.5	□	□
J ₈₉	7.7	□	□

[†] d¹-CDCl₃ used as solvent.

□ Difficult to calculate, due to multiplet.

* Two sets of values, due to the heteroaromatic rings. # Difficult to calculate, due to overlapping.

spectrum, the spectrum of **4** revealed only one Cp signal. This means that the Cp rings are all in the same chemical environment in **4**, but that the heteroaromatic ligands are in different chemical environments. In Chapter 3 the possibility of isomers was mentioned for **2**, but this is unlikely here, based on the Cp resonances.

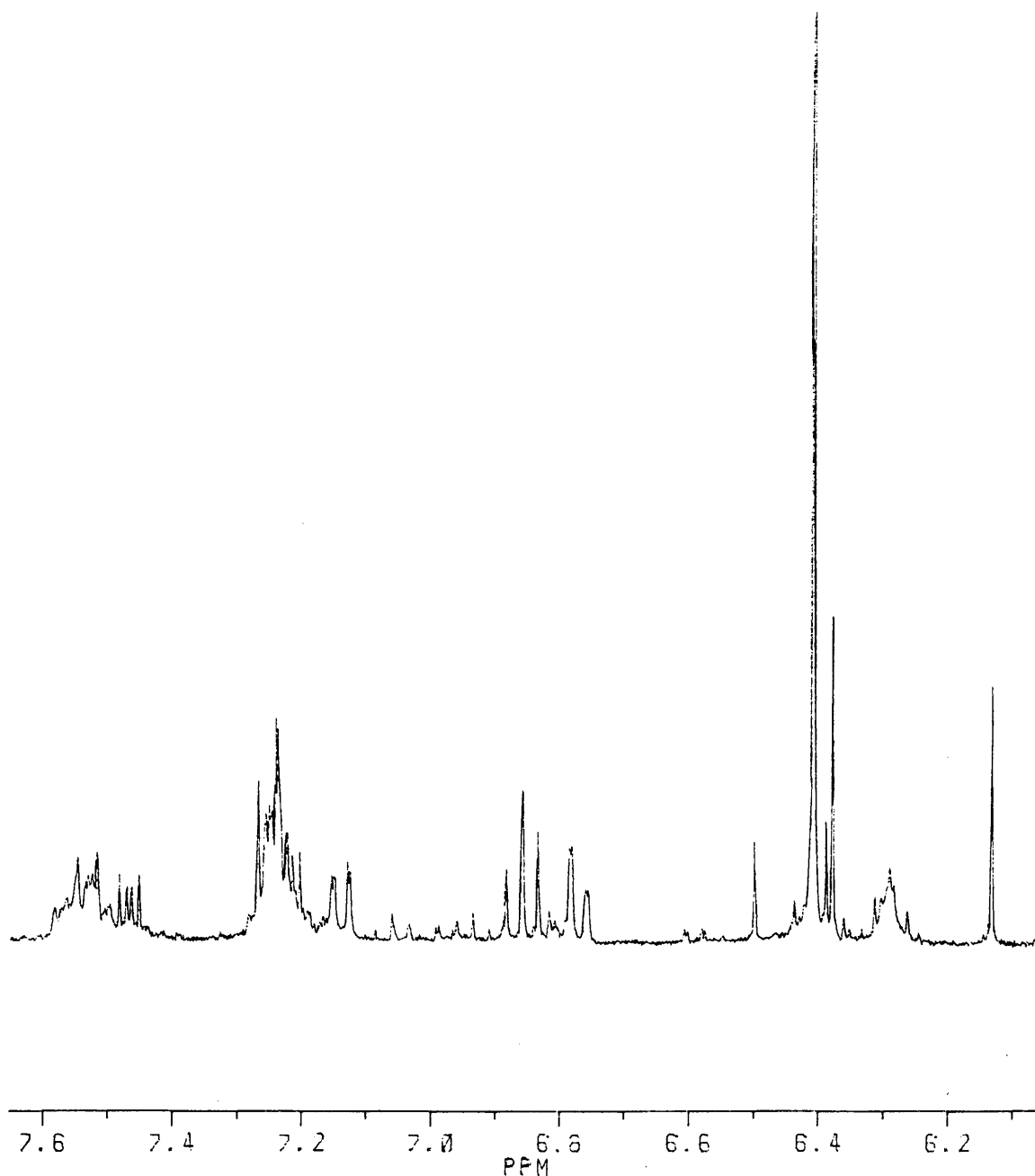


Fig. 4.2. The ¹H NMR spectrum of [TiCp₂(Th)Cl] showing the multiplet.

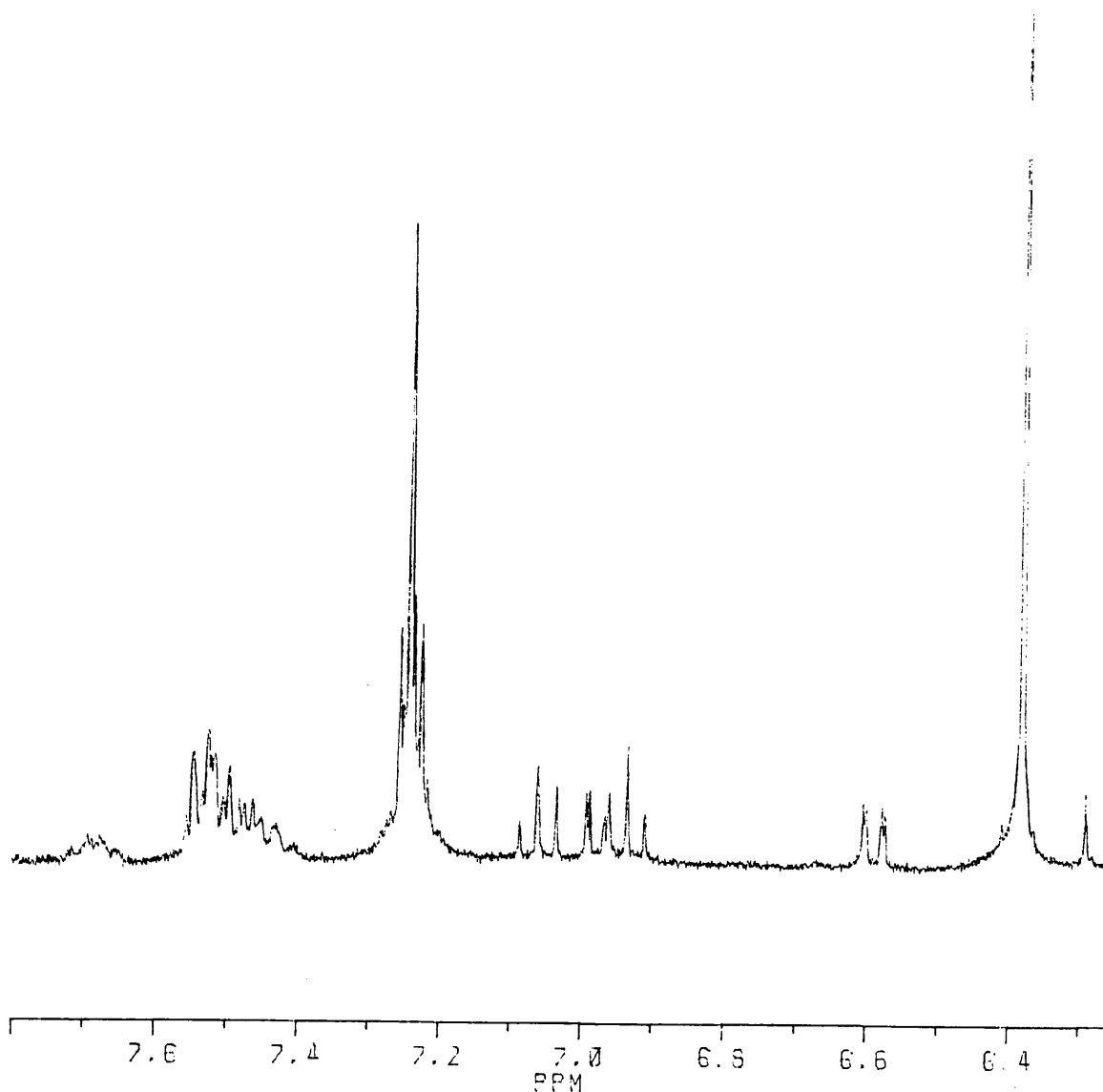
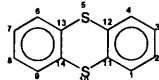
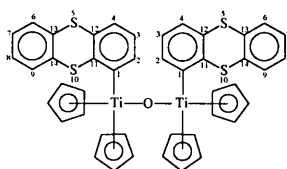


Fig. 4.3. The ^1H NMR spectrum of $[\{\text{TiCp}_2(\text{Th})\}_2\text{O}]$ showing the multiplet.

^{13}C NMR Spectroscopy

Due to the instability of **3**, the ^{13}C NMR spectrum could not be obtained. Complex **4** displayed enough peaks for two thianthrene ligands in different chemical environments. The reasons for this difference in chemical environment was already discussed in Chapter 3. In the rings containing the metal substituent, the carbon atoms closest to the metals were affected most. The carbon atoms in the rings without metals were almost unaffected. As in the proton spectrum there is only one Cp signal.

Table 4.3. ^{13}C NMR spectroscopic data for thianthrene and $[\{\text{TiCp}_2(\text{Th})\}_2\text{O}]$.

		
Chemical Shift, δ (ppm) [†]		
C1	128.7	207.1 and *200.9
C2	127.7	137.5 and *139.7
C3	127.7	125.7 and *126.6
C4	128.7	114.8 and *116.8
C6	128.7	‡ 128.1, 128.3, 128.6 or
C9	128.7	128.7
C7	127.7	‡ 127.4, 127.5, 127.7, 127.7
C8	127.7	
C11	135.5	150.2 and *150.2
C12	135.5	° 135.0-136.0
C13	135.5	
C14	135.5	
Cp	---	115.4

[†] $\text{d}^1\text{-CDCl}_3$ used as solvent.

[‡] Difficult to assign to specific carbons.

^{*} Two sets of values, due to two heteroaromatic ligands. [°] Three signals not clear on the spectrum.

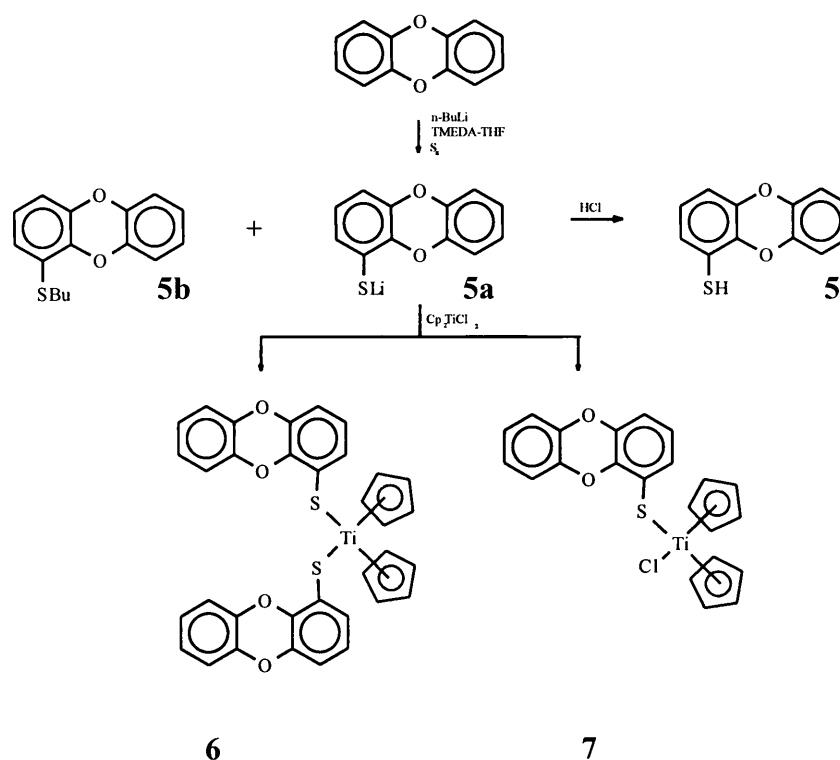
4.3 Conclusion

The aim was to synthesize $[\text{TiCp}_2(\text{Th})\text{Cl}]$ **3** and this was done by the described method, but due to instability, **3** decomposed to yellow $[\{\text{TiCp}_2(\text{Th})\}_2\text{O}]$ **4**. Whereas **3** was only characterized by ^1H NMR spectroscopy, the more stable **4** could be characterized by mass spectrometry, ^1H and ^{13}C NMR spectroscopy. These complexes will be compared to the dibenzodioxin analogues in Part III and the possible antitumour properties will be discussed. However it was clear that serious handling problems would eliminate them as possible candidates for further testing in biological systems.

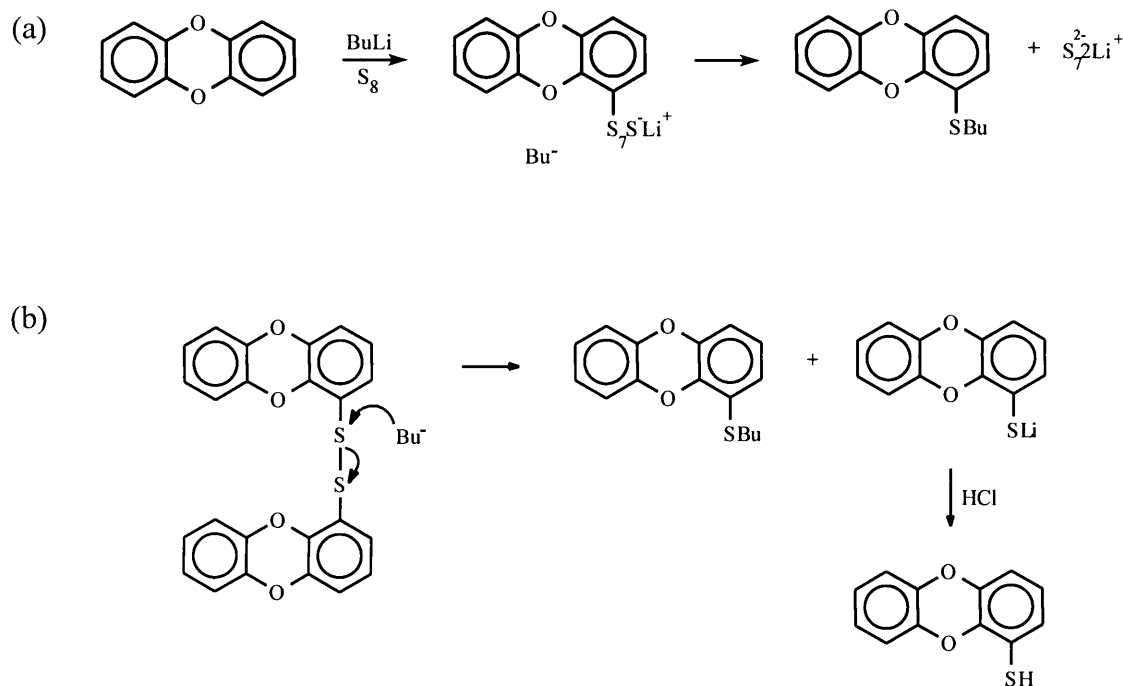
5. Titanocene Complexes with Dibenzdioxinthiolate as Ligand

5.1 Synthesis

The lithiation of dibenzo[1,4]dioxin [DbH] was performed as before and flowers of sulfur was added at low temperature. The lithiated dibenzodioxin-1-thiolate [DbS] **5a** was protonated by bubbling HCl gas through the solution, which formed dibenzodioxinthiol **5** [DbSH], a white precipitate (**Scheme 5.1**). A side reaction resulting in the formation of a thioether was also observed. The formation of dibenzodioxinbutylthioether **5b** is difficult to explain, but a possible reaction route is shown in **Scheme 5.2**. Attack of the lithiated Db on S₈ is followed by a second attack with the release of a sulphide in (a) or an intermediate disulphide is cleaved by a butyl



Scheme 5.1



Scheme 5.2

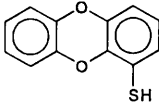
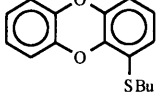
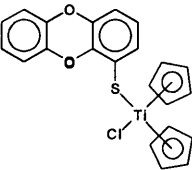
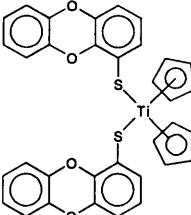
nucleophile in (b) to give the thioether and thiolate. No information on [DbSH] could be found in the literature and it was fully characterized. The reaction of lithiated thiolate with titanocene dichloride was expected to yield chlorobis(cyclopentadienyl)(dibenzodioxin-1-thiolato)titanium(IV) **6** and bis(cyclopentadienyl)bis(dibenzodioxin-1-thiolato)titanium(IV) **7** (Scheme 5.1). The reaction of Li[DbS] and titanocene dichloride was accompanied by a colour change from orange-brown to dark red-brown for the reaction mixture. Thin layer chromatography revealed the formation of two products. A red major product and a second purple compound. On the silica gel column, used for purification, the less polar purple product was collected first and thereafter the red product. Both fractions were characterized by mass spectrometry and NMR spectroscopy and it was confirmed that they were the predicted complexes, [TiCp₂(DbS)Cl] **6** and [TiCp₂(DbS)₂] **7**. The complexes were light sensitive and lost colour within a few hours when exposed to normal daylight.

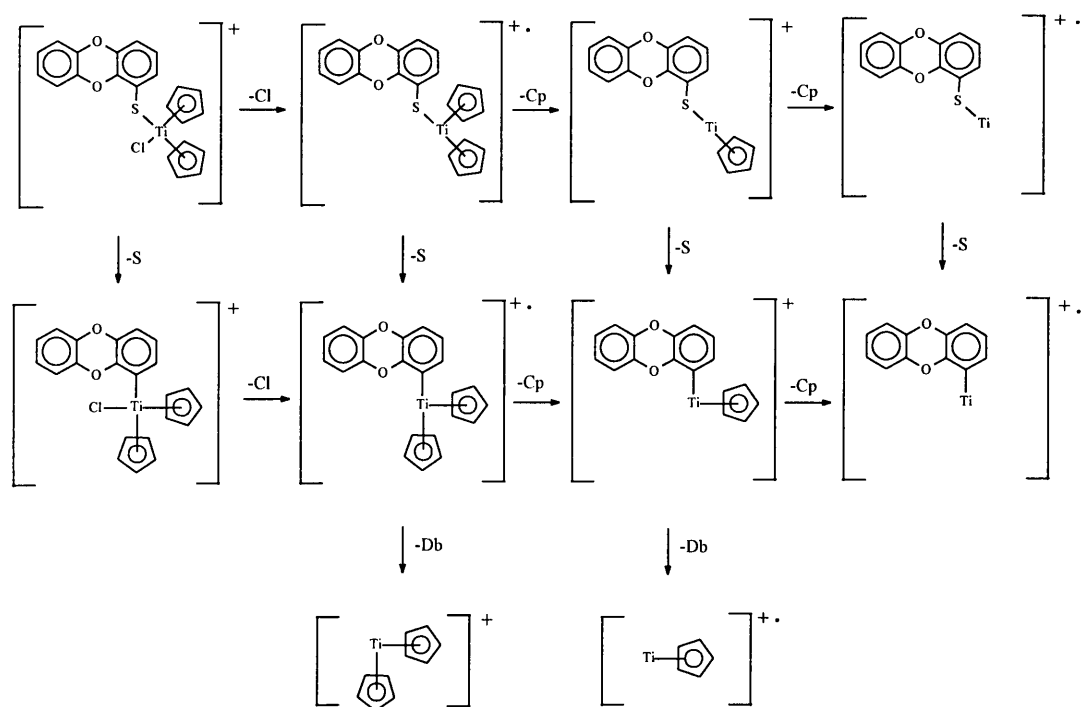
5.2 Characterization

Mass spectrometry

The mass spectra of **5**, **5b**, **6** and **7** were recorded and the data are summarized in **Table 5.1**. In the spectrum of **5b**, the additional fragment ions due to a butyl group are seen. A fragmentation pattern for **6** is given in **Scheme 5.3**. The major decomposition pathway involves the competitive fragmentation of the chloro ligand and the elimination of the sulfur atom from the DbS ligand. The resulting Db moiety is observed in many fragment ions in the spectrum.

Table 5.1. Mass spectral data for DbSH, DbSBu, [TiCp₂(DbS)Cl] and [TiCp₂(DbS)₂].

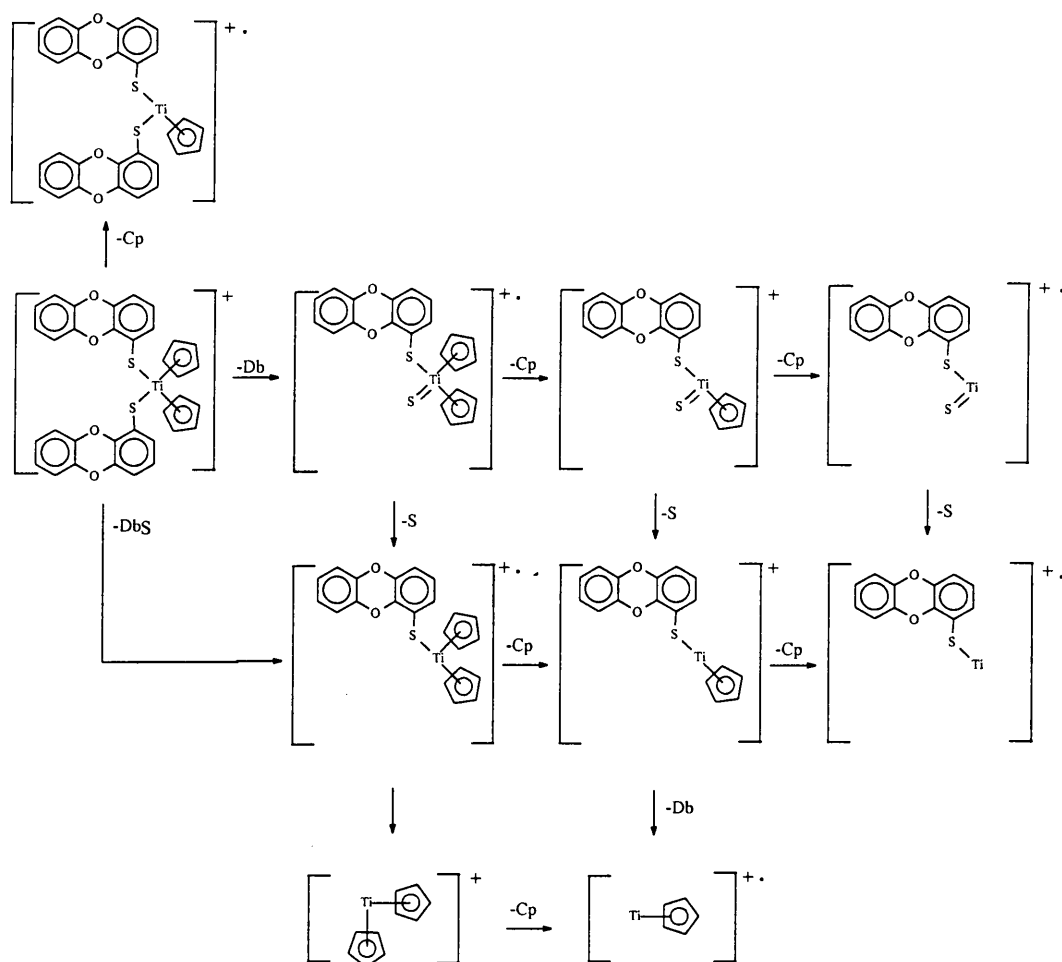
 5	 5b	 6	 7
Mass peaks, m/z (I%)	Mass peaks, m/z (I%)	Mass peaks, m/z (I%)	Mass peaks, m/z (I%)
216 (100) [M] ⁺ 184 (26) [DbH] ⁺ 155 (4) [M-CHO] ⁺ 127 (6) [M-2CO] ⁺	272 (2) [M] ⁺ 216 (5) [M-Bu] ⁺ 184 (5) [DbH] ⁺ 57 (5) [Bu] ⁺	428 (2) [M] ⁺ 396 (5) [TiCp ₂ (Db)Cl] ⁺ 393 (1) [TiCp ₂ (DbS)] ⁺⁺ 361 (7) [TiCp ₂ (Db)] ⁺⁺ 328 (1) [TiCp(DbS)] ⁺⁺ 296 (2) [TiCp(Db)] ⁺ 263 (1) [Ti(DbS)] ⁺⁺ 231 (1) [Ti(Db)] ⁺⁺ 216 (70) [DbS] ⁺⁺ 184 (12) [DbH] ⁺ 178 (3) [TiCp ₂] ⁺ 115 (21) [TiCp] ⁺⁺	610 (66) [M] ⁺ 545 (1) [TiCp(DbS) ₂] ⁺ 425 (5) [TiCp ₂ (DbS)S] ⁺⁺ 393 (12) [TiCp ₂ (DbS)] ⁺⁺ 360 (73) [TiCp(DbS)S] ⁺⁺ 328 (27) [TiCp(DbS)] ⁺⁺ 295 (5) [Ti(DbS)S] ⁺⁺ 263 (10) [Ti(DbS)] ⁺⁺ 213 (100) [DbS] ⁺⁺ 183 (37) [Db] ⁺ 178 (36) [TiCp ₂] ⁺ 115 (13) [TiCp] ⁺⁺


Scheme 5.3.

Notable is the high intensity of the molecular ion for **7** (**Scheme 5.4**), which indicates that the complex is reasonably stable. Interesting to note is the fact that there is no elimination of the sulfur atom as for **6**. Under the prevailing conditions in the mass spectrometer, the major pathway involves the competitive loss of the dioxin fragment from one of the DbS ligands or loss of a total DbS fragment. A large number of fragment ions are the same as those observed for **6** which means that similar fragmentation patterns occur.

¹H NMR Spectroscopy

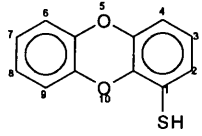
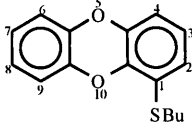
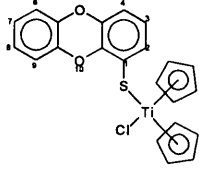
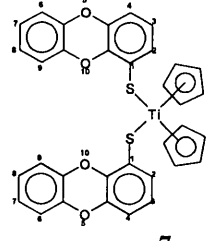
The ¹H NMR data for **5**, **5b**, **6** and **7** are summarized in **Table 5.2**. When comparing the chemical shifts of dibenzodioxinthiol, with dibenzodioxin we can see that the addition of the sulfur atom did not, with the exception of H2, influence the chemical shifts much. The chemical shifts of the ring without the thiol group are roughly the same as for dibenzodioxin, but due to their overlapping signals (**Fig. 5.1**) the specific chemical shifts could not be assigned for H6-H9. The ring with the thiolate group as substituent has a downfield shift of 0.34ppm for H2 and upfield


Scheme 5.4.

shifts of 0.02 and 0.08 ppm for H3 and H4, respectively. The proton closest to the substituent is downfield because of the electron withdrawing effect of the sulfur atom. In the spectrum of **5b** the presence of the butyl group is seen at chemical shift values 2.90, 1.44, and 0.89 ppm. The triplet at 2.9 ppm is indicative of protons on a carbon attached to a sulfur atom and adjacent to a methylene carbon. This supports **5b** of having a thioether unit rather than a butyl substituent on a thiophenol ring of the dioxin molecule.

Coordination of the thiolate to titanium in **6** results in a more shielded proton on C2, which indicates that the phenyl ring is shielded and not really affected by the coordination of the sulfur atom. H2 is 0.14 ppm upfield in **6** which can only be ascribed to π -resonance effects of

Table 5.2. The ¹H NMR data for dibenzodioxin-1-thiol, [TiCp₂(DbS)Cl] and [TiCp₂(DbS)₂].

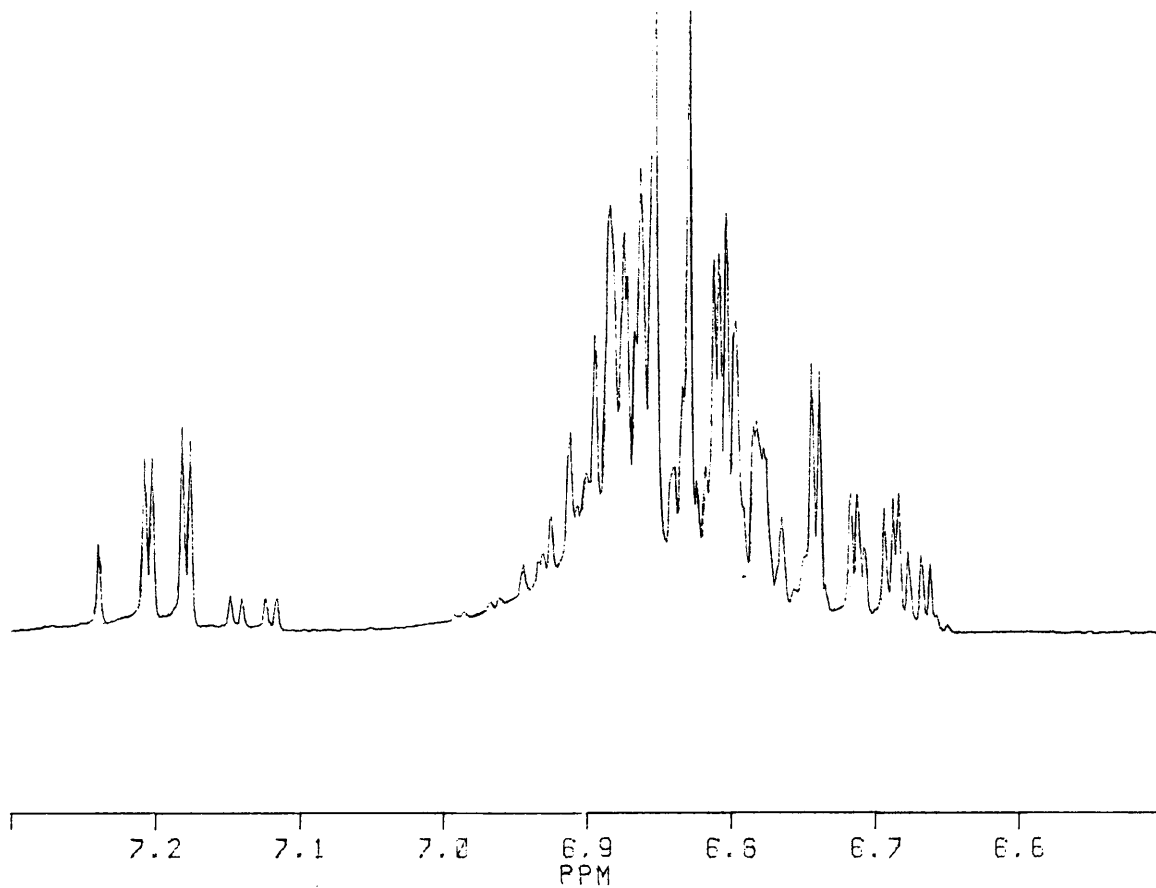
				
	Chemical Shift, δ (ppm) [†]			
H2	7.19 (dd)	7.13 (dd)	6.95 (dd)	7.31 (dd)
H3	6.83 (t)	°	6.87 (t)	6.84 (t)
H4	6.73 (dd)	6.68 (dd)	6.74 (dd)	6.69 (dd)
H6	6.76-6.91 (multiplet)	6.76-6.91 (multiplet)	6.81-6.97 (multiplet)	6.71-6.94 (multiplet)
H7				
H8				
H9				
SH	Not observed	---	---	---
Cp	---	---	6.31 (s)	6.11 (s)
Bu	---	2.90 (t), 1.44 (multiplet) and 0.89 (multiplet)	---	---
	Coupling Constant, ⁿ J _{H-H} (Hz)			
J ₂₃	7.9	7.1	8.0	7.9
J ₂₄	1.6	1.9	1.7	1.6
J ₃₄	8.1	7.7	7.9	8.0
J ₆₇	□	□	□	□
J ₆₈	□	□	□	□
J ₆₉	□	□	□	□
J ₇₈	□	□	□	□
J ₇₉	□	□	□	□
J ₈₉	□	□	□	□

[†] d¹-CDCl₃ used as solvent.

□ Difficult to calculate, due to multiplet.

° Triplet not clear on spectrum.

(a)



(b)

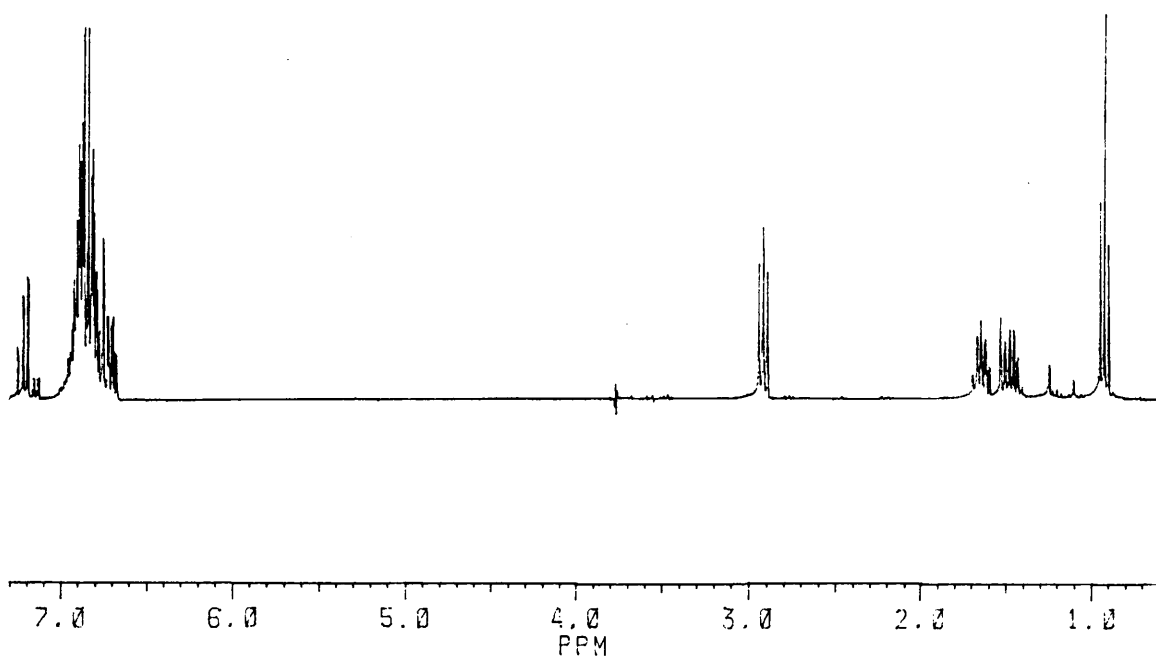


Fig. 5.1. The ¹H NMR spectra for (a) dibenzodioxinthalol showing the multiplet and (b) butyldibenzodioxinsulphide.

a sulphur lone pair to the substituted phenyl ring (**Fig. 5.2**). This will compete with π -donation from the sulphur to the titanium. The unsubstituted ring's protons are assigned as a multiplet (**Fig. 5.3**) and the general tendency of the chemical shifts are slightly downfield. The two Cp rings resonate as a singlet due to similar chemical environments. When a chloro ligand was replaced in **6**, it caused an upfield chemical shift for the Cp rings, revealing more electron density on the metal fragment. In **7** the replacement of both chloro ligands caused even more electron density to reside on the metal fragment and the chemical shift of the Cp rings was even further upfield.

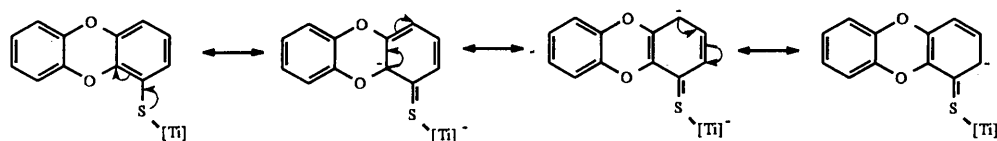


Fig. 5.2. Possible π -resonance effects of sulphur lone pairs in $[\text{TiCp}_2(\text{DbS})\text{Cl}]$.

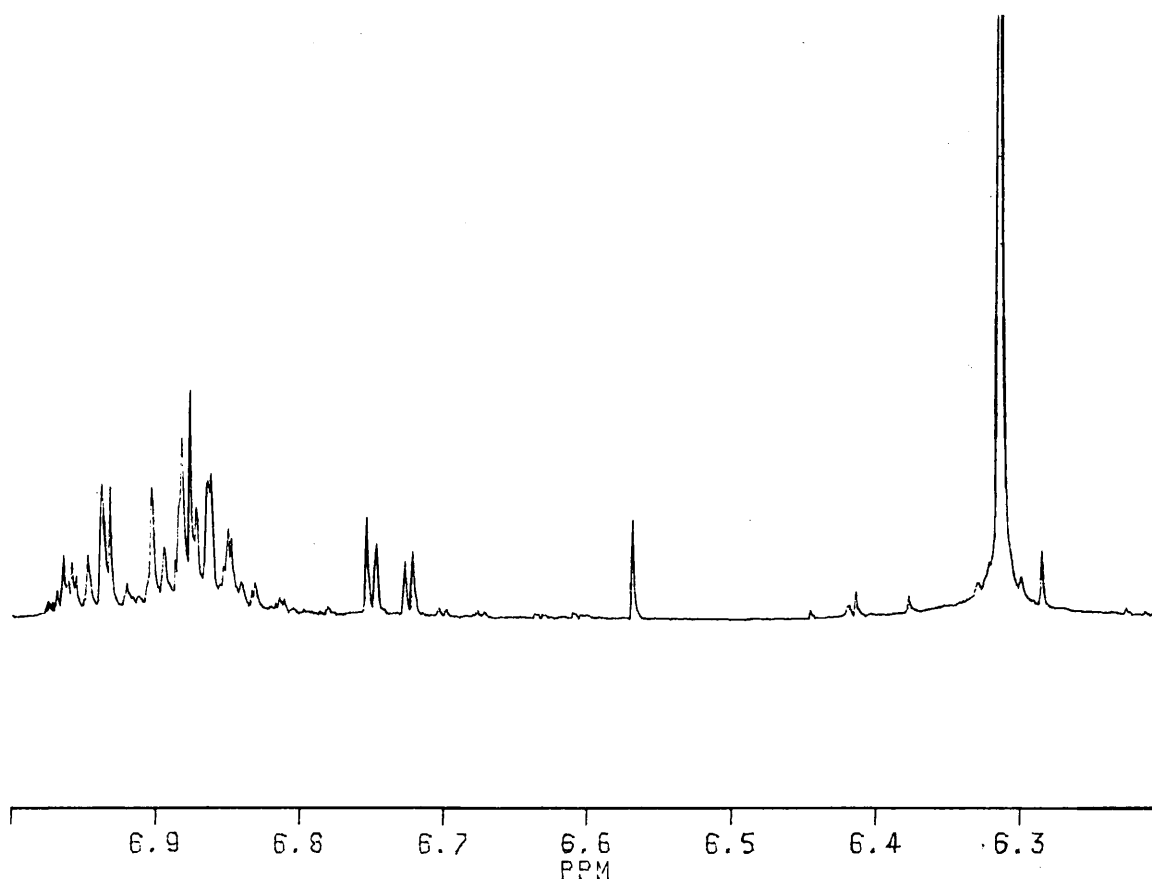


Fig. 5.3. The ^1H NMR spectrum for $[\text{TiCp}_2(\text{DbS})\text{Cl}]$ showing the multiplet.

The spectrum for **7** is shown in **Fig. 5.4**. Again there is a multiplet for H6-H9 and the chemical shifts are roughly the same. Notable is a significant downfield shift for H2 of 0.36ppm for **7** compared to **6**. The chemical shifts of H3 and H4 are about the same as for **5**, **6** and **7**.

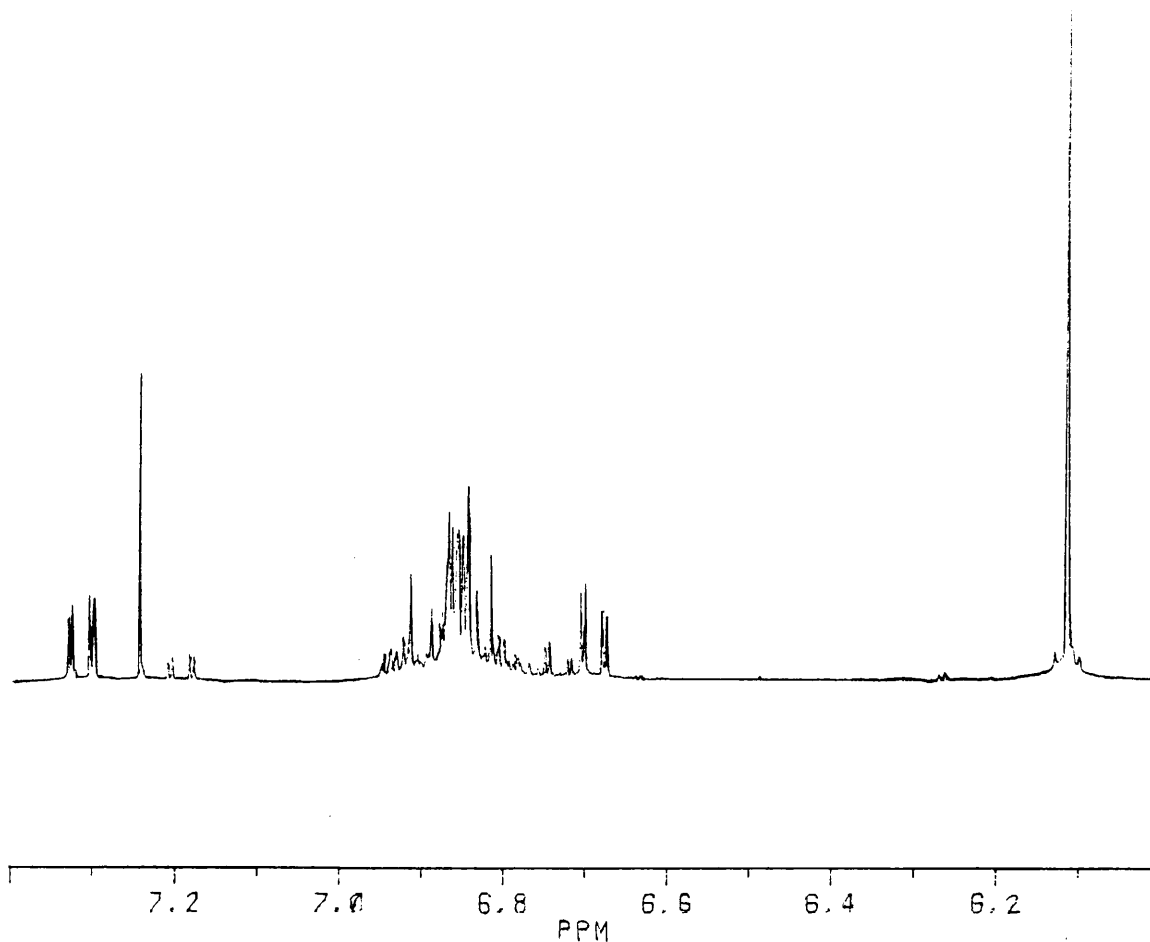


Fig. 5.4. The ^1H NMR spectrum for $[\text{TiCp}_2(\text{DbS})_2]$ showing the multiplet.

COSY

Two-dimensional homonuclear shift correlation spectroscopy (COSY) was used to obtain additional information of compound **5** (**Fig. 5.5**) to aid in assigning and distinguishing between the different ring protons. In spite of this, it was still difficult to assign protons, especially for the protons in the multiplet. It did however aid and confirm the assignment of H2, H3 and H4.

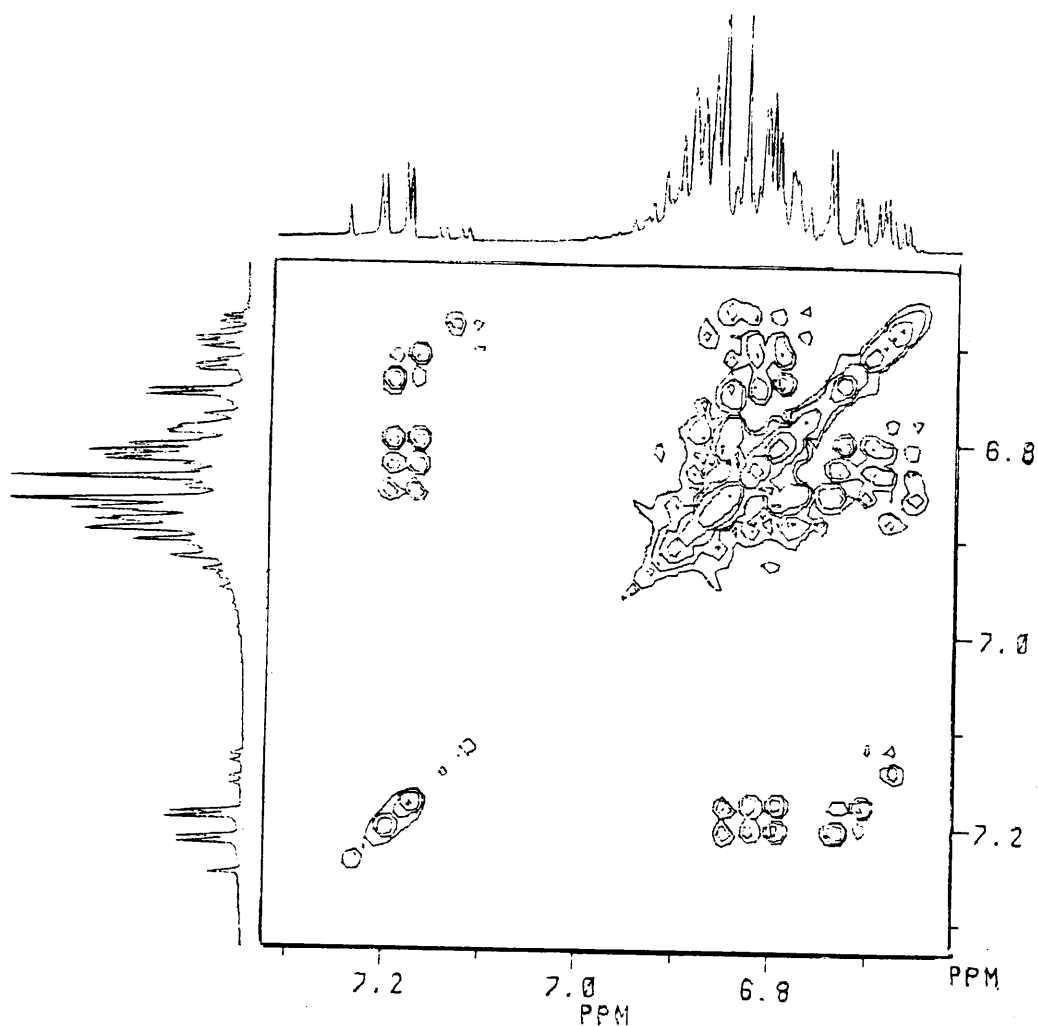
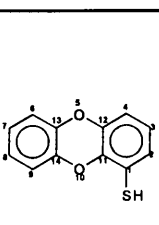
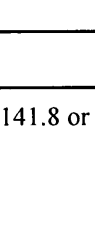
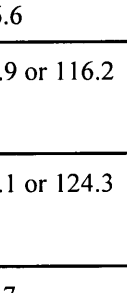
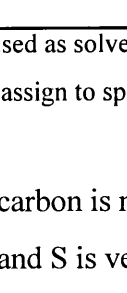


Fig. 5.5. The 2-D spectrum (COSY) for dibenzodioxinthiol.

¹³C NMR Spectroscopy

The ¹³C NMR spectral data for **5**, **5b**, **6** and **7** are given in **Table 5.3**. In **5** C1 is about 10ppm downfield from its position in [DbH]. The rest of the carbons are rather unaffected. In **5b** the four signals for the butyl group is present in the area of 30ppm.

Table 5.3. The ^{13}C NMR data for dibenzodioxinthalate, butyldibenzodioxinsulphide, $[\text{TiCp}_2(\text{DbS})\text{Cl}]$ and $[\text{TiCp}_2(\text{DbS})_2]$.

				
	5	5b	6	7
Chemical Shift, δ (ppm) [†]				
C1	126.7	126.7	°142-143 or 150.17	‡142.17, 142.23, 142.51 or 150.17
C12	‡141.7, 141.8 or	°141.5-143.0		
C13	142.4			
C14				
C2	124.7	124.4	129.67	129.50
C3	123.5	123.3	122.99	123.00
C4	116.6	116.8	120.44	116.88
C6	‡115.9 or 116.2	‡ 114.3 or 114.3	‡116.19 or 116.83	‡114.44 or 116.07
C9				
C7	‡124.1 or 124.3	‡ 123.8 or 124.1	‡123.52 or 124.06	‡123.59 or 123.65
C8				
C11	167.7	150.1	178.74	178.75
Cp	---	---	115.95	112.81
Bu	---	13.6, 22.0, 31.1 and 32.4	---	---

[†] $\text{d}^1\text{-CDCl}_3$ used as solvent.

[°] Carbons not clear on spectrum.

[‡] Difficult to assign to specific carbons.

In **6** the C1 carbon is not as far downfield as was observed in **1**. This confirms that the bonding between Ti and S is very much restricted to a localized interaction and the ring is little affected by it. Carbons, C11 and C12, are further downfield because of the effects of the neighbouring oxygen atoms. The rest of the carbons are rather unaffected, while the Cp resonances are shifted upfield due to the increased electrondensity on the metal fragment.

In **7** C1 is downfield as expected and the rest of the signals are about the same as for **6**. The resonances of the carbon atoms of the substituted ring are almost identical to those of **6**.

HETCOR

The HETCOR spectrum of compound **5** is shown in **Fig. 5.6**. This was useful to assign the specific proton peaks to their carbons resonances, especially for H2, H3 and H4. Again this was impossible for the protons in the unsubstituted ring.

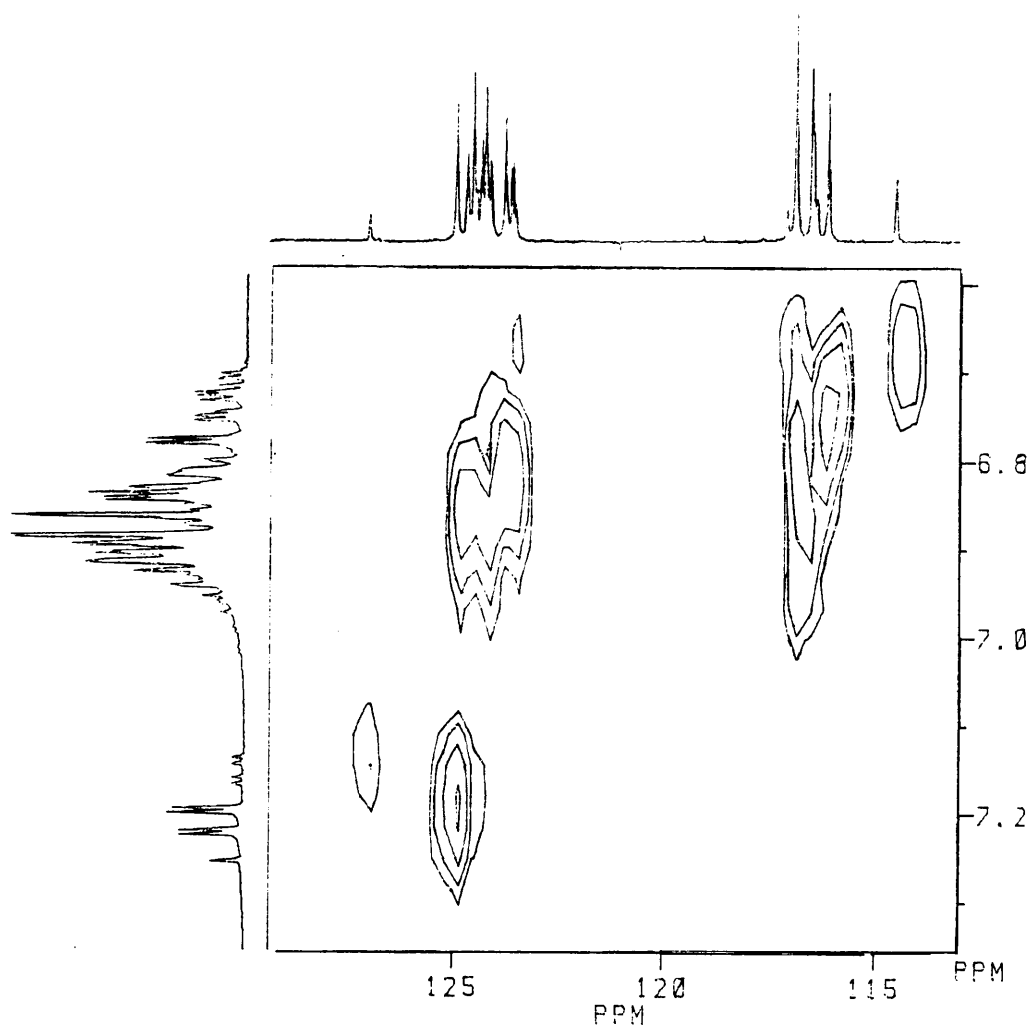
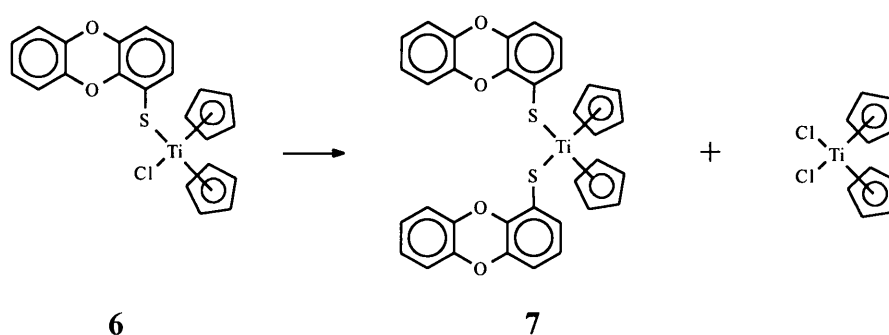


Fig. 5.6. The 2-D spectrum (HETCOR) for dibenzodioxinthiol

5.3 Conclusion

Dibenzodioxinithiol **5** and its thiolato complexes of titanium were successfully characterized. The inserted sulfur in **6** or **7** moves the titanium out of the plane of the dioxin ring ligand and different antitumour properties are expected. The compound is easily handled and its conversion into the bithiolate is slow (**Scheme 5.5**).



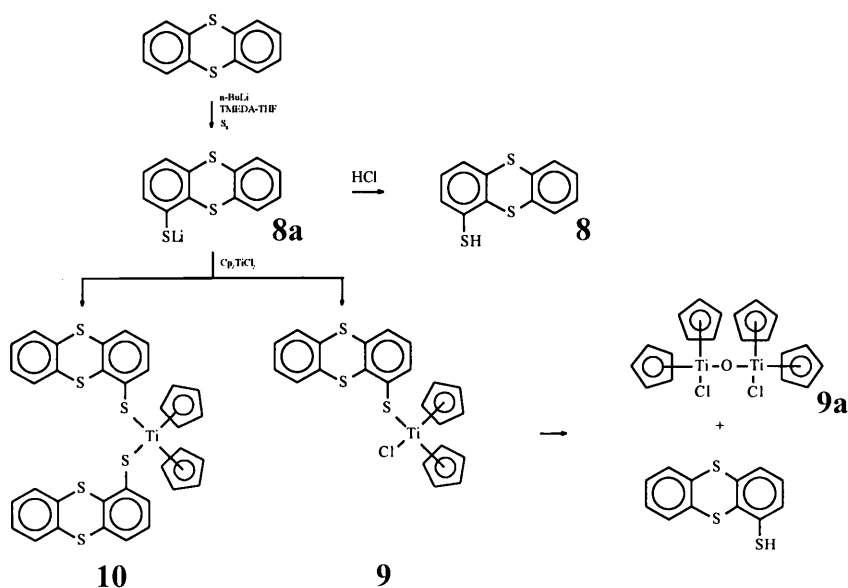
Scheme 5.5.

Unfortunately the thiolate ligand is of a comparable lability with the chloro ligand and the loss of the potential intercalator is a strong possibility. Surprisingly, no literature evidence could be found indicating that the dibenzodioxinithiol has been prepared before. The formation of the thioether was unexpected and needs further investigation. The possible antitumour properties of **6** and **7** will be discussed in Part III.

6. Titanocene Complexes with Thianthrenethiolate as Ligand

6.1 Synthesis

The reaction of lithiated thianthrene [ThH] with flowers of sulfur yielded lithiated thianthrene-1-thiolate **8a**, which formed a white powder thianthrenethiol **8** [ThSH], when protonated with HCl gas. No information of this product could be found in literature and it was also fully characterized. In **8** the compound did not react with butyl to give the corresponding thioether as was found for [DbH] **5**. The reaction of the lithiated thiolate with titanocene dichloride was expected to yield chlorobis(cyclopentadienyl)(thianthrene-1-thiolato)titanium(IV) **9** and bis(cyclopentadienyl)bis(dibenzodioxin-1-thiolato) titanium(IV) **10** (Scheme 6.1). The reaction products were purified by chromatography on a silica gel column affording a purple product which was collected before the second red product.



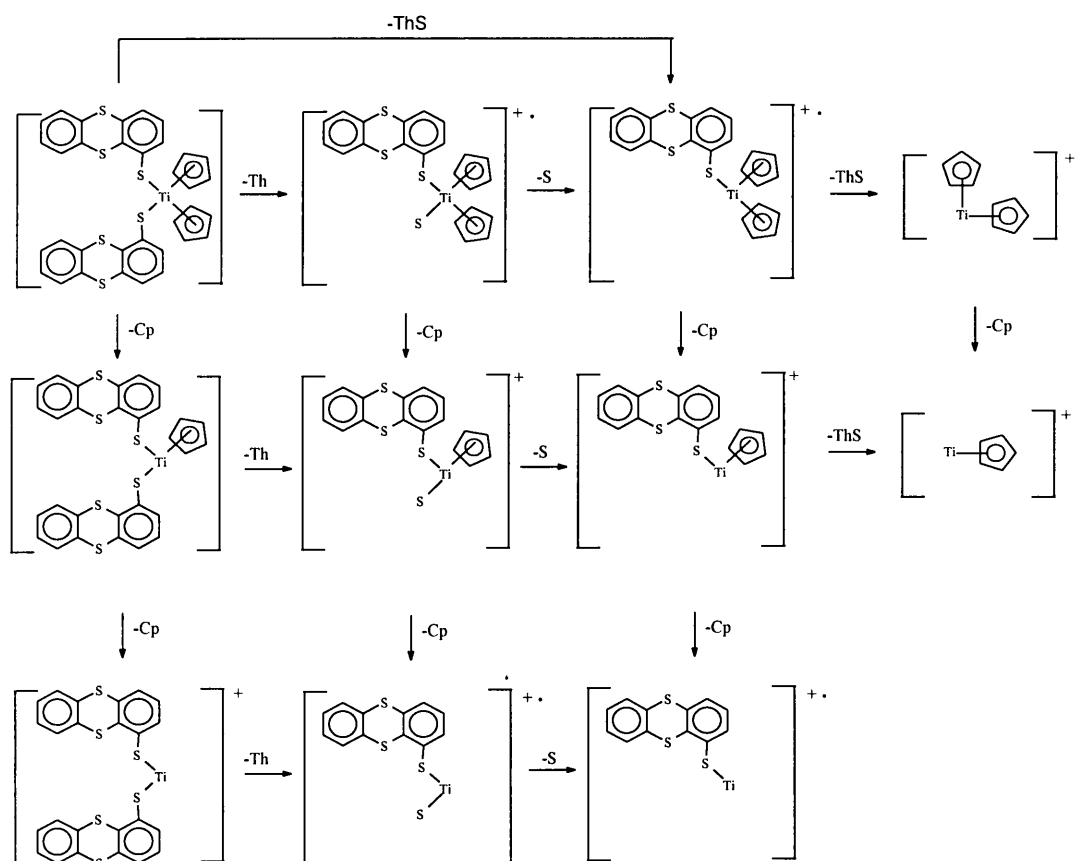
Scheme 6.1

The purple fraction was characterized as $[\text{TiCp}_2(\text{ThS})_2]$ **10**, a very light sensitive complex, which lost colour within a few hours after being exposed to light. The red fraction $[\text{TiCp}_2(\text{ThS})\text{Cl}]$ **9** was also unstable and the ^1H NMR showed that it decomposed to the free ligand and the oxygen bridged dimer μ -oxobis{chlorobis(cyclopentadienyl)titanium(IV)}¹.

6.2 Characterization

Mass spectrometry

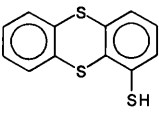
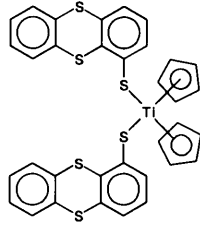
The mass spectra of **8** and **10** were recorded and the data are summarized in **Table 6.1**. Fragmentation patterns for **10** are shown in **Scheme 6.2** and the competitive pathways are shown and represent the fragmentation of Cp and ThS ligands.



Scheme 6.2.

1. S. A. Giddings, *Inorg. Chem.*, 1964, 5, 684; D. Nath, R. K. Sharma, A. N. Bhat, *Inorg. Chim. Acta*, 1976, 20, 109.

Table 6.1. Mass spectral data for thianthrene-1-thiol and [TiCp₂(ThS)₂].

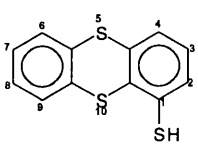
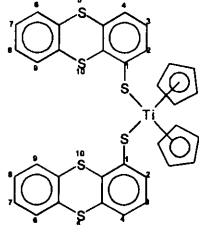
 8	 10
Mass peaks ² , m/z (I%)	Mass peaks, m/z (I%)
248 (100) [M]	674 (6) [M] ⁺
216 (13) [ThH] ⁺	609 (66) [TiCp(ThS) ₂] ⁺⁺
215 (78) [Th] ⁺	544 (47) [Ti(ThS) ₂] ⁺
184 (53) [M-S] ⁺	457 (6) [TiCp ₂ (ThS)S] ⁺⁺
171 (38) [Th-CSH] ⁺	425 (4) [TiCp ₂ (ThS)] ⁺⁺
152 (1) [Th-2S] ⁺	392 (100) [TiCp(ThS)S] ⁺⁺
139 (13) [Th-(CSH+S)] ⁺	360 (5) [Ti(ThS)S] ⁺⁺
	327 (6) [Ti(ThS)S] ⁺⁺
	295 (6) [Ti(ThS)] ⁺⁺
	263 (9) [Ti(Th)] ⁺⁺
	248 (2) [ThSH] ⁺
	216 (22) [ThH] ⁺
	215 (6) [Th] ⁺
	178 (81) [TiCp ₂] ⁺
	113 (4) [TiCp] ⁺⁺

¹H NMR Spectroscopy

The data from the ¹H NMR spectra of **8** and **10** is summarized in **Table 6.2**. In **8**, the addition of the sulfur did not influence the chemical shifts of the protons too much, compared to thianthrene. The chemical shifts of the ring protons without the thiolate group are roughly the same as those for thianthrene. Due to the overlapping of signals (**Fig. 6.1**) the specific chemical shifts for H6-H9 could not be assigned. The ring with the thiolate groups displayed downfield

2. N. P. Buu-Hoi, G. Saint-Ruf, M. Mangane, *J. Heterocycl. Chem.*, 1972, 9, 691.

Table 6.2. ¹H NMR spectral data for thianthrene-1-thiol and [TiCp₂(ThS)₂].

 8		 10	
Chemical Shift, δ (ppm) [†]			
H1	---	---	
H2	7.48	7.72	(dd)
H3	7.13	7.13	(dd)
H4	7.33	7.27	(dd)
H6	7.18-7.29 (multiplet)	7.18-7.24 (multiplet)	
H9			
H7	7.43-7.57 (multiplet)	7.43-7.50 (multiplet)	
H8			
SH	Not observed	---	
Cp	---	6.31	(s)
Coupling Constant, ⁿ J _{H-H} (Hz)			
J ₂₃	7.8	7.8	
J ₂₄	1.4	1.4	
J ₃₄	7.7	7.6	
J ₆₇	□	□	
J ₆₈	□	□	
J ₆₉	□	□	
J ₇₈	□	□	
J ₇₉	□	□	
J ₈₉	□	□	

[†] d¹-CDCl₃ used as solvent.

□ Difficult to calculate, due to multiplet.

shifts of 0.24ppm for H2 and the resonances of H3 and H4 are little affected. The proton closest to the thiolate is also closest to the site of the more electronegative sulphur and loses more electron density than the other protons.

Coordination of ThS to titanium in **10** causes the withdrawal of even more electron density from the aromatic system and leaves the substituted ring with a partial positive charge. This is most pronounced in the chemical shifts of the H2 protons. The proton on C2 is closest to the positions

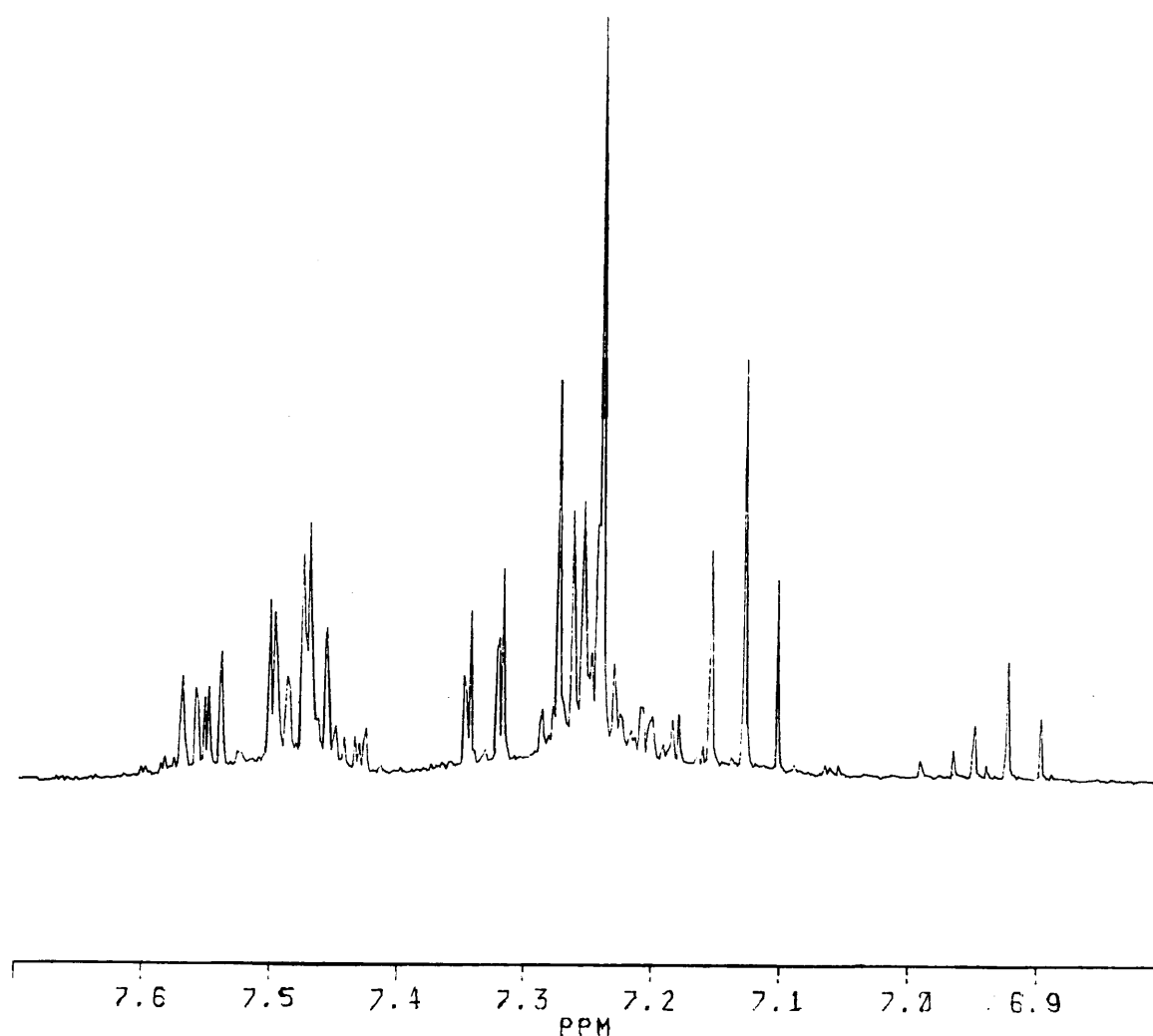


Fig. 6.1. The ¹H NMR spectrum for [ThSH] showing the region of the multiplet.

of coordination and hence the most affected. The unsubstituted ring's protons are a multiplet (**Fig. 6.2**) and the general trend of chemical shifts is slightly downfield. The two Cp rings resonate as a singlet due to similar chemical environments. In **10** the replacement of both chloro ligands caused more residual electron density on the metal fragment and the chemical shift of the Cp rings is more upfield.

The spectrum for **9** showed resonances indicating that the complex decomposes quickly to the free ligand and $[\{\text{TiCp}_2\text{Cl}\}_2(\mu\text{-O})]$ **9a**. The two Cp signals are in a 1:1 ratio and it means that the two sets of Cp rings are in different chemical environments.

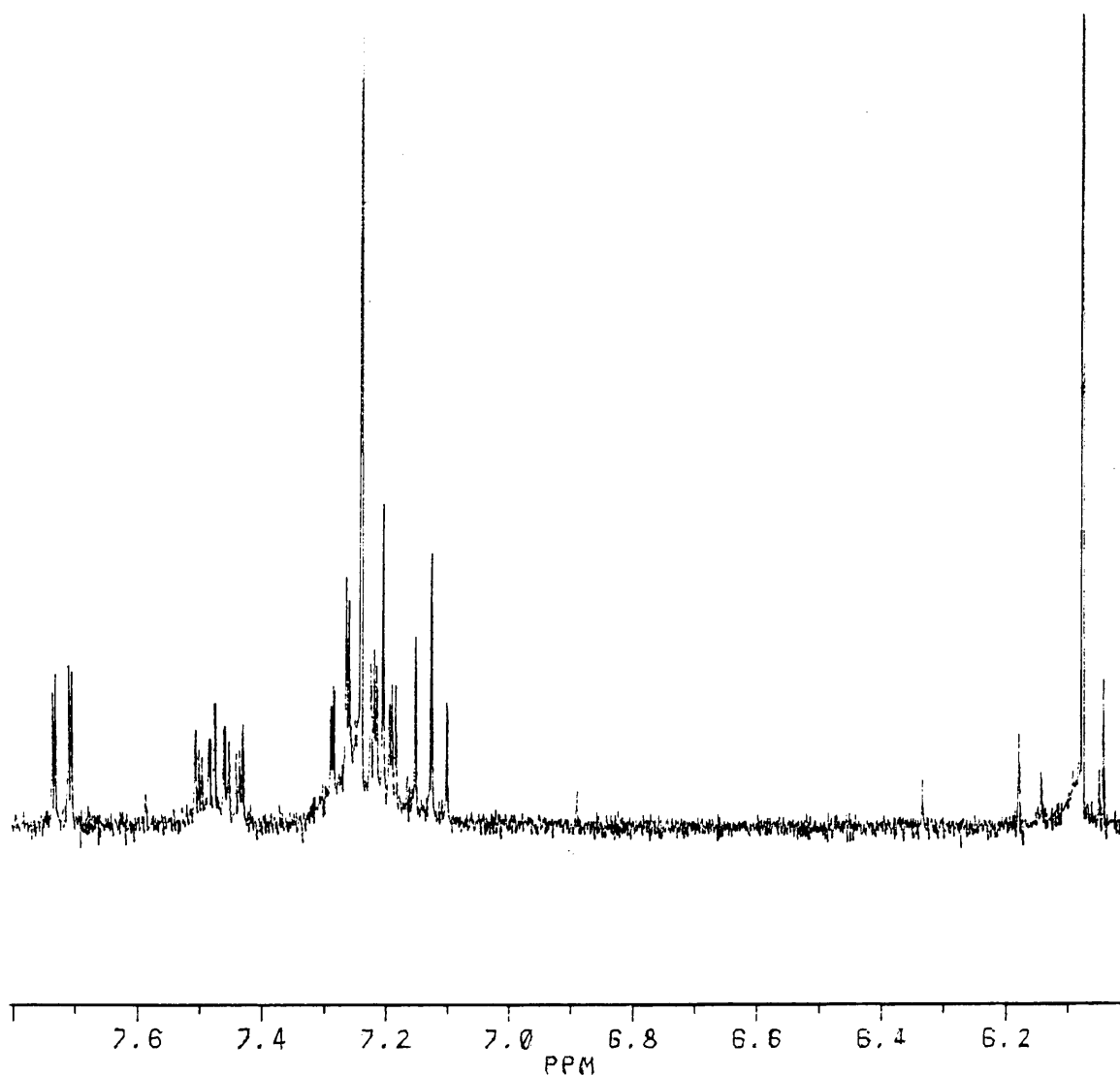


Fig. 6.2. The ^1H NMR spectrum for $[\text{TiCp}_2(\text{ThS})_2]$ showing the multiplet.

COSY

Two-dimensional homonuclear shift correlation spectroscopy (COSY) was used to assign protons to the phenyl rings of compound **8** (Fig. 6.3). This problem could not be solved for the protons in the multiplet. It was possible, however, to discriminate between the sets H6 and H9 and H7 and H8, respectively.

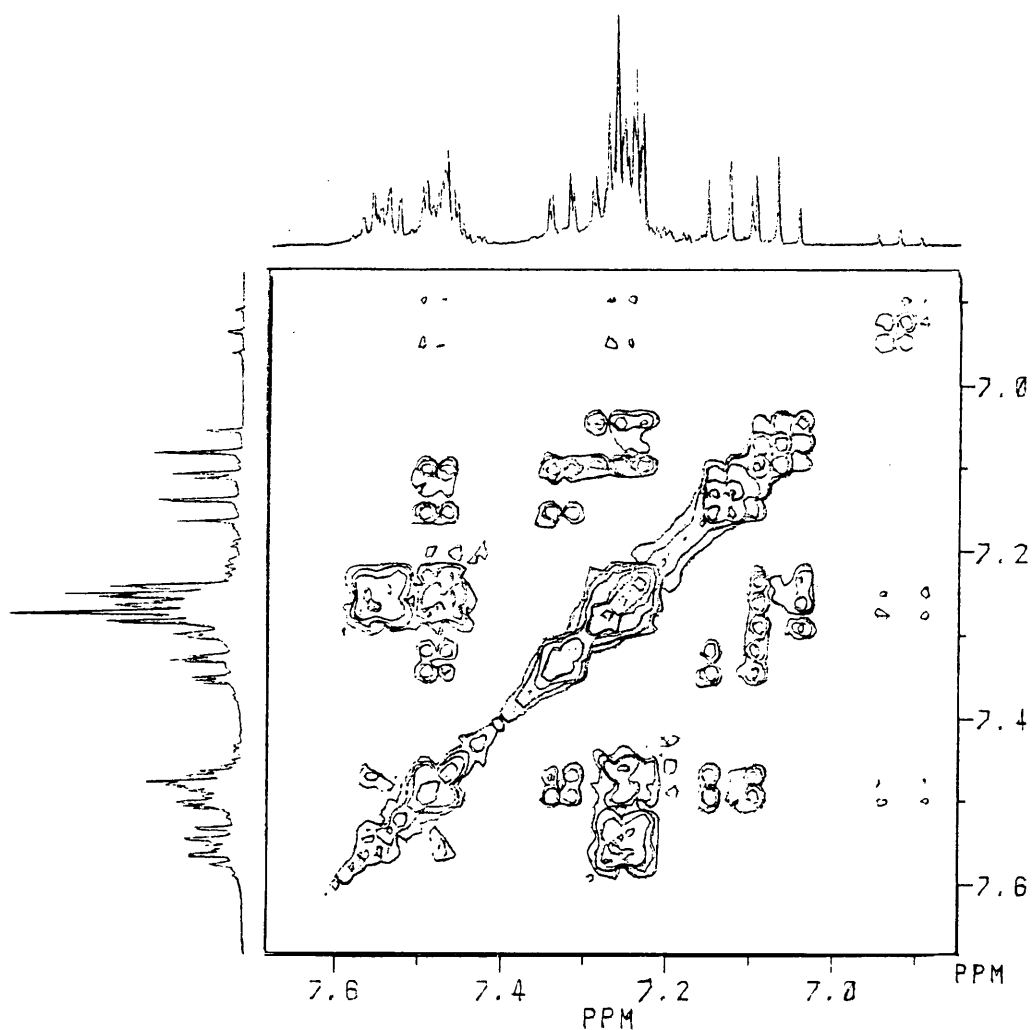
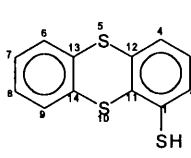
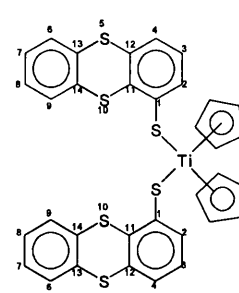


Fig. 6.3. The 2-D spectrum (COSY) for thianthrenethiolate.

¹³C NMR Spectroscopy

The ¹³C NMR spectral data for **8** and **10** is given in Table 6.3. In **8** C1 is downfield due to the electron withdrawing effect of the sulfur atom. The other carbons are little affected and have about the same chemical shifts compared to the corresponding carbons in [ThH]. The carbons C2 and C3 are also downfield and this correlates with the results from the ¹H NMR spectrum.

Table 6.3. ¹³C NMR spectral data for thianthrene-1-thiol and [TiCp₂(ThS)₂].

		
Chemical Shift, δ (ppm) [†]		
C1	136.9	176.0 and *178.1
C2	129.2	132.5 and *133.2
C3	128.7	128.7 [▪]
C4	123.5	128.3 [▪]
C6	126.2 or 127.7	‡126.9 or 126.4 [▪]
C9		
C7	127.8 or 128.2	‡127.5 or 127.7 [▪]
C8		
C11	176.0	148.0 or *148.0
C12	134.2, 135.7 or 136.2	‡135.7, 135.9 or 137.4 [▪]
C13		
C14		
Cp	---	112.8 or *113.4

[†] d¹-CDCl₃ used as solvent.

^{*} Two signals due to two heteroaromatic ligands.

[‡] Difficult to assign to specific carbons.

[▪] Second signal difficult to assign.

In **10** the Cp signals appear as two single peaks in a ratio of 3:1. This ratio is repeated for the rest of the spectrum and can be ascribed to two different isomers in solution. The C1 carbon is far downfield as expected, due to the electron density transferred to sulfur and the metal centre. The neighbouring carbons, C2 and C11, are less downfield than C1. The rest of the carbons are rather unaffected, while the Cp's carbons resonate upfield due to the increased electron density on the metal fragment.

6.3 Conclusion

The aim was to synthesize lithiated thianthrene-1-thiolate **8a** and from this, $[\text{TiCp}_2(\text{ThS})\text{Cl}]$ **9** and $[\text{TiCp}_2(\text{ThS})_2]$ **10**. This was done by the methods described. The new ligand **8** was a white powder and the complexes were purple and red compounds respectively. Thianthrenethiol **8** and $[\text{TiCp}_2(\text{ThS})_2]$ **10** were characterized by mass spectrometry and NMR spectroscopy. The possible antitumour properties will be discussed in Part III. Complex **9** was very unstable and NMR spectra showed that it decomposed to the free ligand and complex **9a**.

Unfortunately the desired monosubstituted thiolate **9** was very unstable and not suitable for further studies. A high lability for the remaining chloro ligand in **9** was hoped for, but in this case it was too high to be practically useful and under normal conditions led to the destruction of the targeted complex. However, the possible antitumour properties will be discussed in Part III.

Interestingly no report could be found that the thiol **8** have been reported before. Also, during the synthesis the analogous thioether ThSBu, did not form as was found for DbSBu.

7. Titanocene Complexes with Thianthrene as Ring-Opened Ligand

7.1 Introduction

The insertion of transition metals between the S and C bond of thiophene derivatives was recognized and have been widely studied. This is seen as the key step in the hydrodesulfurisation process; important for the removal of thiophenes from fossil fuels. Examples have been found for many late and middle transition metals, such as Pt¹, Ir², Rh³, Fe⁴, Mn⁵, etc., but none for the early transition metals such as Ti(IV). This can be understood on the basis of metal insertions being promoted by transition metals in low oxidation states and the insertions are described to be oxidative addition reactions. Recently Rauchfuss and co-workers⁶ opened a thiophene C-S bond of dibenzothiophene reductively by reacting the thiophene with lithium biphenylide. After subsequent reaction with titanocene dichloride, the titanacycle shown in **Fig. 7.1** was obtained.

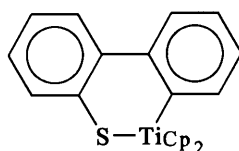
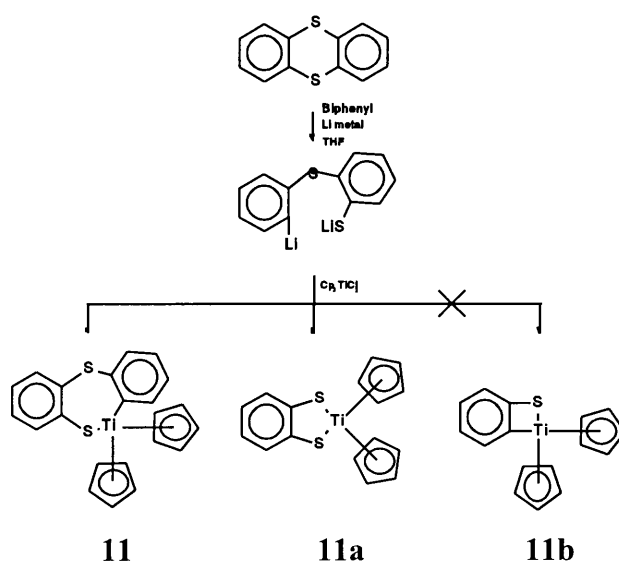


Fig. 7.1 The titanacycle synthesized from dibenzothiophene.

1. J. J. Garcia, B. E. Mann, H. Adams, N. A. Bailey, P. M. Maitlis, *J. Am. Chem. Soc.*, **1995**, *117*, 2179.
2. J. Chen, C. M. Daniels, R. J. Angelici, *J. Am. Chem. Soc.*, **1990**, *112*, 199.
3. C. Binanchini, V. Herra, M. V. Jiménez, F. Laschi, A. Meli, R. Sanches-Delgado, F. Vizza, P. Zanello, *Organometallics*, **1995**, *14*, 4390.
4. C. Blonski, A. W. Meyers, M. Palmer, S. Harris, W. D. Jones, *Organometallics*, **1997**, *16*, 3819.
5. C. A. Dullaghan, S. Sun, G. B. Carpenter, B. Weldon, D. A. Sweigart, *Angew. Chem. Int. Ed. Engl.*, **1996**, *35*, 212.
6. P. R. Stafford, T. B. Rauchfuss, A. K. Verma, S. R. Wilson, *J. Organomet. Chem.*, **1996**, *256*, 203.

7.2 Synthesis

In this chapter we will look at the resulting complex where the Ti-fragment is inserted into the thianthrene ligand. The insertion of the titanocene fragment into the ring-opened thianthrene ligand was done according to the method described by Rauchfuss⁶. The outline for the reaction is given in **Scheme 7.1**. In this case, the reaction was expected to yield as many as three products. Complex **11** and possibly two other products, caused by the unsymmetric and symmetric cleavage of the ligand, represented by complexes **11a** and **11b**, respectively. On the column three fractions were indeed collected. A red zone, followed by a green and finally an orange fraction. The main product was a light sensitive red complex, which was characterized as complex **11**. The green complex, characterized as **11a**, was already described in literature^{7,8} and will not be discussed in this section. From the mass spectra it was concluded that the orange fraction was not **11b**, but an organic product where two ring-opened ligands were released from the metal and combined to form a dimer. The metal centre acted as a template and facilitated the dimer formation, which consisted of a cyclic compound, with four thiophenylene units [(1,2-C₆H₄S)₄] (**Fig. 7.2**). All complexes were characterized by NMR spectroscopy and mass spectrometry.



Scheme 7.1.

7. H. Köpf, *Angew. Chem.*, **1971**, *83*, 146.

8. A. Kutoglu, *Z. Anorg. Allg. Chem.*, **1972**, *390*, 195.

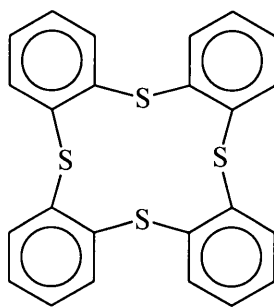
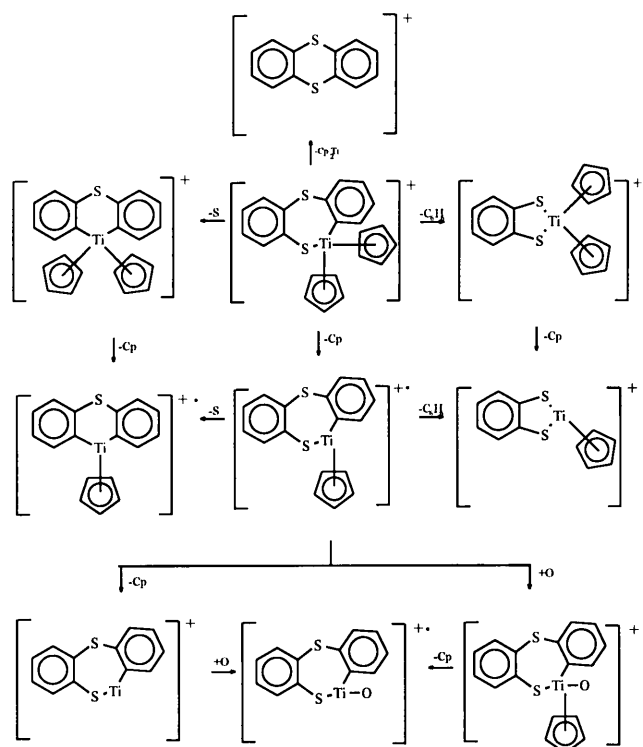


Fig. 7.2 The cyclic dimer [(1,2-C₆H₄-S)₄].

7.3 Characterization

Mass spectrometry

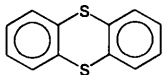
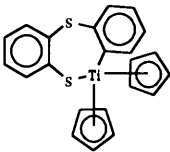
The mass spectra for thianthrene ⁹ and complex **11** are given in **Table 7.1**. The molecular ion [M⁺] of **11** was observed, but is of low intensity and the principal ion is at m/z-value 184,



Scheme 7.2.

9. N. P. Buu-Hoi, G. Saint-Ruf, M. Mangane, *J. Heterocycl. Chem.*, 1972, 9, 691.

Table 7.1 The mass spectral data for thianthrene and [TiCp₂(SC₆H₄SC₆H₄)].

	 11
Mass peaks, m/z (I%)	Mass peaks, m/z (I%)
216 (100) [M] ⁺	394 (9) [M] ⁺
184 (70) [M-S] ⁺	362 (1) [TiCp ₂ (C ₁₂ H ₈ S)] ⁺
171 (22) [M-CSH] ⁺	345 (38) [TiCp(C ₁₂ H ₈ S ₂)O] ⁺
152 (5) [M-2S] ⁺	329 (7) [TiCp(C ₁₂ H ₈ S ₂)] ⁺⁺
139 (22) [M-(CS ₂ H)] ⁺	318 (15) [TiCp ₂ (C ₆ H ₄ S ₂)] ⁺
	297 (1) [TiCp(C ₁₂ H ₈ S)] ⁺
	280 (3) [Ti(C ₁₂ H ₈ S ₂)O] ⁺
	264 (1) [Ti(C ₁₂ H ₈ S ₂)] ⁺
	253 (36) [TiCp(C ₆ H ₄ S ₂)] ⁺
	217 (76) [ThH] ⁺
	216 (35) [Th] ⁺⁺
	184 (100) [Th-(HS)] ⁺
	178 (12) [TiCp ₂] ⁺
	113 (6) [TiCp] ⁺

corresponding to the fragment ion of dibenzothiophene. There are several possible fragmentation pathways as shown in **Scheme 7.2**. The major pathway is the one where thianthrene is regenerated. It is interesting to note that whereas the fragmentation of one Cp is important, the peaks where two Cp rings are lost are either absent or of very low intensity. There is also a pathway whereby oxygen from the atmosphere is added to the titanium centre.

¹H NMR Spectroscopy

The ¹H NMR spectroscopic data for thianthrene and **11** are tabulated in **Table 7.2**. In the spectrum of **11** the existence of two isomers is clearly visible and there is an isomeric ratio of

about 1:3. **Fig. 7.3** illustrates that the ligand is not planar and that there is a reversible inversion of the conformation. This will correspond to a fluxional process in the molecule and it is not clear that this could cause the duplication of resonances. If the process is fast, a single set of signals would be expected and if slow, two sets of equal intensity should appear. The aromatic ring closest to the titanium was affected most. H1 and H3 are downfield from their original position and H2 and H4 are upfield. This can be explained by the fact that when thianthrene is lithiated, there is a negative charge on the lithiated ring which causes all resonances to move upfield. The addition of titanium removes electron density from the ring by π -resonance effects and there is a downfield shift of some of the signals.

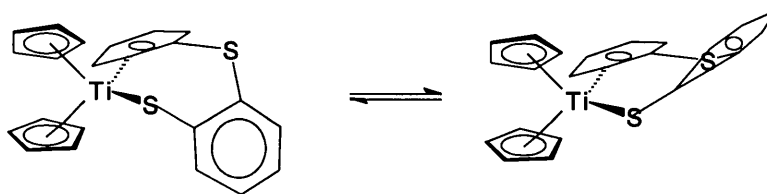
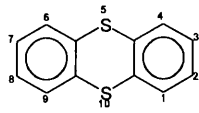
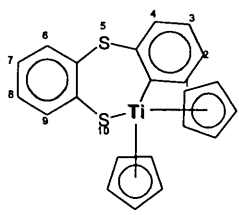


Fig. 7.3. Two isomers of $[\text{TiCp}_2(\text{SC}_6\text{H}_4\text{SC}_6\text{H}_4)]$.

As explained in Chapter 3, there are two possible ways to explain the shifts in electrondensity. Now however, the σ -inductive effect is between the metal and C11 and the π -resonance effects are illustrated in **Fig. 7.4**. Note that H1 and H3 if left with less electron density corresponding to a shift further downfield compared to H2 and H4. H1 is influenced most because it is closest to titanium. The other phenyl ring was quite unaffected and due to overlapping and the appearance of peaks belonging to the isomers, these protons could not be specifically identified and assigned (**Fig.7.5**). It is possible to discriminate between the combinations of H6 and H9 and H7 and H8, respectively. The isomer ratio is also reflected in the Cp signals which are upfield from those of titanocene dichloride. Therefore, the chloro ligands have a more deshielding effect on the metal than the thianthrene ligand, which is inserted.

Table 7.2. The ^1H NMR spectroscopic data for thianthrene and $[\text{TiCp}_2(\text{SC}_6\text{H}_4\text{SC}_6\text{H}_4)]$.

  11		
Chemical Shift, δ (ppm) [†]		
H1	7.48	7.81 (dd)
H2	7.24	7.07 (dt)
H3	7.23	7.56 (dt)
H4	7.48	6.75 (dd)
H6	7.48	7.35-7.49 (multiplet)
H9	7.48	
H7	7.23	7.12-7.33 (multiplet)
H8	7.24	
Cp	---	6.10 and 6.02 (s)
Coupling Constant, $^nJ_{\text{H-H}}$ (Hz)		
J_{12}	7.7	7.7
J_{13}	1.5	1.5
J_{14}	0.4	---
J_{23}	7.5	7.7
J_{24}	1.5	1.5
J_{34}	7.7	7.9
J_{67}	7.7	□
J_{68}	1.5	□
J_{69}	0.4	□
J_{78}	7.5	□
J_{79}	1.5	□
J_{89}	7.7	□

[†] $d^1\text{-CDCl}_3$ used as solvent.

□ Difficult to calculate, due to multiplet.

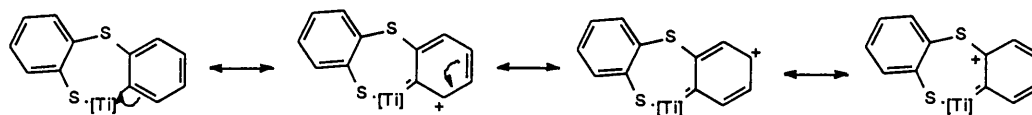


Fig. 7.4. The inductive effect of $[\text{TiCp}_2(\text{SC}_6\text{H}_4\text{SC}_6\text{H}_4)]$.

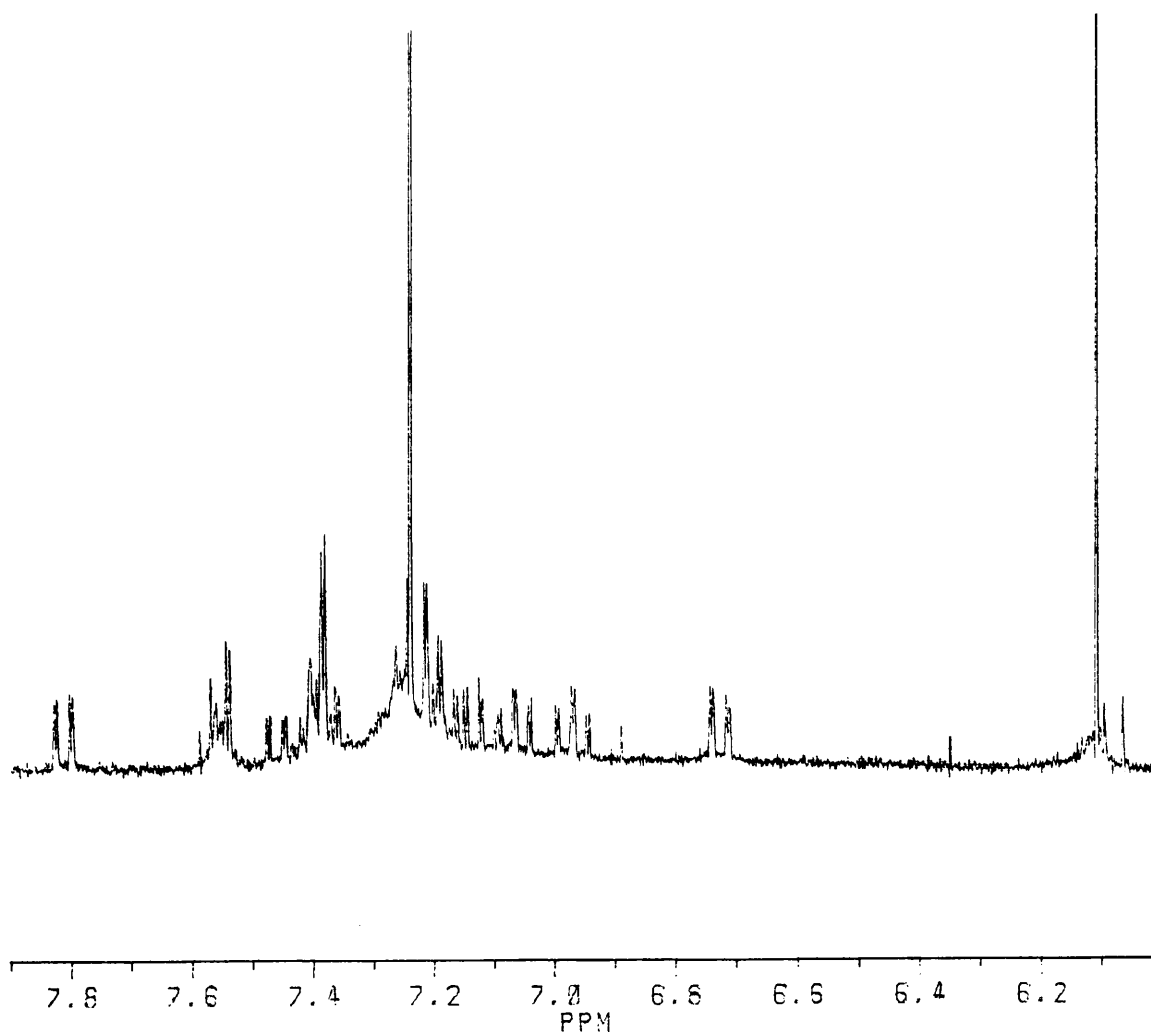
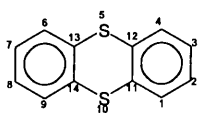
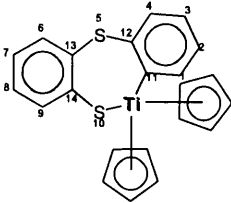


Fig. 7.5. The ^1H NMR spectrum of $[\text{TiCp}_2(\text{SC}_6\text{H}_4\text{SC}_6\text{H}_4)]$ showing multiplets.

^{13}C NMR Spectroscopy

The ^{13}C NMR spectral data for thianthrene and **11** are tabulated in **Table 7.3**. In this case no isomeric ratio was observed and only a single set of carbon resonances was obtained. The Ti-C

Table 7.3. The ^{13}C NMR spectral data for thianthrene and $[\text{TiCp}_2(\text{SC}_6\text{H}_4\text{SC}_6\text{H}_4)]$.

		
Chemical Shift, δ (ppm) [†]		
C1	128.7	176.0
C2	127.7	118.1
C3	127.7	112.7
C4	128.7	109.7
C6	128.7	‡123.5 or 129.4
C7	127.7	
C8	127.7	
C9	128.7	
C11	135.5	189.8
C12	135.5	141.9
C13	135.5	‡133.5 or 135.0
C14	135.5	
Cp	---	150.1

[†] $\text{d}^1\text{-CDCl}_3$ used as solvent.

[‡] Difficult to assign to specific carbons.

bond properties caused C11 to be shifted far downfield and also C1 is found further downfield than what was anticipated. This is ascribed to the π -resonance effects in the coordinated ring. The values of C6-C9 are difficult to assign but it was noticed that some of these were more upfield than expected. This can be due to the ring opening, which caused the aromaticity to be disturbed.

7.4. Conclusion

The method described by Rauchfuss¹⁰ could be successfully extended to insert a titanium biscyclopentadienyl fragment into thianthrene, between a phenyl carbon and a sulfur atom. Complex **11** is light sensitive, leading to the elimination of the titanium fragment and regeneration of the thianthrene ligand, as well as decomposition products. Also interesting is the template effect of titanium in constructing the cyclic tetraphenylthioether, compound **11b**. None of these products have any relevance to the theme of the study, relating to compounds designed for biological activity, but nevertheless extended the chemistry of titanium complexes with thianthrene.

10. P. R. Stafford, T. B. Rauchfuss, A. K. Verma, S. R. Wilson, *J. Organomet. Chem.*, **1996**, 256, 203.

Part III

Comparison and Antitumour Properties

8. Comparison of Geometries	86
9. Antitumour Properties	92

8. Comparison of Geometries

8.1 Chalcanthrenes

As structural orientations of the plane of the condensed ring ligand with respect to the labile chloro ligand and the stopper cyclopentadienyl rings are of utmost importance in the design of the complexes, the structural features of the new complexes will be studied and compared.

When the ball-and-stick model of the actual crystal structure determination of [TiCp₂(Db)Cl] **1** (Fig. 8.1) and the spacefill model generated by computer software (Fig. 8.2) is compared with the computer generated model of [TiCp₂(Th)Cl] **3** (Fig. 8.3), we can see that the heteroaromatic ligands have different geometries. The spacefill models represent the lowest energy arrangement as constructed by computer modelling. The results were obtained by using SYBYL¹. In Fig. 8.1 and 8.2 it can be seen that the dibenzodioxin ligand is practically planar when σ -bonded to titanium. In Fig. 8.3 the thianthrene ligand displays a bent geometry. The only difference between the two ligands is the heteroatoms, but this difference causes the ligands to behave totally different.

According to Amato², dibenzodioxin shows an upfield chemical shift for the protons closest to the heteroatom, when compared to the other chalcanthrenes, due to the modification of the paramagnetic term by oxygen. Oxygen is not able to participate in the π -delocalization effects and therefore the C-O-C bond angle is smaller than expected. It is also known that the angle of the fold in the chalcanthrenes, decreases with an increase of molecular mass of the heteroatom. The angle of the fold of dioxin is the greatest and therefore dioxin tends to be more planar. This is because the localization of the HOMO is higher on the heavier heteroatom, which leads to a

1. *Tripes (1997) SYBYL Version 6.4*, Tripos Inc. 1997.

2. M. E. Amato, A. Grassi, K.J. Irolic, G.C. Pappalardo, L. Radics, *Organometallics*, 1993, 12, 775.

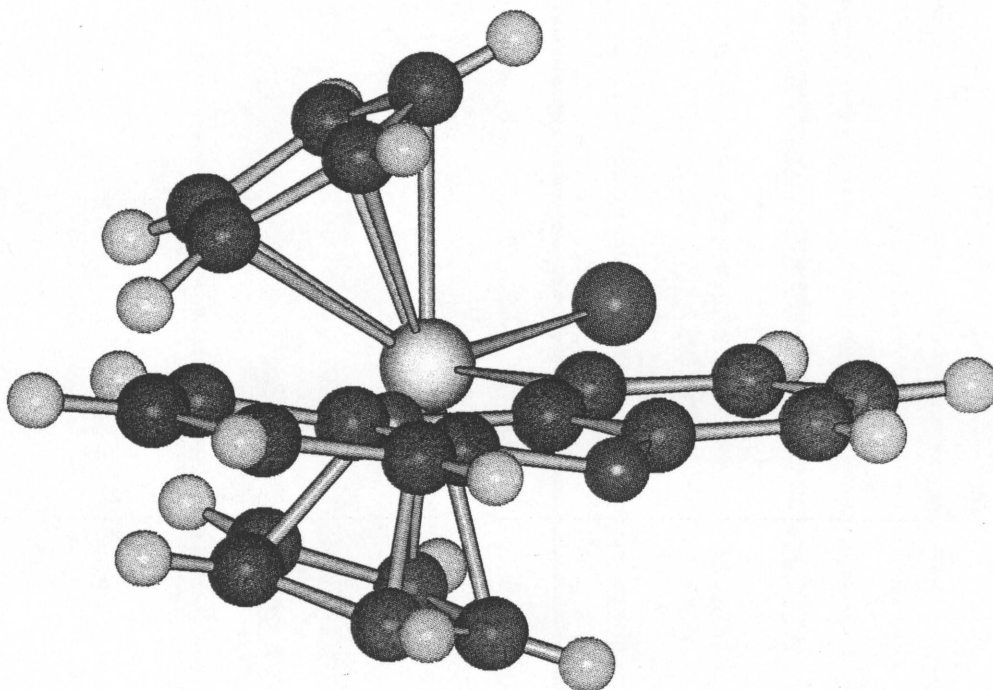


Fig. 8.1. A ball-and-stick diagram for [TiCp₂(Db)Cl].

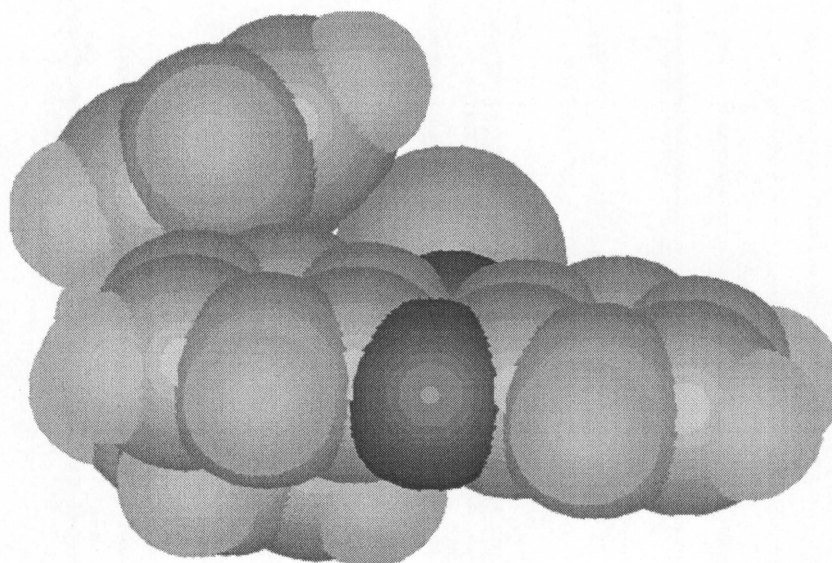


Fig. 8.2. A spacefill model for [TiCp₂(Db)Cl].

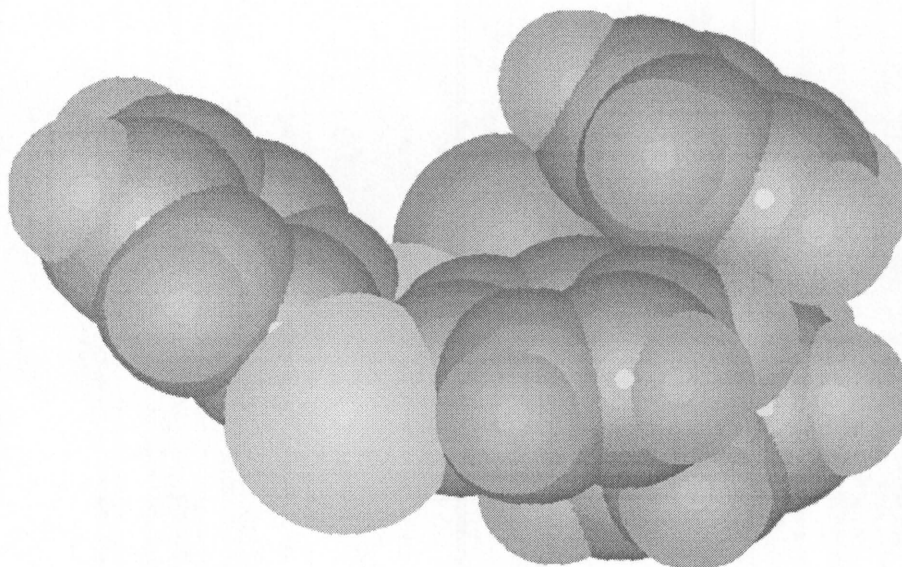


Fig. 8.3. A spacefill model for $[\text{TiCp}_2(\text{Th})\text{Cl}]$.

decrease of the p_z - π -interactions. With dioxin the HOMO is only an antibonding combination of the two highest π -orbitals of the rings with the two p_z -orbitals of oxygen.

When we look at the position of the chloro ligand in **1**, we can see that the ligand is in the plane of the metal and the planar heteroaromatic ligand. The cyclopentadienyl ligands are situated above and below this plane at an angle.

8.2 Chalcanthrenethiolates

In the chalcanthrenethiolates the same effect as above was experienced. In **Fig. 8.4** and **8.5** the models for $[\text{TiCp}_2(\text{DbS})\text{Cl}]$ **6** and $[\text{TiCp}_2(\text{DbS})_2]$ **7** can be seen. Again the heteroaromatic rings are planar, while in $[\text{TiCp}_2(\text{ThS})\text{Cl}]$ **9** and $[\text{TiCp}_2(\text{ThS})_2]$ **10** (**Fig 8.6** and **8.7**) the ligands are bent. The sulfur is sp^3 hybridized and there is a bent geometry around the sulfur. This allows for more space around the metal centre and is the reason why both chloro ligands can be replaced when the chalanthrenethiolates are used.

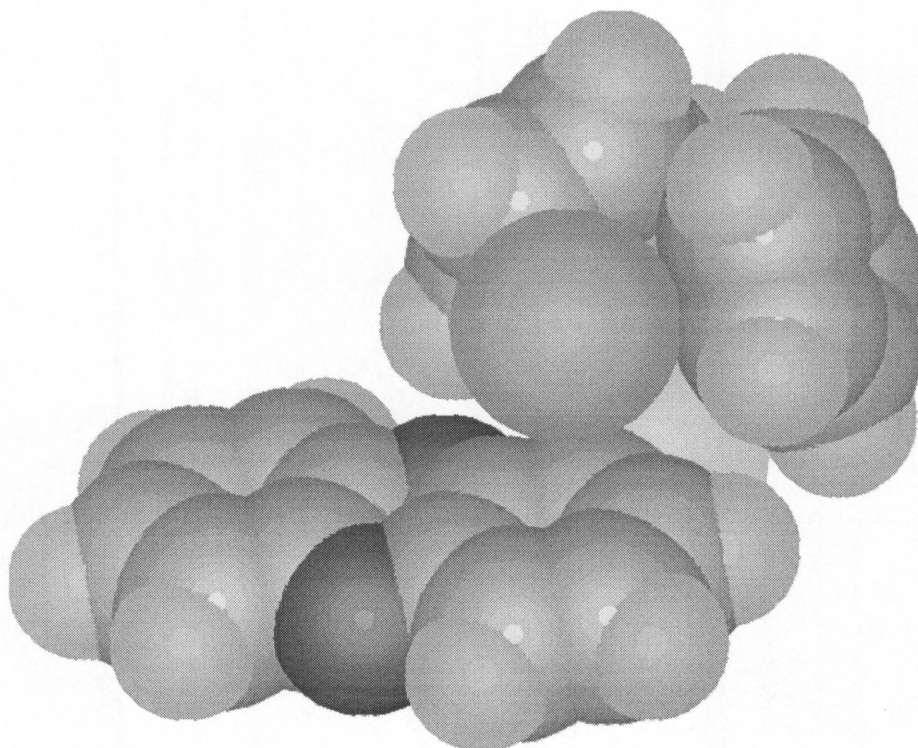


Fig. 8.4. A spacefill model for [TiCp₂(DbS)Cl].

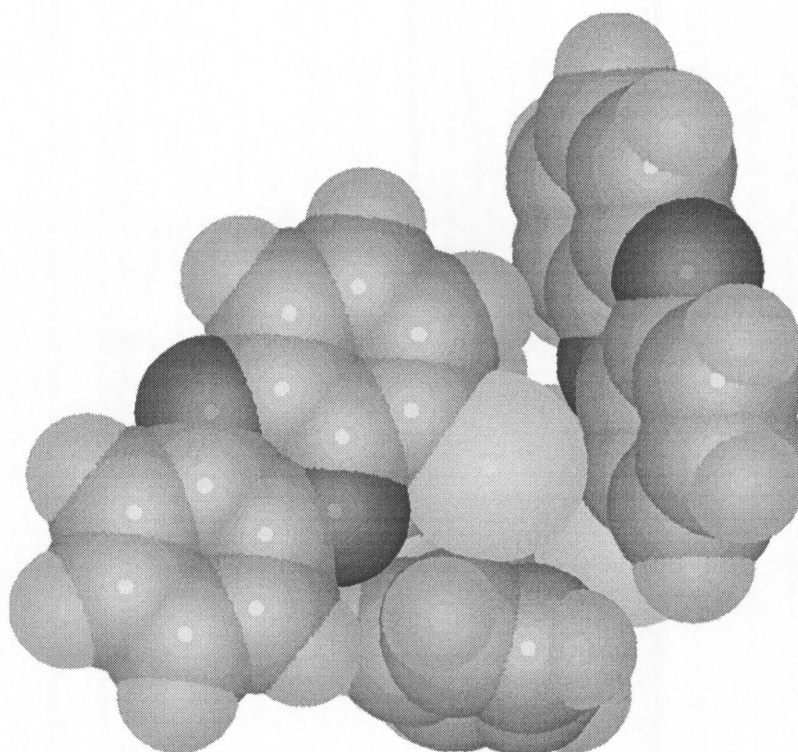


Fig. 8.5. A spacefill model for [TiCp₂(DbS)₂].

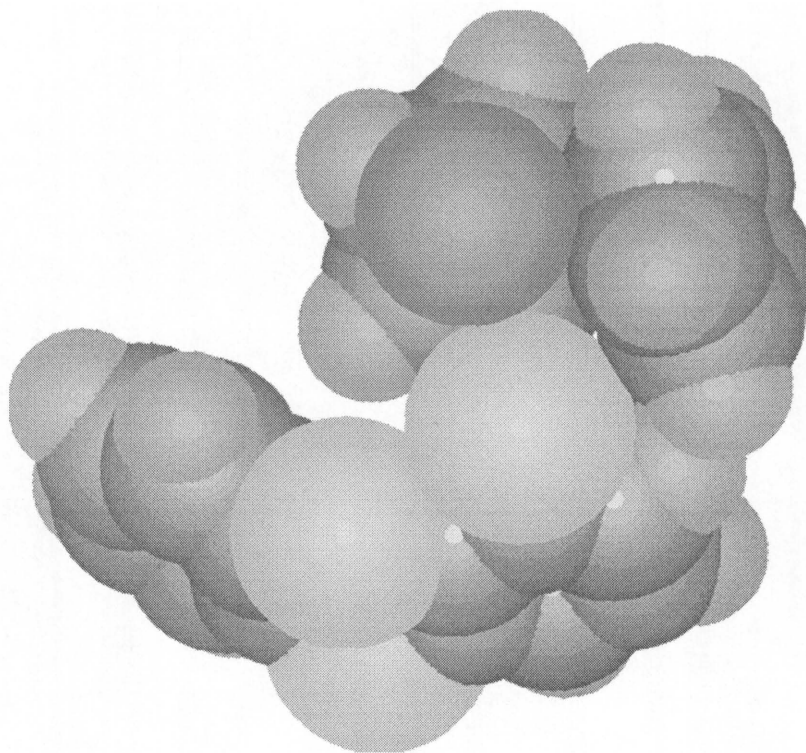


Fig. 8.6. A spacefill model for [TiCp₂(ThS)Cl].

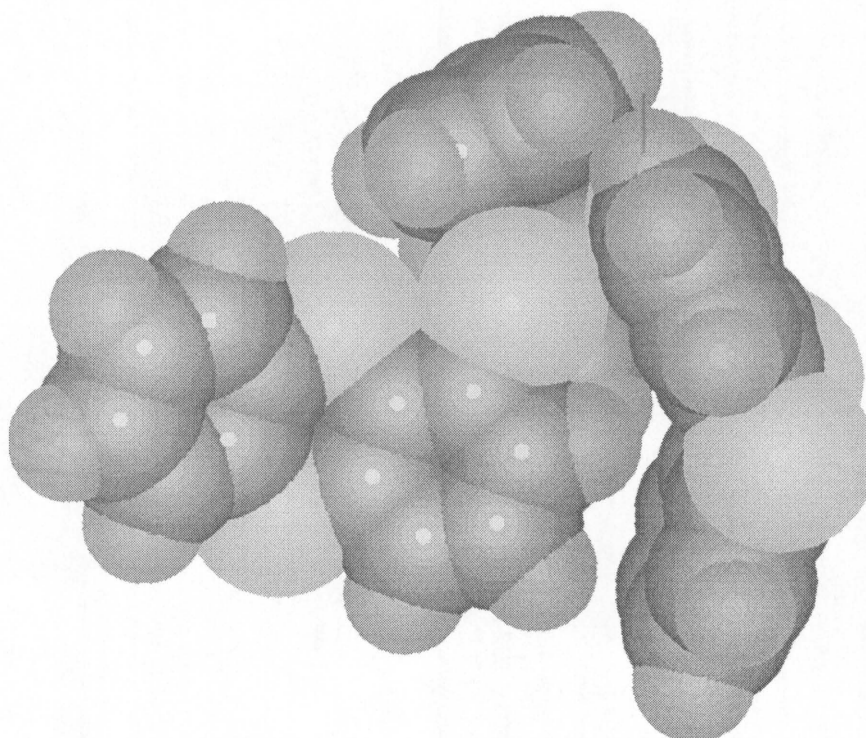


Fig. 8.7. A spacefill model for [TiCp₂(ThS)₂].

Comparing **Fig. 8.4** with **Fig. 8.2** we can see that the chloro ligand and metal are not in the plane of the heteroaromatic ligand anymore. The cyclopentadienyl rings are also away from the ligand and are not arranged around the plane of the ligand as in **Fig. 8.2**.

8.3 Conclusion

The computer generated spacefill models and the crystal structure of **1**, made it possible to see that the dibenzodioxin ligand has a planar geometry when complexed with titanium, while the thianthrene ligand has a bent geometry. The geometries for the thiolate analogues are the same and the sulfur allowed for the doubly substituted products to form. The presence or absence of the sulfur atom, between the metal and the heteroaromatic ligand, has a great influence on the position of the chloro ligand and the orientation of the cyclopentadienyl ligands.

9. Antitumour Properties

9.1 Geometry and Intercalation

In 1988 Palmer¹ reported that the dibenzo[1,4]dioxin-1-carboxamide (**Fig. 9.1**) has significant antitumour activity. After studying the geometries and the intercalation abilities of a series of analogous compounds, it was concluded that the best antitumour results were obtained when the ligand intercalated. The intercalator must compose of a planar tri- or tetracyclic chromophore with one or two side chains added, especially on the 1-position. There must be a heteroatom, preferably nitrogen or oxygen, *peri* to the side chain.

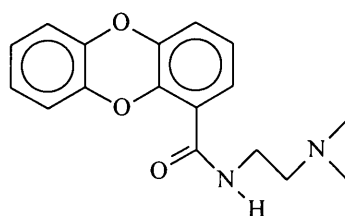


Fig. 9.1. Dibenzo[1,4]dioxin-1-carboxamide.

From the above study and the structural study in Chapter 8, it can be predicted that the complexes with the planar dibenzodioxin ligands could intercalate with DNA and cause an increase in the distance between two stacked base pairs. This will cause the cell to die, because the enzymes will not be able to execute important biological functions. The complexes with thianthrene ligands are not planar and it is expected that they might not be very successful as intercalators. Thianthrene ligands will be able to intercalate partially on the outside of the groove, with its bent geometry.

In Chapter 8 we compared **Fig. 8.2** with **Fig. 8.6** and saw that the cyclopentadienyl ligands are close to the heteroaromatic ligand in $[\text{TiCp}_2(\text{Db})\text{Cl}]$ **1** and further away from the ligand in $[\text{TiCp}_2(\text{DbS})\text{Cl}]$ **6**. This means that the cyclopentadienyl ligands will prevent proper intercalation

1. B. D. Palmer, G. W. Rewcastle, G. J. Atwell, B. C. Baguley, W. A. Denny, *J. Med. Chem.* **1988**, *31*, 707.

of **1**, while in **6** it will allow the ligand to intercalate more effectively.

The complex with the one thiolate ligand **6**, is expected to intercalate best and the one with two thiolate ligands [TiCp₂(DbS)₂] **7** is expected not to intercalate, because of two possible reasons. When the heteroaromatic ligands are parallel to each other, the distance between the two ligands is not enough to intercalate between two sets of base pairs and when the ligands are not parallel, the one ligand will prevent the other to intercalate.

9.2 Geometry and Covalent Bonding

Comparing the titanium complex² in **Fig. 2.13** and complexes of molybdenocene with nucleobases³ (**Fig. 2.15**), it can be predicted that the synthesized derivatives could also form covalent bonds between the titanium and the nitrogen of a nucleobase by replacing the chloro ligand. Comparing **Fig. 8.2** with **Fig. 8.6** it is clear that the chloro ligand is in different positions for the two complexes. In **1** the covalent bond is expected to form on the side of the major groove with the negatively charged oxygen of the phosphate group in the DNA backbone being a good candidate. In **6** the bond is expected to form in the groove with one of the nitrogen or oxygen atoms of the base pairs above or below the intercalating heteroaromatic ligand.

9.3 Conclusion

From the results by Palmer¹ and preliminary test results in our laboratories⁴, it can be concluded that the complexes with the dibenzodioxin ligands will probably intercalate best because of their planar nature, while the bent thianthrene complexes may be poor intercalators. It is also suggested that **6** will intercalate best because of the sulfur spacer between the metal and the heteroaromatic ligand, which causes the metal to be out of the plane of the ligand. The ligand is

2. A. L. Beauchamp, D. Cozac, A. Mardhy, *Inorg. Chim. Acta*, **1984**, *92*, 191.

3. B. Lippert in *Progress in Inorganic Chemistry*, S. J. Lippard (Ed.), John Wiley and Sons, New York, **1989**, 1.

4. S. Brink, R. Meyer, S. Lotz, Unpublished Results.

then free to intercalate completely and is not hindered by the metal fragment. The presence or absence of this spacer also determines where the chloro ligand will be relative to the heteroaromatic ligand and this determines where a possible covalent bond could form in the DNA. A little disappointing however is the fact that the thiolate ligands are relatively labile and may be readily substituted in the body. Nevertheless, complexes **1** and **6** need to be further investigated.

9.4 Future

Extending Palmer's work into coordination chemistry, it was decided to repeat the procedure on two more ligands, phenothiazine and phenothiolate, since one intercalated well and the other showed positive antitumour results. The work will also be continued to include other metals and heteroaromatic ligands. Ruthenium has more space available around the metal for ligands and form stable +2 and +3 complexes. Rhenium and iridium have photosensitive properties and this may also be important for mechanisms relying on electron transfer processes in the body.

Complexes **1** and **6** of this study will be screened *in vitro* and if good results are obtained, tested *in vivo* to prove the above statements and to see which complexes could form the basis for further studies.

Part IV

Experimental

Information Concerning all Reactions 96

10. Experimental 97

Information concerning all reactions

In the experimental part, standard Schlenk methods¹ were used in the synthesis of new complexes. Column chromatography was done by circulating cooled *iso*-propanol through the column jacket. Products were stored at 5°C under dry argon gas. All the solvents were distilled under inert reflux conditions and stored under dry nitrogen gas². THF was used immediately after distillation. Characterization of complexes was done under an inert atmosphere, where possible. Melting points were determined on a Gallenkamp Melting Point Apparatus. Nuclear magnetic resonance spectra were obtained on a Bruker AC-300 spectrometer. The ¹H and ¹³C NMR spectra were recorded at 300.135 and 75.469MHz, respectively. Micro analysis was obtained from the analytic section of the Division for Energy Technology of the CSIR in Pretoria. The high resolution mass spectra were recorded on a Finnegan 8200 spectrometer. Silica gel plates, silica gel and all other chemicals used were commercially available, except dibenzo[1,4]dioxin which was synthesized according to the method described in literature³. All solid reagents were used without prior purification, while the liquid reagents were distilled first, except for *n*-BuLi which was 1.6mol/dm³ in a hexane solution.

1. D. F. Shriver, M. A. Drezdson in *The Manipulation of Air-Sensitive Compounds*, 2nd edition, John Wiley and Sons, New York, 1986.

2. D. D. Perrin, W. L. F. Armarego, D. R. Perrin in *Purification of Laboratory Chemicals*, 2nd edition, Pergamon, New York, 1980.

3. H. H. Lee, W. A. Denny, *J. Chem. Soc. Perkin Trans. 1*, 1990, 1071-1074.

10. Experimental

10.1 Experimental Procedures

Lithiation of Dibenzodioxin at the 1-position

A solution of dibenzodioxin (0.54g, 3.0mmol) was dissolved in 30ml THF and cooled to -30°C . TMEDA (1.02ml, 3.3mmol) was added and the resulting solution was treated with n-BuLi (2.1ml of a $1.6\text{mol}/\text{dm}^3$ hexane solution, 3.3mmol). After stirring at -30°C for 1h the colour changed from pale yellow to clear bright yellow and the mixture was ready for subsequent reactions. Note that it is important to immediately proceed with subsequent reactions.

Lithiation of Thianthrene at the 1-position

The same procedure as above, but with thianthrene (1.08 g, 5.0mmol) instead of dibenzodioxin, dissolved in 50ml of THF was employed. TMEDA (0.75ml, 5.5mmol), n-BuLi (3.4ml of a $1.6\text{mol}/\text{dm}^3$ hexane solution, 5.5mmol) was added and the solution was stirred for 2h at -30°C .

Synthesis of Chlorobis(cyclopentadienyl)(dibenzodioxinyl)titanium(IV) 1 and μ -Oxobis{bis(cyclopentadienyl)(dibenzodioxinyl)titanium(IV)} 2.

The lithiated dibenzodioxin was cooled to -50°C and a solution of titanocene dichloride (0.75g, 3.0mmol) dissolved in 30ml THF, was added. After stirring for 30min. at -50°C the colour changed from bright red to clear orange-brown. The solution was heated to room temperature and stirred for another hour, until the colour was dark orange brown. The solvent was removed under reduced pressure and the residue was filtered through silica gel with dichloromethane. The resulting orange product was chromatographed on silica, with hexane:dichloromethane (6:4) mixture as eluent, to give chlorobis(cyclopentadienyl)(dibenzo-1,4-dioxin)titanium(IV). (Yield: 0.44g, 37%). Recrystallization from hexane/THF (1:1) gave bright orange, diamond shaped crystals (mp.: 92°C). *Anal.* Calc. for $\text{C}_{22}\text{H}_{17}\text{ClO}_2\text{Ti}\cdot\text{C}_6\text{H}_{14}\cdot\text{C}_4\text{H}_8\text{O}$: C, 69.24%; H, 7.10%. Found: C, 69.45%; H, 7.22%. A yellow fraction was collected before the major product, but turned black

on attempts to filter it with a chlorinated solvent. Finally, a yellow product, μ -oxobis{bis(cyclopentadienyl)(dibenzodioxinyl)titanium(IV)}, was collected by extracting and filtrating the black residue with benzene. This product was characterized spectroscopically.

Synthesis of Chlorobis(cyclopentadienyl)(thianthrenyl)titanium(IV) **3** and μ -oxobis(bis(cyclopentadienyl)(thianthrenyl)titanium(IV)) **4**.

The same procedure as above, but now with lithiated thianthrene, was used. Titanocene dichloride (1.25g, 5.0mmol) dissolved in 50ml THF was added and the colour changed from bright red to clear red-brown. The mixture was stirred for two hours, instead of one hour. Chromatography gave chlorobis(cyclopentadienyl)(thianthrenyl)titanium(IV) **3**, an orange band which quickly converted to μ -oxobis{bis(cyclopentadienyl)(thianthrenyl)titanium(IV)} **4**, a yellow band. Both products were characterized with spectroscopic methods.

Synthesis of Lithiated Dibenzo-1,4-dioxin-1-thiolate **5a**, Dibenzo-1,4-dioxin-1-thiol **5** and Dibenzo-1,4-dioxin-1-butylthioether **5b**.

The lithiation procedure for dibenzodioxin was followed and the solution was cooled to -40°C . Flowers of sulfur, S_8 (0.10g, 3.0mmol) was added and the solution was stirred for about 15 minutes to dissolve the sulfur, with a colour change from yellow to orange-brown. The mixture, containing the lithiated dibenzodioxin-1-thiolate **5a**, was then ready for subsequent reactions, which was executed immediately afterwards. To protonate the lithiated product, HCl gas was bubbled through the solution for about 5 min. The clear orange-brown solution turned into a pale yellow, milky colour and the solvent was evaporated under reduced pressure. The pale yellow residue was filtered through silica gel with dichloromethane and the resulting residue was again filtered with hexane to wash away the unreacted dibenzodioxin. Chromatography with dichloromethane:hexane (1:1) as eluent, gave a white-yellow product, dibenzodioxin-1-thiol **5** and dibenzodioxin-1-butylthioether **5b**, (Yield: 0,48g, 74%) which precipitated as soon the solvent started evaporating. The two products were difficult to separate and were not very soluble in hexane or dichloromethane. *Anal.* Calc. for $\text{C}_{12}\text{H}_9\text{O}_2\text{S}$: C, 66.35%; H, 6.31%. Found: C, 66.66%; H, 6.49%.

Synthesis of Lithiated Thianthrene-1-thiolate **8a** and Thianthrene-1-thiol **8**.

Same procedure as above was used, but starting with the lithiation method for thianthrene instead and adding S₈ (0.17g, 5.0mmol). Protonation gave a pale yellow product, thianthrene-1-thiol **9** (Yield: 0.89g, 71%). *Anal.* Calc. for C₁₂H₈S₃: C, 57.83%; H, 3.65%. Found: C, 57.97%; H, 3.78%.

Synthesis of Chlorobis(cyclopentadienyl)(dibenzodioxin-1-thiolato)titanium(IV) **6** and Bis{(cyclopentadienyl)(dibenzodioxin-1-thiolato)}titanium(IV) **7**

The same method as for **1** was used, but starting from lithiated dibenzodioxin-1-thiolate instead. The colour change was from red to dark red and chromatography gave the expected chlorobis(cyclopentadienyl)(dibenzodioxin-1-thiolato)titanium(IV) **6**, a red band (Yield: 1.29 g, 18%). *Anal.* Calc. for C₂₂H₁₇ClO₂STi: C, 61.63%; H, 4.00%. Found: C, 62.09%; H, 4.23%. Before the expected fraction, there was a red-purple band, bis{(cyclopentadienyl)(dibenzodioxin-1-thiolato)}titanium(IV) **7**, (Yield: 1.83 g, 22%; mp.: 189°C). *Anal.* Calc. for C₃₄H₂₄O₄STi: C, 67.11%; H, 3.98%. Found: C, 67.39%; H, 4.11%.

Synthesis of Chlorobis(cyclopentadienyl)(thianthrene-1-thiolato)titanium(IV) **9** and Bis{(cyclopentadienyl)(thianthrene-1-thiolato)}titanium(IV) **10**.

The same method was used as for **2**, but using lithiated thianthrene-1-thiolate instead. The colour change was from red to purple-red and chromatography gave the expected chlorobis(cyclopentadienyl)(thianthrene-1-thiolato)titanium(IV) **9**, a red band, which started to decompose on the column to a dinuclear product and the ligand. The next product was a purple-red band, bis{(cyclopentadienyl)(thianthrene-1-thiolato)}titanium(IV) **10** (Yield: 0.84g, 25%). *Anal.* Calc. for C₃₄H₂₄S₆Ti: C, 60.72%; H, 3.60%. Found: C, 60.90%; H, 3.72%.

Synthesis of the Titanium(IV) complex with Thianthrene as Ring-Opened Ligand **11**.

The method described by Rauchfuss⁴ was used, but thianthrene instead of dibenzothiophene was used. Small pieces of Li (5.0mmol, 0.078g) were added to a mixture of biphenyl (5.0mmol, 0.77g) and 20ml THF. After the colour changed from green to blue, the mixture was cooled to

4. P. R. Stafford, T. B. Rauchfuss, A. K. Verma, S. R. Wilson, *J. Organomet. Chem.*, 1996, 256, 203-214.

0°C. A solution of thianthrene (5.0mmol, 1.08g) in 20ml THF was also cooled to 0°C and added to the first mixture. Diethyl ether was added slowly over a period of 30min. The mixture was heated to room temperature and a red precipitate formed. After four hours the mixture was cooled to -78°C and was added to a mixture of titanocene dichloride (5.0mmol, 1.25g) dissolved in 20ml THF. The reaction was protected against light and the mixture was left to warm to room temperature overnight. The solvent was removed under reduced pressure and column chromatography with a toluene:hexane (6:4) mixture as eluent gave the red, ring-opened thianthrene product, $[\text{Ti}(\text{C}_5\text{H}_5)_2\text{S}_2\text{C}_{12}\text{H}_8]$ **11** (yield: 0.61g, 31%). *Anal.* Calc. for $\text{C}_{22}\text{H}_{18}\text{S}_2\text{Ti}$: C, 67.01%; H, 4.93%. Found: C, 67.34%; H, 5.01%. After the major product, there was a green fraction, $[\text{Ti}(\text{C}_5\text{H}_5)_2\text{S}_2\text{C}_6\text{H}_4]$, (yield: 0.41g, 21%), which was already mentioned in literature.

10.2 Crystal Structure Determination of $[\text{TiCp}_2(\text{Db})\text{Cl}]$

The X-ray data set was collected on a novel 1K SMART Siemens CCD area detector system using Mo radiation⁵. X-rays were generated using a regular sealed tube and an X-ray generator operating at 50kV 30mA. The 9cm wide CCD area detector was mounted 4.5cm from the crystal and the data set collected at low temperature (-100°C). A graphite monochromator followed by a 5mm collimator was used. The selected crystal was mounted on a thin glass fibre.

In order to obtain an initial set of cell parameters and an orientation matrix for data collection, reflections from three sets of 15 frames each were collected, covering three perpendicular sectors of space. The data collection nominally covered over a hemisphere of reciprocal space, by a combination of 3 sets of exposures of 1271 frames. Each set had a different ϕ angle for the crystal and each exposure covered 0.3° in ω , with 10 seconds exposure per frame. In order to monitor crystal and instrument stability and to enable crystal decay corrections, the first 50 frames of the first set were measured again at the end of the data collection. Crystal decay was found to be negligible after analysing the duplicate reflections. The final data set after scaling consisted of 16945 reflections to 0.751Å resolution. Coverage of data is 67.87 % complete to at least 28.26° in θ . The data collection took about 5 hours. A detailed presentation of the data collection statistics is given in **Table 10.1**.

5. G. M. Sheldrick, *SADABS User Guide*, University of Göttingen, Germany, 1996.

Empirical formula	C ₃₃ H ₄₁ Cl O ₃ Ti
Molecular weight	569.01
Temperature, K	296(2)
Wavelength, Å	0.71073
Space group	P2(1)/n
Unit cell dimensions: a, Å.	10.0318(5)
b, Å.	17.6700(10)
c, Å.	15.3214(8)
α, °	90
β, °	103.728(1)
γ, °	90
Z	4
Volume, Å ³	2638.3(2)
Density (calculated), Mg/m ³	1.433
Absorption coefficient, mm ⁻¹	0.461
F(000)	1208
Crystal size, mm	0.28 x 0.36 x 0.44
Scan range (θ°)	1.79 ≤ θ ≤ 28.26
Zone collected	-12 ≤ h ≤ 9 -22 ≤ k ≤ 21 -19 ≤ l ≤ 20
Reflections collected	16714
Independent reflections	6010
R _{int}	0.0209
Data / restraints / parameters	6010 / 0 / 411
Goodness-of-fit on F ²	1.840
Final R indices [I > 2σ(I)]	R1 = 0.0610, wR2 = 0.2122
R indices (all data)	R1 = 0.0674, wR2 = 0.2187
Residual electron density, (eÅ ⁻³)	Max = 1.564 Min = -0.710

Table 10.1. Crystal data and structure refinement for [TiCp₂(Db)Cl].

H atoms were placed geometrically and refined with a riding model and with U_{iso} constrained to be 0.08\AA^2 .

Refinement on F^2 for ALL reflections, except for 0 with a very negative F^2 or flagged by the user for potential systematic errors. Weighted R-factors (wR) and all goodness-of-fit (S) are based on F^2 , while conventional R-factors (R) are based on F, with F set to zero for negative F^2 . The observed criterion of $F^2 > 2\sigma(F^2)$ is used only for calculating R-factor observed, etc. and is not relevant to the choice of reflections for refinement. R-factors based on F^2 are statistically about twice as large as those based on F, and R-factors based on ALL data will be even larger.

All esds, except the esd in the dihedral angle between two l. s. planes, were estimated using the full covariance matrix. The cell esds were taken into account individually in the estimation of esds in distances, angles and torsion angles; correlations between esds in cell parameters were only used when they were defined by crystal symmetry. An approximate (isotropic) treatment of cell esds was used for estimating esds involving l. s. planes.

The determination of the unit cell parameters, crystal orientation and data collection were performed with the SMART (Siemens 1995)⁶. The crystallographic raw data frames were integrated, all reflections extracted, reduced and Lp-corrected using the program SAINT (Siemens 1995)⁷. The cell refinement using all data was also performed by SAINT (Siemens 1995). The program SHELXTL ver. 5.0 (Siemens 1995) was used for the structure solution, refinement, molecular graphics and publication preparation⁸.

6. Siemens (1996) *SMART Reference Manual*, Siemens Analytical X-ray Instruments Inc., Madison, Wisconsin, USA, 1996.

7. Siemens (1995b) *ASTRO and SAINT. Data Collection and Processing for the SMART System*, Siemens Analytical X-ray Instruments Inc., Madison, Wisconsin, USA, 1995.

8. Siemens (1995a) *SHELXTL Version 5.0 (Dos version) - Structure Determination Programme*, Siemens Analytical X-ray Instruments Inc., Madison, Wisconsin, USA, 1995.

Appendix

Crystallographic data for [TiCp₂(Db)Cl] 1.

Table 1. Fractional atomic coordinates ($\times 10^4$) and equivalent isotropic displacement parameters ($\text{Å}^2 \times 10^3$) for [TiCp₂(Db)Cl].

Atom	x/a	y/b	z/c	U _{eq}
Ti	1229(1)	1961(1)	9799(1)	21(1)
Cl	1952(1)	838(1)	10619(1)	31(1)
O(1)	2028(2)	3106(1)	8226(2)	35(1)
C(1)	7618(4)	-1127(2)	3281(2)	51(1)
C(2)	8098(4)	-395(2)	3483(3)	54(1)
O(2)	4402(2)	3185(1)	7529(1)	34(1)
C(3)	9038(4)	-183(2)	4235(3)	49(1)
C(4)	9411(3)	573(2)	4360(2)	35(1)
O(3)	-1151(3)	4258(1)	8588(2)	58(1)
C(5)	10390(4)	748(2)	5150(3)	49(1)
C(6)	10785(4)	1493(2)	5308(3)	55(1)
C(7)	11771(5)	1709(2)	6094(4)	68(1)
C(8)	-739(3)	1180(2)	9250(2)	42(1)
C(9)	-1170(3)	1931(2)	9220(2)	41(1)
C(10)	-589(3)	2321(2)	8592(2)	36(1)
C(11)	189(3)	1793(2)	8235(2)	32(1)
C(12)	114(3)	1096(2)	8648(2)	38(1)
C(13)	506(4)	2732(2)	10858(3)	47(1)
C(14)	822(4)	3215(2)	10205(2)	47(1)
C(15)	2234(4)	3156(2)	10279(2)	38(1)
C(16)	2769(3)	2642(2)	10971(2)	40(1)
C(17)	1694(4)	2404(2)	11325(2)	45(1)
C(18)	2950(3)	2049(1)	9134(2)	22(1)
C(19)	4044(3)	1542(2)	9384(2)	27(1)

C(20)	5194(3)	1567(2)	9014(2)	31(1)
C(21)	5295(3)	2107(2)	8385(2)	28(1)
C(22)	4242(3)	2626(2)	8134(2)	26(1)
C(23)	3090(3)	2589(1)	8490(2)	24(1)
C(24)	3240(3)	3597(2)	7155(2)	29(1)
C(25)	2060(3)	3545(1)	7487(2)	28(1)
C(26)	3276(3)	4080(2)	6448(2)	33(1)
C(27)	2128(3)	4509(2)	6064(2)	37(1)
C(28)	938(3)	4444(2)	6382(2)	37(1)
C(29)	901(3)	3957(2)	7083(2)	33(1)
C(30)	-770(5)	5034(3)	8506(4)	77(1)
C(31)	-2008(5)	5398(2)	7920(3)	61(1)
C(32)	-3136(5)	4968(3)	8141(5)	89(2)
C(33)	-2569(5)	4233(3)	8443(5)	87(2)

U_{eq} is defined as one third of the trace of the orthogonalized U_{ij} tensor.

Table 2. Bond lengths [Å] for [TiCp₂(Db)Cl].

Ti-C(18)	2.208(2)	C(7)-C(1)#1	1.439(6)
Ti-C(10)	2.356(3)	C(8)-C(9)	1.394(5)
Ti-C(9)	2.360(3)	C(8)-C(12)	1.406(5)
Ti-C(14)	2.364(3)	C(9)-C(10)	1.417(5)
Ti-C(13)	2.362(3)	C(10)-C(11)	1.408(4)
Ti-Cl	2.3684(7)	C(11)-C(12)	1.395(4)
Ti-C(15)	2.381(3)	C(13)-C(17)	1.365(6)
Ti-C(11)	2.394(3)	C(13)-C(14)	1.408(6)
Ti-C(8)	2.392(3)	C(14)-C(15)	1.397(5)
Ti-C(16)	2.397(3)	C(15)-C(16)	1.404(5)
Ti-C(12)	2.400(3)	C(16)-C(17)	1.383(5)
Ti-C(17)	2.404(3)	C(18)-C(19)	1.397(4)
O(1)-C(25)	1.379(3)	C(18)-C(23)	1.404(3)
O(1)-C(23)	1.389(3)	C(19)-C(20)	1.403(4)
C(1)-C(2)	1.391(5)	C(20)-C(21)	1.376(4)
C(1)-C(7)#1	1.439(6)	C(21)-C(22)	1.383(4)
C(2)-C(3)	1.356(5)	C(22)-C(23)	1.392(3)
O(2)-C(24)	1.378(3)	C(24)-C(26)	1.387(4)
O(2)-C(22)	1.389(3)	C(24)-C(25)	1.397(4)
C(3)-C(5)#1	1.398(5)	C(25)-C(29)	1.387(4)
C(3)-C(4)	1.388(4)	C(26)-C(27)	1.388(4)
C(4)-C(5)	1.400(5)	C(27)-C(28)	1.398(4)
O(3)-C(33)	1.387(6)	C(28)-C(29)	1.383(4)
O(3)-C(30)	1.437(5)	C(30)-C(31)	1.494(7)
C(5)-C(6)	1.380(6)	C(31)-C(32)	1.467(7)
C(5)-C(3)#1	1.398(5)	C(32)-C(33)	1.449(6)
C(6)-C(7)	1.417(7)		

Symmetry transformations used to generate equivalent atoms:

#1 -x+2,-y,-z+1

Table 3. Bond angles [°] for [TiCp₂(Db)Cl].

C(18)-Ti-C(10)	99.42(10)	C(3)-C(2)-C(1)	125.5(4)
C(18)-Ti-C(9)	131.90(11)	C(24)-O(2)-C(22)	115.7(2)
C(10)-Ti-C(9)	34.98(12)	C(2)-C(3)-C(5)#1	117.9(4)
C(18)-Ti-C(14)	104.94(12)	C(2)-C(3)-C(4)	119.5(3)
C(10)-Ti-C(14)	78.65(12)	C(5)#1-C(3)-C(4)	122.6(3)
C(9)-Ti-C(14)	84.01(13)	C(3)-C(4)-C(5)	116.3(3)
C(18)-Ti-C(13)	132.65(11)	C(33)-O(3)-C(30)	107.5(3)
C(10)-Ti-C(13)	94.38(13)	C(6)-C(5)-C(3)#1	120.5(4)
C(9)-Ti-C(13)	79.56(12)	C(6)-C(5)-C(4)	118.4(3)
C(14)-Ti-C(13)	34.67(14)	C(3)#1-C(5)-C(4)	121.1(3)
C(18)-Ti-Cl	97.42(7)	C(5)-C(6)-C(7)	121.3(4)
C(10)-Ti-Cl	136.53(8)	C(6)-C(7)-C(1)#1	118.4(4)
C(9)-Ti-Cl	109.72(9)	C(9)-C(8)-C(12)	108.2(3)
C(14)-Ti-Cl	134.10(9)	C(9)-C(8)-Ti	71.7(2)
C(13)-Ti-Cl	102.94(11)	C(12)-C(8)-Ti	73.2(2)
C(18)-Ti-C(15)	76.09(10)	C(8)-C(9)-C(10)	108.1(3)
C(10)-Ti-C(15)	101.24(12)	C(8)-C(9)-Ti	74.2(2)
C(9)-Ti-C(15)	117.09(12)	C(10)-C(9)-Ti	72.4(2)
C(14)-Ti-C(15)	34.26(13)	C(11)-C(10)-C(9)	107.2(3)
C(13)-Ti-C(15)	56.79(11)	C(11)-C(10)-Ti	74.3(2)
Cl-Ti-C(15)	121.68(9)	C(9)-C(10)-Ti	72.7(2)
C(18)-Ti-C(11)	75.54(10)	C(12)-C(11)-C(10)	108.3(3)
C(10)-Ti-C(11)	34.47(11)	C(12)-C(11)-Ti	73.3(2)
C(9)-Ti-C(11)	57.16(11)	C(10)-C(11)-Ti	71.3(2)
C(14)-Ti-C(11)	108.55(11)	C(11)-C(12)-C(8)	108.1(3)
C(13)-Ti-C(11)	128.85(13)	C(11)-C(12)-Ti	72.9(2)
Cl-Ti-C(11)	115.69(8)	C(8)-C(12)-Ti	72.6(2)
C(15)-Ti-C(11)	118.11(11)	C(17)-C(13)-C(14)	108.3(3)
C(18)-Ti-C(8)	123.28(11)	C(17)-C(13)-Ti	75.1(2)
C(10)-Ti-C(8)	57.28(12)	C(14)-C(13)-Ti	72.8(2)

C(9)-Ti-C(8)	34.11(13)	C(15)-C(14)-C(13)	107.0(3)
C(14)-Ti-C(8)	117.03(14)	C(15)-C(14)-Ti	73.5(2)
C(13)-Ti-C(8)	102.27(12)	C(13)-C(14)-Ti	72.6(2)
Cl-Ti-C(8)	80.02(9)	C(14)-C(15)-C(16)	108.0(3)
C(15)-Ti-C(8)	150.98(13)	C(14)-C(15)-Ti	72.2(2)
C(11)-Ti-C(8)	56.57(11)	C(16)-C(15)-Ti	73.6(2)
C(18)-Ti-C(16)	82.80(10)	C(17)-C(16)-C(15)	107.4(3)
C(10)-Ti-C(16)	133.93(12)	C(17)-C(16)-Ti	73.6(2)
C(9)-Ti-C(16)	135.35(12)	C(15)-C(16)-Ti	72.3(2)
C(14)-Ti-C(16)	56.82(12)	C(13)-C(17)-C(16)	109.3(3)
C(13)-Ti-C(16)	56.20(12)	C(13)-C(17)-Ti	71.6(2)
Cl-Ti-C(16)	87.75(9)	C(16)-C(17)-Ti	73.0(2)
C(15)-Ti-C(16)	34.17(12)	C(19)-C(18)-C(23)	115.2(2)
C(11)-Ti-C(16)	149.62(12)	C(19)-C(18)-Ti	118.5(2)
C(8)-Ti-C(16)	152.22(12)	C(23)-C(18)-Ti	126.2(2)
C(18)-Ti-C(12)	89.17(10)	C(18)-C(19)-C(20)	122.4(2)
C(10)-Ti-C(12)	57.09(11)	C(21)-C(20)-C(19)	120.7(2)
C(9)-Ti-C(12)	56.89(12)	C(20)-C(21)-C(22)	118.4(2)
C(14)-Ti-C(12)	135.33(12)	C(21)-C(22)-O(2)	117.1(2)
C(13)-Ti-C(12)	134.97(12)	C(21)-C(22)-C(23)	120.7(2)
Cl-Ti-C(12)	83.52(8)	O(2)-C(22)-C(23)	122.2(2)
C(15)-Ti-C(12)	151.82(11)	C(22)-C(23)-O(1)	120.4(2)
C(11)-Ti-C(12)	33.85(11)	C(22)-C(23)-C(18)	122.6(2)
C(8)-Ti-C(12)	34.12(12)	O(1)-C(23)-C(18)	117.1(2)
C(16)-Ti-C(12)	167.29(12)	C(26)-C(24)-O(2)	118.3(2)
C(18)-Ti-C(17)	115.65(11)	C(26)-C(24)-C(25)	120.4(3)
C(10)-Ti-C(17)	127.63(12)	O(2)-C(24)-C(25)	121.3(2)
C(9)-Ti-C(17)	108.53(13)	C(29)-C(25)-O(1)	118.7(2)
C(14)-Ti-C(17)	56.25(12)	C(29)-C(25)-C(24)	119.8(2)
C(13)-Ti-C(17)	33.28(13)	O(1)-C(25)-C(24)	121.5(2)
Cl-Ti-C(17)	78.00(9)	C(24)-C(26)-C(27)	119.6(3)

C(15)-Ti-C(17)	55.97(11)	C(26)-C(27)-C(28)	119.9(3)
C(11)-Ti-C(17)	162.10(12)	C(29)-C(28)-C(27)	120.3(3)
C(8)-Ti-C(17)	118.92(13)	C(25)-C(29)-C(28)	119.9(3)
C(16)-Ti-C(17)	33.47(12)	O(3)-C(30)-C(31)	105.2(4)
C(12)-Ti-C(17)	150.56(12)	C(32)-C(31)-C(30)	102.4(4)
C(25)-O(1)-C(23)	116.3(2)	C(33)-C(32)-C(31)	105.8(4)
C(2)-C(1)-C(7)#1	116.5(4)	O(3)-C(33)-C(32)	109.4(4)

Symmetry transformations used to generate equivalent atoms:

#1 $-x+2, -y, -z+1$

Table 4. Anisotropic displacement parameters ($\text{Å}^2 \times 10^3$) for $[\text{TiCp}_2(\text{Db})\text{Cl}]$.

Atom	U(11)	U(22)	U(33)	U(23)	U(13)	U(12)
Ti	20(1)	20(1)	23(1)	-1(1)	7(1)	-3(1)
Cl	38(1)	27(1)	31(1)	6(1)	12(1)	0(1)
O(1)	34(1)	33(1)	45(1)	16(1)	23(1)	10(1)
C(1)	66(2)	41(2)	46(2)	-5(2)	14(2)	2(2)
C(2)	47(2)	47(2)	62(2)	-10(2)	5(2)	5(2)
O(2)	30(1)	38(1)	40(1)	16(1)	18(1)	4(1)
C(3)	55(2)	39(2)	53(2)	-2(2)	11(2)	3(2)
C(4)	43(2)	24(1)	32(1)	4(1)	-5(1)	0(1)
O(3)	46(2)	38(1)	86(2)	0(1)	9(1)	11(1)
C(5)	47(2)	48(2)	54(2)	9(2)	15(2)	4(1)
C(6)	60(2)	51(2)	57(2)	5(2)	22(2)	10(2)
C(7)	65(3)	38(2)	120(4)	8(2)	57(3)	10(2)
C(8)	37(2)	49(2)	36(2)	2(1)	0(1)	-24(1)
C(9)	18(1)	62(2)	43(2)	-13(1)	9(1)	-5(1)
C(10)	29(1)	36(2)	37(2)	3(1)	-2(1)	4(1)
C(11)	25(1)	42(2)	26(1)	-2(1)	3(1)	-4(1)
C(12)	40(2)	31(2)	36(2)	-9(1)	-5(1)	-3(1)
C(13)	43(2)	47(2)	58(2)	-27(2)	29(2)	-11(1)
C(14)	60(2)	27(1)	47(2)	-15(1)	-2(2)	11(1)
C(15)	52(2)	31(1)	38(2)	-14(1)	21(1)	-19(1)
C(16)	35(2)	43(2)	38(2)	-20(1)	3(1)	-4(1)
C(17)	71(2)	39(2)	30(1)	-10(1)	18(2)	-8(2)
C(18)	21(1)	23(1)	22(1)	-3(1)	7(1)	-3(1)
C(19)	24(1)	24(1)	34(1)	6(1)	7(1)	1(1)
C(20)	25(1)	31(1)	37(1)	5(1)	9(1)	7(1)
C(21)	19(1)	32(1)	35(1)	0(1)	10(1)	-1(1)
C(22)	24(1)	27(1)	27(1)	3(1)	9(1)	-2(1)
C(23)	24(1)	22(1)	28(1)	1(1)	10(1)	2(1)
C(24)	31(1)	24(1)	34(1)	4(1)	14(1)	-1(1)
C(25)	31(1)	23(1)	32(1)	6(1)	11(1)	0(1)

C(26)	39(2)	31(1)	31(1)	3(1)	15(1)	-5(1)
C(27)	47(2)	34(2)	32(1)	6(1)	10(1)	-5(1)
C(28)	37(2)	30(1)	39(2)	5(1)	3(1)	-1(1)
C(29)	28(1)	26(1)	43(2)	4(1)	7(1)	-1(1)
C(30)	64(3)	59(3)	112(4)	-32(3)	29(3)	-10(2)
C(31)	83(3)	38(2)	61(2)	-3(2)	13(2)	-1(2)
C(32)	59(3)	85(4)	118(4)	36(3)	12(3)	25(2)
C(33)	58(3)	76(3)	134(5)	31(3)	38(3)	10(2)

The anisotropic displacement factor exponent takes the form:

$$-2 \pi^2 [h^2 a^{*2} U(11) + \dots + 2 h k a^* b^* U(12)]$$

Table 5. Hydrogen coordinates ($\times 10^4$) and isotropic displacement parameters ($\text{Å}^2 \times 10^3$) for $[\text{TiCp}_2(\text{Db})\text{Cl}]$.

Atom	x	y	z	U_{eq}
H(8)	-939(59)	925(31)	9595(39)	89(17)
H(9)	-1709(39)	2100(20)	9474(27)	41(10)
H(10)	-720(45)	2910(23)	8459(30)	57(11)
H(11)	687(40)	1861(20)	7814(28)	45(10)
H(12)	525(45)	652(24)	8615(29)	56(11)
H(13)	-366(45)	2654(23)	10910(28)	50(11)
H(14)	107(50)	3538(27)	9875(33)	66(14)
H(15)	2764(48)	3289(26)	9936(32)	70(13)
H(16)	3635(35)	2511(19)	11143(23)	31(8)
H(17)	1600(67)	2033(31)	11747(47)	103(21)
H(19)	3969(40)	1167(23)	9786(27)	51(10)
H(20)	5916(44)	1193(25)	9162(27)	57(11)
H(21)	5986(40)	2170(20)	8093(26)	42(9)
H(26)	4094(42)	4119(21)	6236(28)	49(10)
H(27)	2175(38)	4798(21)	5586(26)	42(9)
H(28)	83(37)	4772(21)	6121(24)	42(9)
H(29)	28(38)	3881(20)	7359(24)	41(9)
H(30A)	7(5)	5067(3)	8233(4)	93
H(30B)	-530(5)	5276(3)	9090(4)	93
H(31A)	-2061(5)	5930(2)	8064(3)	73
H(31B)	-2009(5)	5347(2)	7289(3)	73
H(32A)	-3467(5)	5220(3)	8611(5)	107
H(32B)	-3892(5)	4916(3)	7616(5)	107
H(33A)	-2822(5)	4096(3)	8996(5)	104
H(33B)	-2937(5)	3853(3)	7994(5)	104